NAL LABORATORY
operated by
UNION CARBIDE CORPORATION
for the
U.S. ATOMIC ENERGY COMMISSION

ORNL - TM - 1

CHEMICAL TECHNOLOGY DIVISION

CHEMICAL DEVELOPMENT SECTION B

QUARTERLY PROGRESS REPORT

APRIL–JUNE 1961

ORNL-TM-1

CHEMICAL TECHNOLOGY DIVISION

Chemical Development Section B

QUARTERLY PROGRESS REPORT FOR CHEMICAL DEVELOPMENT SECTION B

APRIL-JUNE, 1961

R. E. Blanco

DATE ISSUED

NOV 15 1961

OAK RIDGE NATIONAL LABORATORY
Oak Ridge, Tennessee
Operated by
UNION CARBIDE NUCLEAR COMPANY
for the
U.S. ATOMIC ENERGY COMMISSION

ABSTRACT

Graphite Fuels

The 90% HNO_3, Combustion-Dissolution, and Grind-Leach processes were studied as methods for recovering uranium and thorium from graphite reactor fuel elements containing pyrolytic carbon-coated dicarbide or Al_2O_3-coated oxide fuel particles. Greater than 99% of the uranium and thorium can be recovered from fuel containing carbon-coated particles by either the Grind-Leach (70% HNO_3) or Combustion-Dissolution processes. High recoveries were achieved by leaching with boiling acid only when the fuel specimens were ground finer than 200 mesh, which ensured crushing of the fuel particles. The ThO_2-U_3O_8 ash from combustion of specimens containing coated UC_2-ThC_2 particles was dissolved in less than 7 hr in boiling 13 M HNO_3-0.04 M NaF-0.1 M $Al(NO_3)_3$ to yield a solution 1 M in thorium. High recoveries from fuels containing Al_2O_3-coated oxide fuel particles were obtained only with the Grind-Leach process. Grinding specimens containing Al_2O_3-coated UO_2 finer than 200 mesh and leaching with boiling 15.8 M (70%) HNO_3 resulted in uranium recoveries of about 99%.

Uranium Monocarbide

Uranium monocarbide reacted with water at temperatures between 40 and 99°C to produce a gelatinous, greenish-brown uranium(IV) compound and 93.0 ml (STP) of gas consisting of 86% (vol) methane, 11% hydrogen, 1.8% ethane, 0.7% propane, 0.3% butanes, 0.07% pentanes, 0.03% hexanes, and a trace of heptane. There was no evidence of any change in product concentration with temperature as reported by Litz. The gas evolution rate increased rapidly with increasing temperature, 50% of the gas was evolved in 6 hr at 40°C vs 20 min at 90°C. A material balance for uranium and carbon was obtained. A satisfactory procedure was developed for analyzing the gaseous products from the reaction of metal carbides with aqueous solutions, whose vapors do not react appreciably with mercury at 25°C.

Beryllium and Beryllium Oxide

Studies of the dissolution of BeO-based fuel specimens in boiling fluoride and sulfate solutions were continued. The initial dissolution rates of BeO-5% UO_2 were 0.07, 1.5, and 3.3 mg $min^{-1}cm^{-2}$ in 8 M NH_4F, 8 M NH_4F--5 M HF, and 8 M NH_4F--20 M HF, respectively. In 3.2 M KF-5 M HF, the initial dissolution rate was only 0.36 mg $min^{-1}cm^{-2}$, or one-third the rate in the corresponding NH_4F-HF mixture. In boiling sulfuric acid solutions, BeO and BeO-5% UO_2 dissolved at rates which increased from about 0.01 to about 3.5 mg $min^{-1}cm^{-2}$ as the acid concentration increased from 4 to 16 molar. Rates were slightly higher in sulfuric acid solutions containing 0.2 M NaF.

Volatilization of Chloride with Hydrogen Peroxide

The chloride concentration in a 1.33 M $ZrOCl_2$-8 M HCl solution was

decreased to 1 M by adding 10 M H_2O_2 at 99°C. Chloride analyses indicate nearly 100% efficiency according to the reaction $2HCl + H_2O_2 \longrightarrow Cl_{2(g)} + 2H_2O$.

Acid Thorex Process

Diluent studies using the Acid Thorex flowsheet showed that decontamination factors obtained with fresh secbutyl benzene were five times higher than values obtained with Amsco or Solvesso 100. After the solvents were subjected to similar degradation conditions, the decontamination factors obtained with Amsco were twice as large as those obtained with the other diluents.

Extraction of uranium and thorium using an Acid Thorex flowsheet and a Darex declad solution as the extraction section salting agent, resulted in decontamination factors from ruthenium, zirconium, and rare earths of 560, 9000, and 2.5×10^5, respectively. Uranium and thorium losses were <0.001% and 0.4%.

Extraction of Uranium from Zirconium Fuel Solutions

Extraction of uranium from zirconium fuel solutions using a 5% TBP-Acid scrub flowsheet resulted in decontamination factors from ruthenium of 2600 and from zirconium-niobium of $>2 \times 10^5$. The uranium loss was <0.02%.

Extraction of Niobium with TBP

The distribution coefficient of niobium-95 from 0.09 to 4.1 M HNO_3 into 30% TBP-dodecane with 10% of the TBP degraded by refluxing 6 hr with 6 M HNO_3, ranged from 0.2 to 0.6. The values obtained in organic to aqueous experiments ranged from 0.3 to 1.6. In both cases the minimum values were obtained with 2 M HNO_3. Accurate values could not be obtained with acid deficient solutions but were approximately 10^{-4}. Additional experiments with 2 and 4 M HNO_3 showed that the coefficients are higher when degraded TBP and Amsco are present. Values obtained for freshly purified TBP and 2 and 4 M HNO_3, ranged from 0.003 to 0.01.

Separation of Thorium from Uranium 233 by Ion Exchange

Uranium may be effectively separated from thorium with Dowex 50W ion exchange resin using 0.5 N HNO_3 as the eluant. Product cuts contain 99% of the uranium with about 1% of the original thorium, and about 99% of the thorium containing less than 1% of the uranium.

IMMI Mixer-Settler Studies

Results of performance studies of the intermediate-scale mixer-settlers using the standard Purex flowsheet show that stage efficiencies up to 93% for uranium extraction and up to 95% for uranium stripping can be attained with modified impellers operated at speeds up to 1200 rpm. These efficiencies were realized while operating the extraction-scrub bank at

an aqueous throughput of 92 ml/min, ~85% flooding capacity, the back extraction-partition bank at an aqueous throughput of 25 ml/min, ~23% flooding capacity, and the strip bank at an aqueous throughput of 350 ml/min, ~90% flooding capacity. Uranium extraction was quantitative, 0.001% loss, with five actual stages; uranium stripping was quantitative, 0.001% loss, with seven actual stages.

It was established that, using the standard Purex flowsheet, stable operation of the IMMI mixer-settlers can be conducted at an aqueous feed throughput of 52 ml/min, i.e., a uranium mass throughput of 23.7 kg per day, with high stage efficiencies. With this flowsheet, aqueous throughput in the strip bank is limiting; 350 ml/min equivalent to 90% of flooding capacity.

Corrosion Studies

Unwelded Haynes 21 corroded at a maximum rate of 0.75 mil/mo in flowing Modified Zirflex dissolver solution (689 hr exposure) vs 6.4 mils/mo for welded Type 347 stainless steel (500 hr) and 3.6 mils/mo for as-welded Haynes 6B (192 hr). Type 347 stainless steel and LCNA corroded at uniform maximum rates of 0.26 mil/mo during 336 hr exposure in Modified Zirflex solvent extraction solutions (50°C) varying in composition from 0.75 to 1.5 $\underline{M}$ HNO_3, 0.6 to 1.0 $\underline{M}$ in Al^{+3}, 0.36 to 0.49 $\underline{M}$ in Zr^{+4} and 3.44 to 3.33 $\underline{M}$ in F^-. Both Type 304L stainless steel and Carpenter 20 SCb showed localized attack in these solutions. In 90 vol % 21 $\underline{N}$ HNO_3-10 vol % 40 $\underline{N}$ H_2SO_4 INOR-8 and Nichrome V showed uniform maximum rates of 0.16 and 0.20 mil/mo, respectively, vs accelerated localized attack observed on LCNA, CD4MCu, Carpenter 20 SCb and Types 304L, 347 and 309 SCb stainless steels. INOR-8 corroded rapidly (~375 mils/mo) in boiling 4 $\underline{M}$ HNO_3 vs 0.14 mil/mo for Nichrome V.

Type 304L stainless steel showed overall rates of 0.75 and 0.36 mil/mo accompanied by intergranular attack during 4000-6000 hr exposure to Darex-Purex waste solutions 5 $\underline{M}$ and 2 $\underline{M}$, respectively, in HNO_3 at 80°C. Corresponding maximum rate in the same solution containing polyethylene chips was 0.02 mil/mo.

Haynes 25, Nichrome V, INOR-8 and Pyroceram corroded at maximum rates of 0.25, 0.16, 0.03 and <0.01 mil/mo, respectively, for 360 hr exposure to anhydrous HCl at 350°C. At 600°C maximum rates were 5.30, 5.63, 16.4, and 1.2 mils/mo, respectively, for 34 hr exposure. At 200°C rates for all these materials were ≦0.01 mil/mo for 192 hr exposure. Nickel, Haynes 25, Nichrome V, INOR-8, and Pyroceram corroded at maximum rates of 11.4, 35.2, 8.8, 27.1, and 0, respectively for 24 hr exposure in dry Cl_2 at 600°C. At 350°C all rates ≦0.08 mil/mo and at 200°C all materials showed either a weight gain or no change in weight. In oxygen at 725°C (188 hr exposure) nickel, Haynes 25, Nichrome V, INOR-8 and Pyroceram 9608 showed maximum rates of 0.10, 0.02, 0.01, 0.01 and 0, respectively. In nitrogen saturated at room temperature with CCl_4 and heated to 600°C, specimens of Haynes 25

Nichrome V and INOR-8 were consumed during 18 hr exposure while Pyroceram 9608 corroded at a maximum rate of 108 mils/mo. At 450°C maximum rates (24 hr) were 7.33, 1.13, 1.16 and 0.02 mil/mo, respectively, and all were ≦0.12 mil/mo at 300°C. Specimens located "downstream" in the reactor usually corroded at considerably higher rates than those located upstream.

Radiation Damage to TBP--Amsco 125-82 Systems

Further studies on the radiolysis of 1 M TBP in solutions in Amsco 125-82 containing dissolved H_2O and HNO_3 showed that the yield of nitric acid destruction, $G(-HNO_3)$, increases from ~4 to ~11 molecules/100 ev at a dose of 45 whr/l as the acidity in the organic phase increases from ~0.1 to ~0.7 M, corresponding to equilibrium with aqueous phases containing ~0.7 and ~4.5 M HNO_3. Associated yields of dibutyl phosphoric acid formed, G(HDBP), increase from ~1 to ~3 molecules/100 ev under these same conditions. At a constant acidity, the value of G(HDBP) at a dose of 135 whr/l is only 60-80% of its value at 45 whr/l. These results were used to show that the ~25°C rate of decomposition of TBP, as ~1 M TBP and 0.1 M HNO_3 in a kerosene solvent, in a radiation field of 1 w/l is about the same as would be observed if the same solution were heated to ~100°C in the absence of radiation.

Foam Separation

Using the soft β emitter Ca-45 for surface counting, it was found that the calcium distribution coefficient with the sulfonate surfactant RWA-100 achieved a surface/bulk (Γ/c) Ca value at least as large as 1.4×10^{-2} cm, although potentially practical values are in the range 4×10^{-3} cm. Further evidence was obtained, with cerium solutions, in support of the concept, developed with H^+, Na^+, and Ca^{++} solutions, that for a specified concentration of a complex between a cation and the sulfonate group of RWA-100, surface activity is independent of cation valence to a first approximation. Thus separation of cesium from strontium occurs because the latter complexes the sulfonate strongly while cesium does not; instead, the cesium compound is largely ionized in aqueous solutions. Foam density was found to be dependent on bubble size when foam linear flow rates exceed 2-3 cm/min but to be nearly independent of bubble size at linear rate <1 cm/min. Specific foam areas ranged up to 3×10^5 cm^2/cm^3 of foam condensate. Cesium was removed to the extent of 95% from 6 M $NaNO_3$-10^{-5} M $CsNO_3$, a synthetic 1WW-NS, by frothing $K_2Cu_3[Fe(CN)_6]_2$ formed *in situ*. The cesium was subsequently separated from sodium and ferrocyanide by dissolution in triethanol amine, sorption on Duolite S-30 resin, and elution with 6.5×10^{-3} M HCl solution.

Distribution of Nitric Acid Between Aqueous and TBP-Amsco 125-82 Solutions

It was previously reported that the distribution of 0-5 M HNO_3 between aqueous and TBP--Amsco 125-82 solutions can be accurately described by equation (1), wherein square brackets refer to molal activities, parentheses

to molal concentrations, subscripts org and aq to organic and aqueous phases, respectively, and a and b are apparently functions only of the ratio (Amsco)/(TBP).

$$\log \frac{(HNO_3)_{org}}{[HNO_3]_{aq}\,(3.75493 - (HNO_3)_{org})} = a + b\,(HNO_3)_{org} \qquad (1)$$

The applicability of this equation in conjunction with material balance equations and the measured H_2O and HNO_3 concentrations of the organic phases lead to the conclusion that the fundamental equilibrium reaction for HNO_3 extraction at low acidity is

$$\left.\begin{matrix} TBP_{org} \\ + \\ TBP\cdot H_2O_{org} \end{matrix}\right\} + HNO_{3aq} \rightleftharpoons \left\{\begin{matrix} TBP\cdot HNO_3 \\ + \\ TBP\cdot HNO_3\cdot H_2O \end{matrix}\right.$$

The quantity (a) in equation 1 may be interpreted as the product of the equilibrium constant K_1^m for this extraction reaction and the mean activity coefficient, γ_T, of the species TBP and $TBP\cdot H_2O$. $K_1^m\gamma_T$ increases from 0.27 to 1.51 as the TBP concentration in Amsco increases from 5 to 100 vol %.

Vapor Pressure of Tributyl Phosphate

The vapor pressure of TBP over 0.2 wt % and 50 mole %, i.e., water saturated, solutions of water in TBP were measured by a transpiration technique to be ~0.80 and 0.51 microns, respectively, at 25°C. The former value is lower nearly by a factor of 10 than the vapor pressure estimated from a literature vapor pressure equation.

Waste Fixation in Borate and Phosphate Glasses

"Glasses" were prepared from simulated high sulfate Purex waste solution by the addition of phosphate and borate as fluxing agents and CaO and MgO to prevent sulfate volatility. Densities varied between 2.6-2.8 g/cc and 5.2 to 6.9 gal of solid product represented one ton of uranium processed. Similar "glasses", prepared with phosphate fluxes, had densities of 2.7 to 2.8 g/cc and 4.9 to 5.7 gal of solid represented one ton of U processed. Softening points of the magnesium melts were between 825°and 875°C while a calcium melt softened at ~950°C. A glassy borophosphate product, softening point ~900°C, was prepared from TBP-25 waste. Leach tests on high sulfate Purex waste "glass" spiked with mixed fission products gave an initial rate of 3.2×10^{-2} g $cm^{-2}day^{-1}$ which decreased to 6.6×10^{-5} g $cm^{-2}day^{-1}$ after 37 days.

Addition of 0.4 M H_3PO_3 to simulated Purex waste resulted in volatilization of 4.92% of the Ru during calcination vs 1.38% when the initial feed was 0.1 M in H_3PO_3 and the remaining phosphite was added (total of 0.4 M)

before decomposition of the salt nitrates. Lowering the phosphite in the initial feed to 0.05 M followed by later increase to 0.4 M resulted in volatilization of 7.7% to 12.2% of the Ru. Substitution of Ca for Mg did not affect ruthenium volatility.

Low Level Waste Treatment

Decontamination of low-level ORNL waste by means of a precipitation-phenolic ion exchange process demonstrated the feasibility of lowering the activity of the effluent to 54% of MPC_w (gross β assuming 100% Sr^{90}). Decontamination factors for strontium and cesium were >1000 and >100 respectively, or a reduction of <1% of MPC_w for each.

Fission Product Recovery by Ion Exchange

A head-end double precipitation step prior to using ion exchange for the recovery of strontium from 1WW Purex waste solution was studied on a laboratory scale. Excess ferric ion was added to the waste solution and the mixture diluted with 90% nitric acid to 50-55% HNO_3, precipitating >85% of the sulfate ion in the system as iron sulfate. Evaporation of the filtrate to the point of nitrate decomposition (130°C), dilution with fuming nitric acid to 63% HNO_3, and heating the solution to 65-70°C yielded a precipitate which contained 85% of the original strontium with <10% and ~30% of the original iron and aluminum, respectively. A feed solution for further purification by ion exchange was obtained by dissolving the precipitate in dilute nitric acid.

Radiation Damage to Ion Exchange Resins

Amberlite 200 (16-50 mesh), a highly crosslinked, yet porous, sulfonated styrene-divinylbenzene resin, was placed in a circulating system of demineralized water and irradiated in a 10,000 curie cobalt-60 source. A dose of 0.82×10^9 r decreased the resin volume by 2%.

Exposure of Dowex 50W X-8 (20-50 mesh) resin to a dose of 0.85×10^9 r lowered the specific resin capacity by 30%, decreased the resin volume by 20% and lowered the moisture content from its original 42.7% to 38.6%. A dose of 3.9×10^9 r lowered the specific capacity by ~60%, decreased the resin volume by 85% and increased the moisture content to 55.1%.

Chemical Applications of Nuclear Explosions (CANE)

Tritium exchange studies under diffusion controlled conditions were completed. The maximum exchange of T observed was 26% at 600°C when a mixture of $HTO-H_2-H_2O$ was flowing over layers of $CaSO_4$ powders of 1.6 in. bed dia with flow rates of 4.1×10^{-11}, 6.5×10^{-3}, and 4.5×10^{-4} moles/min, respectively. Under the same experimental conditions and flowrate, using forced flow through 1 in. dia fixed beds of 20-30 mesh $CaSO_4$, 66-70% exchange was observed with bed lengths of 3 to 12 in. at 600°C, where the calculated equilibrium exchange would be 93%. An apparatus has been designed and is being tested for utilizing the plasma jet for studying high temperature chemical and exchange reactions.

CONTENTS

1.0 FUEL DISSOLUTION
(L. M. Ferris)

1.1 Graphite Fuels (L. M. Ferris and A. H. Kibbey)

Recovery of uranium and thorium from fuel elements containing coated fuel particles was studied. Fuels of major interest are those which contain pyrolytic carbon-coated UC_2 or ThC_2 particles (such as General Atomic's Philadelphia Electric reactor) and those containing Al_2O_3-coated UO_2 fuel particles (one of the types being tested for the Pebble Bed Reactor). Recoveries by three methods, the 90% HNO_3 (1), Combustion-Dissolution, and the Grind-Leach (2) processes, were determined for the above fuel types. In addition, experiments involving the 90% HNO_3 and Combustion-Dissolution processes were made with uncoated specimens containing uranium and thorium and with prototype TURRET reactor fuel specimens.

Experiments with prototype Philadelphia Electric graphite reactor fuel specimens (9.74% uranium and 33.5% thorium as carbon-coated dicarbide particles dispersed in a graphite matrix) indicated that both the Combustion-Dissolution and Grind-Leach processes were potentially applicable to the recovery of uranium and thorium from this type of fuel. However, uranium and thorium recoveries were less than 10% with the two-leach, boiling 90% HNO_3 process (1). Since the fuel particles were approximately 150 microns in diameter, Grind-Leach experiments were conducted with specimens ground finer than 200 mesh to ensure crushing of all the fuel particles. In two, 4-hr leaches under flowsheet conditions (2), uranium and thorium recoveries were as follows:

Leaching Agent	Losses to the Graphite Residue, %	
	Uranium	Thorium
15.8 M HNO_3	1.2	0.051
13 M HNO_3-0.04 M NaF-0.1 M $Al(NO_3)_3$	0.65	0.036

The achievement of higher thorium recoveries than uranium recoveries, particularly when the leachant contained no fluoride catalyst, was unexpected. Unexpected, also, was the higher uranium recovery in the leachant containing only 13 M HNO_3, since recoveries generally increase with increasing acid concentration (2). In future experiments, the effect of longer leaching periods on the uranium recovery will be tested.

Only the Grind-Leach process appears applicable to the processing of fuels containing Al_2O_3-coated fuel particles. Grinding a prototype Pebble Bed Reactor fuel specimen (Sanderson and Porter code FA-22 containing 125-micron dia fuel particles) finer than 200 mesh and leaching the powder twice for 4 hr with boiling 15.8 M HNO_3 resulted in a uranium recovery of

99%. In other tests with this type of fuel, it was found that the ungraphitized matrix could readily be disintegrated with boiling 90% HNO_3 but that little attendent leaching of the uranium occurred. Combustion of the matrix in oxygen left the fuel particles essentially intact. Attempts to leach out the UO_2 with boiling nitric acid were fruitless.

Carbon-coated as well as uncoated fuel specimens containing both uranium and thorium burned readily in a stream of oxygen at 800 to 900°C. Dissolution of the ThO_2-U_3O_8 ash in boiling 13 M HNO_3-0.04 M NaF-0.1 M $Al(NO_3)_3$ was usually complete in less than 7 hr. Solutions containing about 1 M thorium were easily obtained. In some cases, dissolution of the ash was complicated by the presence of up to about 0.7% iron as an impurity in the fuel. The source of the iron was not established, but it could have been introduced into the fuel as an impurity in the graphite flour or uranium constituent or from operations such as ball milling of the ingredients before molding. The U_3O_8-Fe_2O_3 ash from combustion of fuels containing only uranium could be dissolved in less than 5 hr in boiling 8 M HNO_3-0.75 M HCl. When the HCl concentration was less than 0.75 molar, complete dissolution of the iron oxide was not achieved.

The 90% HNO_3 process resulted in high recoveries from fuels containing both uranium and thorium which were not coated and which did not contain coated fuel particles. Two types of fuel samples were used in these studies: 1) HTGR-1, which contained about 1.5% uranium and 7.2% thorium as oxide particles dispersed homogeneously throughout the graphite matrix; and 2) HTGR-2, which contained about 1.2% uranium and 15% thorium as coprecipitated, 150-micron, dicarbide particles. Sample HTGR-2 actually was taken from an early Philadelphia Electric prototype fuel compact having a solid graphite core surrounded by a 3/8-in. annular ring containing a total of 30 wt % of uranium and thorium dicarbides. At least 99.7% of the uranium and thorium could be recovered from these samples by multiple leaching with boiling 90% HNO_3 (Table 1). The high thorium recoveries were obtained only after three leaches with boiling acid. Interestingly, the presence of 0.05 M HF in the leachant had no beneficial effect on the thorium recovery. Leaching temperature was very important. With sample HTGR-2, uranium and thorium losses to the graphite residue were reduced from about 10 to 0.2% when the leaching temperature was increased from 25° to the boiling point, about 93°C (Table 1).

Previously reported Grind-Leach (70% HNO_3) experiments with specimen HTGR-1 showed that uranium and thorium recoveries were both less than 90% even when the specimens were ground finer than 200 mesh (3).

Uranium was easily recovered from TURRET (4) reactor fuel (Type AUC Graphite impregnated with uranyl nitrate solution prior to baking) by leaching with boiling 90% HNO_3. After two, 4-hr leaches with boiling acid under flowsheet conditions (1), the uranium loss to the graphite residue was only 0.012%. Greater than 99.3% of the uranium was recovered in the first leach and subsequent water washes.

Table 1. Recovery of Uranium and Thorium from Uncoated Graphite Fuels by the 90% HNO_3 Process (1)

Sample, HTGR	Content, % U	Content, % Th	Temp, °C	Recoveries, % 1st Leach and Washes U	1st Leach and Washes Th	2nd Leach and Washes U	2nd Leach and Washes Th	3rd Leach and Washes U	3rd Leach and Washes Th	Residue U	Residue Th
1	1.5	7.2	93	96.4	85.5	2.6	7.7	-	-	1.1	6.8
1	1.45	6.95	93	98.6	86.2	1.37	11.8	-	-	0.24	1.93
1[a]	1.47	7.14	93	97.6	87.2	2.37	7.98	-	-	0.16	4.81
1	1.50	7.21	93	97.7	85.5	2.31	13.0	0.10	1.17	0.06	0.25
2	1.18	14.3	25	80.7	83.7	8.0	5.8	-	-	11.4	10.4
2	1.28	15.0	93	95.3	99.0	4.58	0.88	-	-	0.10	0.16

[a]The leachant in this experiment contained 0.05 M HF.

1.2 Uranium Monocarbide (M. J. Bradley)

Studies on the stoichiometry of the reaction between uranium monocarbide and water as a function of temperature are continuing (5). The uranium monocarbide specimens were prepared from high purity uranium metal and carbon by the best arc melting technique yet developed at ORNL* and appear to be nearly stoichiometric UC on the basis of chemical analysis (Table 2) x-ray, and metallographic examination.

Table 2. Chemical Analysis of Uranium Monocarbide

(Theoretical for UC: 4:00 mmoles/g U and C)

Specimen No.	U, mmoles/g a	U, mmoles/g b	Total C, mmoles/g b	Free C, mmoles/g	N ppm b
ORNL-2A	3.97	3.99	3.95	c	105
ORNL-2B	3.99	3.96	3.95	c	60
ORNL-2C		3.91	3.93	0.04	105

[a]Material balance for hydrolysis experiments.

[b]Direct analysis by ORNL Analytical Chemistry Division.

[c]None detected.

*D. W. Bourgette, ORNL Metallurgy Division

When uranium monocarbide was reacted with water in the temperature range of 40 to 99°C the products were a finely divided, greenish-brown solid uranium (IV) compound and 93 ml (STP) of gas per gram of carbide consisting chiefly of methane (86 vol %) and hydrogen (11 vol %). The gas phase also contained 1.8% ethane, 0.7% propane, 0.3% butanes, 0.01% isopentane, 0.06% n-pentane, 0.02% branched hexane isomers, 0.009% n-hexane, and a trace (0.001%) of n-heptane (Table 3). At least three, and probably all four, of the branched hexane isomers were present. (The analytical procedure did not separate 2,3-dimethylbutane from 2-methylpentane). An unidentified peak representing about 0.02% was found between the butanes and the pentanes. No trace of ethylene, propylene, acetylene or the higher alkynes has ever been detected.

There was no evidence of any change in the concentrations of the products with temperature, as reported by Litz (6), who found 12% hydrogen at 83°C, 22% hydrogen at 90°C, and 37% hydrogen at 100°C. Litz gave no analysis for his uranium carbide. If prepared in situ by the methane reaction, it might have contained uranium metal, uranium hydride, and free carbon in addition to carbide.

Within the limits of experimental error, a material balance for carbon and uranium has been obtained. Assuming that the gases were ideal, for each gram of uranium monocarbide (4.00 mmoles) hydrolyzed, an average of 3.88 mmoles of carbon atoms and 16.03 mmoles of hydrogen atoms were found in the gas phase compared with 3.95 mmoles C/g in the starting material. The nonvolatile product of the hydrolysis was a water slurry of a gelatinous greenish-brown colored uranium compound which was amorphous to x-rays. Dissolution of this compound in chlorine-free 6 M HCl yielded a solution containing 95 to 99% of the uranium in the tetravalent state. No insoluble or nonvolatile carbon has been found in the HCl solutions. At present there is no suitable procedure for determining very small quantities of volatile carbon compounds in HCl solutions.

While temperature had no apparent effect on the products of the reaction between 40 and 99°C, the rate increased markedly with increasing temperature. Typical gas evolution curves in the hydrolysis of UC as a function of temperature are shown in Fig. 1. The specimens were irregularly shaped pieces of unknown surface area weighing 3.1 to 4.3 g. Particularly at the lower temperatures, there was an initial induction period when extensive powdering of the sample occurred without much gas evolution. In one experiment at 25°C, the specimen appeared to have disintegrated completely in 6 hr, yet only about 12% of the gaseous products had been evolved.

In these experiments, the carbide specimen (3-4 g) was placed in the reaction vessel, water was placed in the funnel, and the apparatus was assembled as shown in Fig. 2. The reactants were preheated to the desired temperature in a water bath controlled to ±0.05°C. During the 1-hr equilibration period, both the main reaction vessel and the water in the funnel were flushed with helium to remove most of the air in the system.

Table 3. Reaction of UC with Water as a Function of Temperature

Temp, °C	Run No.	UC Batch ORNL	Volatile Products Composition of Gas Produced, Vol % H_2	CH_4	C_2H_6	C_3H_8	C_4H_{10}	iso-C_5H_{12}	n-C_5H_{14}	Branched C_6H_{14}	n-C_6H_{14}	C_7H_{16}	?	Total Vol of Gas ml/g	Total Carbon mmoles per g UC	Total Hydrogen mmoles per g UC	H/C Mole Ratio
99	173	2A	13.3	83.6	1.86	0.74	0.32	0.012	0.077	0.008	0.010	< 0.001	0.012	95.9	3.92	16.40	4.18
	174	2C	10.1	86.8	1.70	0.80	0.40	0.016	0.10	0.031	0.019	< 0.001	0.024	93.0	3.95	16.19	4.10
	176	2C	11.5	85.4	1.89	0.70	0.35	0.010	0.079	0.030	0.012	< 0.001	0.018	92.5	3.85	15.97	4.15
	178	2C	12.6	84.1	2.12	0.69	0.32	0.013	0.078	0.032	0.016	0.011	0.045	95.6	3.95	16.44	4.16
		Avg.	11.9	85.0	1.89	0.73	0.35	0.013	0.083	0.025	0.014	0.003	0.025	94.2	3.92	16.25	4.15
90	167	2A	10.4	86.9	1.70	0.62	0.26	0.016	0.066	0.013	0.008	0.002	0.022	93.7	3.92	16.18	4.13
	169	2A	12.9	84.0	1.85	0.75	0.28	0.016	0.078	0.017	0.010	<0.001	0.025	93.2	3.82	15.97	4.18
	170	2A	12.0	85.1	1.64	0.66	0.32	0.016	0.068	0.024	0.009	0.010	0.031	91.3	3.77	15.68	4.16
	172	2C	10.9	86.5	1.70	0.57	0.26	0.016	0.047	0.013	0.009	<0.001	0.018	93.7	3.90	16.17	4.15
		Avg.	11.6	85.6	1.72	0.65	0.28	0.016	0.065	0.017	0.009	0.003	0.0024	93.0	3.87	16.00	4.16
80	156	2B	10.7	86.6	1.7	0.65	0.23	0.01	0.05	0.03	0.01	<0.01					
	157	2B	10.1	87.0	1.8	0.73	0.31	0.02		0.006	0.004	<0.001		93.6	3.93	16.19	4.12
	158	2B	10.8	86.0	1.90	0.76	0.30	0.023	0.075	0.137	0.017	<0.001		93.4	3.94	16.26	4.13
	159	2B	10.4	86.7	1.8	0.69	0.27	0.009	0.050	0.045	0.010	<0.001		91.9	3.86	15.92	4.12
		Avg.	10.4	86.7	1.8	0.69	0.27	0.009	0.050	0.045	0.010	<0.001		93.0	3.91	16.12	4.12
60	160	2B	10.7	86.6	1.79	0.50	0.31	0.017	0.054	0.020	0.009	0.001	0.014	92.3	3.86	15.95	4.14
	161	2B	12.3	84.8	1.89	0.53	0.30	0.011	0.067	0.020	0.005	<0.001	0.023	91.8	3.82	15.66	4.10
	162	2B	12.5	85.3	1.39	0.53	0.26	0.008	0.060	0.014	0.008	<0.001	0.017	93.4	3.80	15.95	4.20
	163	2B	10.6	86.6	1.72	0.58	0.26	0.016	0.059	0.019	0.006	<0.001	0.04	93.9	3.91	16.19	4.14
	164	2A	10.7	86.8	1.64	0.55	0.26	0.010	0.049	0.010	0.008	0.002	0.018	93.4	3.89	16.12	4.14
		Avg.	11.4	86.0	1.69	0.54	0.28	0.012	0.058	0.017	0.007	<0.001	0.022	93.0	3.86	15.97	4.14
40	165	2A	10.8	86.4	1.73	0.65	0.33	0.013	0.075	0.018	0.005	< 0.001	0.018	92.2	3.87	15.95	4.12
	166	2A	10.9	86.2	1.75	0.63	0.33	0.011	0.045	0.019	0.003	0.002	0.003	92.3	3.85	15.92	4.14
	175	2C	10.8	86.3	1.85	0.61	0.32	0.013	0.072	0.036	0.006	< 0.001	0.026	91.9	3.85	15.89	4.13
	179	2C	9.9	86.1	2.93	0.59	0.30	0.009	0.057	0.028	0.007	0.005	0.06	92.2	3.92	16.07	4.10
		Avg.	10.6	86.2	2.06	0.62	0.32	0.012	0.062	0.023	0.005	0.002	0.027	92.2	3.87	15.96	4.12
Final Avg.			11.2	85.9	1.83	0.65	0.30	0.012	0.064	0.025	0.009	0.002	0.020	93.1	3.89	16.06	4.14

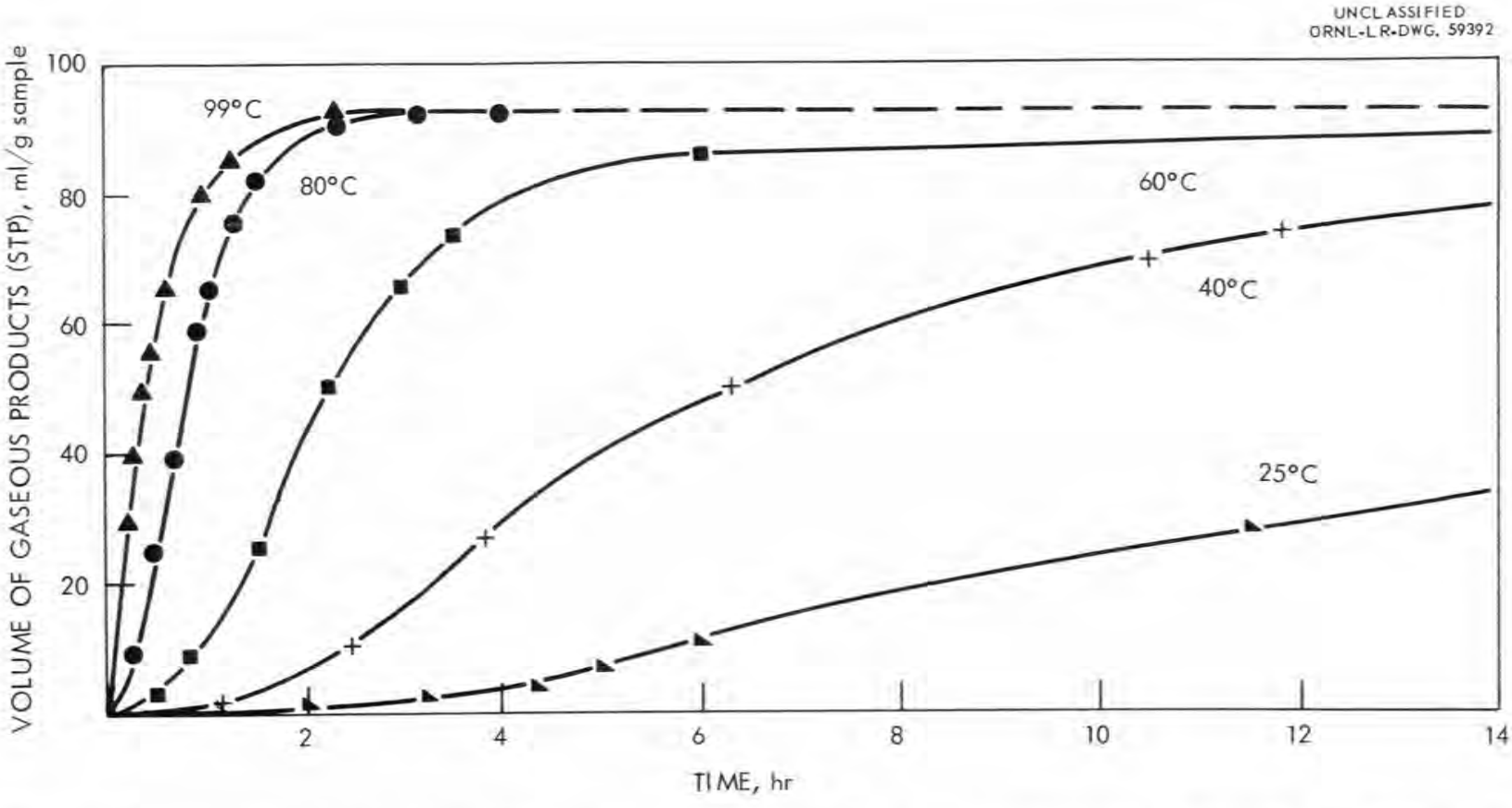

Fig. 1. Typical gas evolution in the hydrolysis of massive UC as a function of temperature. Sample size, 3.1-4.3 g.

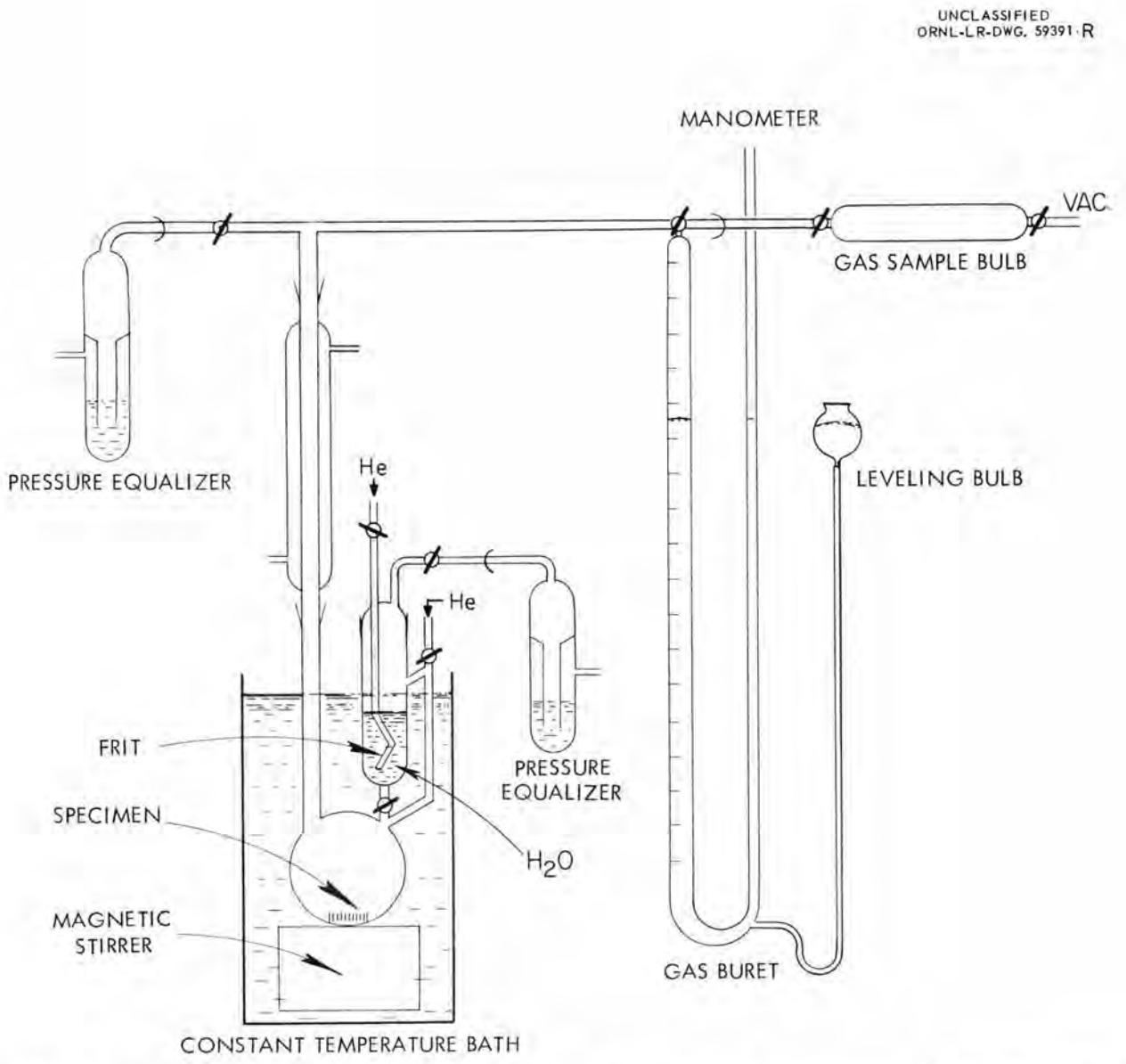

Fig. 2. Apparatus for measuring the volume of gas evolved in the reactions of uranium carbides.

The reaction was initiated by adding water to the carbide. The instantaneous gas expansion caused by the water vapor was usually exhausted to the atmosphere through the pressure equalizer before noticeable carbide reaction occurred. The system was then rapidly isolated from the pressure equalizer, and connected to the mercury filled gas buret. (The instantaneous water vapor expansion at 80°C was collected in the gas buret along with the products, and a correction applied by determining a blank without carbide.) The system was maintained at atmospheric pressure by adjusting the leveling bulb so that the mercury levels in the gas buret and open-end manometer were equal. Gas was transferred from the gas buret to the evacuated sample bulb by raising the leveling bulb. The water bath contained a small amount of glycerol and was covered with a Lucite lid fitted around the apparatus to reduce the rate of evaporation from the bath. When necessary water was added to the bath to hold it at a constant level.

The experimental volume of gas expansion was converted to 0°C and 760 mm pressure assuming that the gases were ideal and corrected for the amount of water vapor present based on the vapor pressure of pure water at the temperature of the gas buret. Two gas samples were taken; one contained the gas evolved from the system and the other the final composition of the gas in the reactor. The weighted averaged composition of the gaseous products could then be calculated knowing the volume of each sample and the analysis. Air contamination of the gas samples was generally less than 0.3% and frequently less than 0.1%.

The gas samples were analyzed by gas chromatography using a Burrell instrument modified with a Gow-Mac thermister detector.* The 5-A Molecular Sieve column was used for the determination of hydrogen, oxygen, nitrogen, methane, and ethane, and a Dow Corning 550 silicon oil (25 wt %) on Celite (75 wt %) column for the higher hydrocarbons. Helium was the carrier gas, and peak areas were determined by the integrator on the Burrell instrument.

The principal reaction between uranium monocarbide and water in the temperature range of 40 to 99°C was:

$$UC + (2 + x)\ H_2O \longrightarrow UO_2 \cdot x\ H_2O + CH_4$$

where the extent of hydration of the UO_2 (or $U(OH)_4$) was unknown.

The formation of hydrogen and hydrocarbons above methane cannot be explained at present, since the sample purity is not completely defined. The U to C ratio, and impurities other than U and C can be determined by chemical analysis. This is insufficient to define the system, since at any given U- to C ratio the sample may contain a mixture of uranium metal, UC, U_2C_3, and UC_2. Theoretically it should be possible to detect impurities by x-ray when 5% of a compound is present. Actually, x-ray analyses of a sample whose mode of preparation and chemical analysis indicated it to be about 20% U metal - 80% UC failed to detect any uranium. Only a faint UC_2 line was detected in a specimen with a C-to-U ratio of 1.3 (30% UC_2-70% UC or 60% U_2C_3-40% UC or mixture). Metallographic examination also has its limitations, in that only insoluble impurities are detected, and only

*A. D. Horton, Analytical Chemistry Division.

one surface can be examined at a time. Uranium metal or any of the three carbides when reacted with water to yield a tetravalent uranium oxide would all yield 4 hydrogen atoms per uranium atom (experimental 4.01). The deficiency of carbon in the products (1.00 U to 0.97 C) and the high H-to-C mole ratio (4.14 vs a theoretical 4.00 for UC) which have been obtained consistantly indicate that the original specimen must have contained at least 3.4% uranium metal, and that at least part of the hydrogen in the off-gas is probably the result of reaction:

$$U + (2 + x)\ H_2O \longrightarrow UO_2 \cdot xH_2O + 2H_2$$

rather than a product of the UC reaction. The hydrocarbons above methane might result from the polymerization of free radicals produced during the UC hydrolysis, or they might be reaction products of U_2C_3 or UC_2 (or a combination of these possibilities). Studies with the 20% U specimen should test the hypothesis that metal impurities yield free hydrogen. Experiments with near stoichiometric specimens of U_2C_3 and UC_2 are needed both to understand the behavior of reactor fuels containing these compounds, and to establish the purity of the monocarbide. While the monocarbide specimens used in these studies may not have been completely pure, they were as close to stoichiometric as any described at the recent AEC carbide meeting (7).

1.3 Beryllium and Beryllium-Oxide (K. S. Warren)

High Beryllia Content Fuels

The initial dissolution rates of high-fired beryllia and BeO-5% UO_2 were measured in boiling sulfuric acid, sulfuric acid--0.2 M NaF, ammonium fluoride, NH_4F--HF, HNO_3-H_2SO_4, and HNO_3-HCl solutions. The highest dissolution rates, 2 to 4 mg $min^{-1}cm^{-2}$, were obtained with boiling 16 M H_2SO_4 and 5 to 8 M NH_4F containing 15 to 20 M HF.

Beryllia and BeO-5% UO_2 dissolved at about the same rates in boiling sulfuric acid solutions, the initial rates increasing from about 0.01 to about 3.5 mg $min^{-1}cm^{-2}$ as the acid concentration increased from 4 to 16 M (Figs. 3 and 4). Approximate initial rates can be calculated from the equation

$$\log_{10}(\text{Rate, mg min}^{-1}\text{cm}^{-2}) = 0.223(H_2SO_4, \text{M}) - 2.81$$

in which the constants for the individual curves were averaged. Dissolution rates of BeO-5% UO_2 were increased slightly by the addition of 0.2 M NaF to 4 to 14 M H_2SO_4 (Fig. 4). The BeO-5% UO_2 rates in H_2SO_4--0.2 M NaF solutions may be calculated from the relationship:

$$\log_{10}(\text{Rate, mg min}^{-1}\text{cm}^{-2}) = 0.168(H_2SO_4, \text{M}) - 2.043.$$

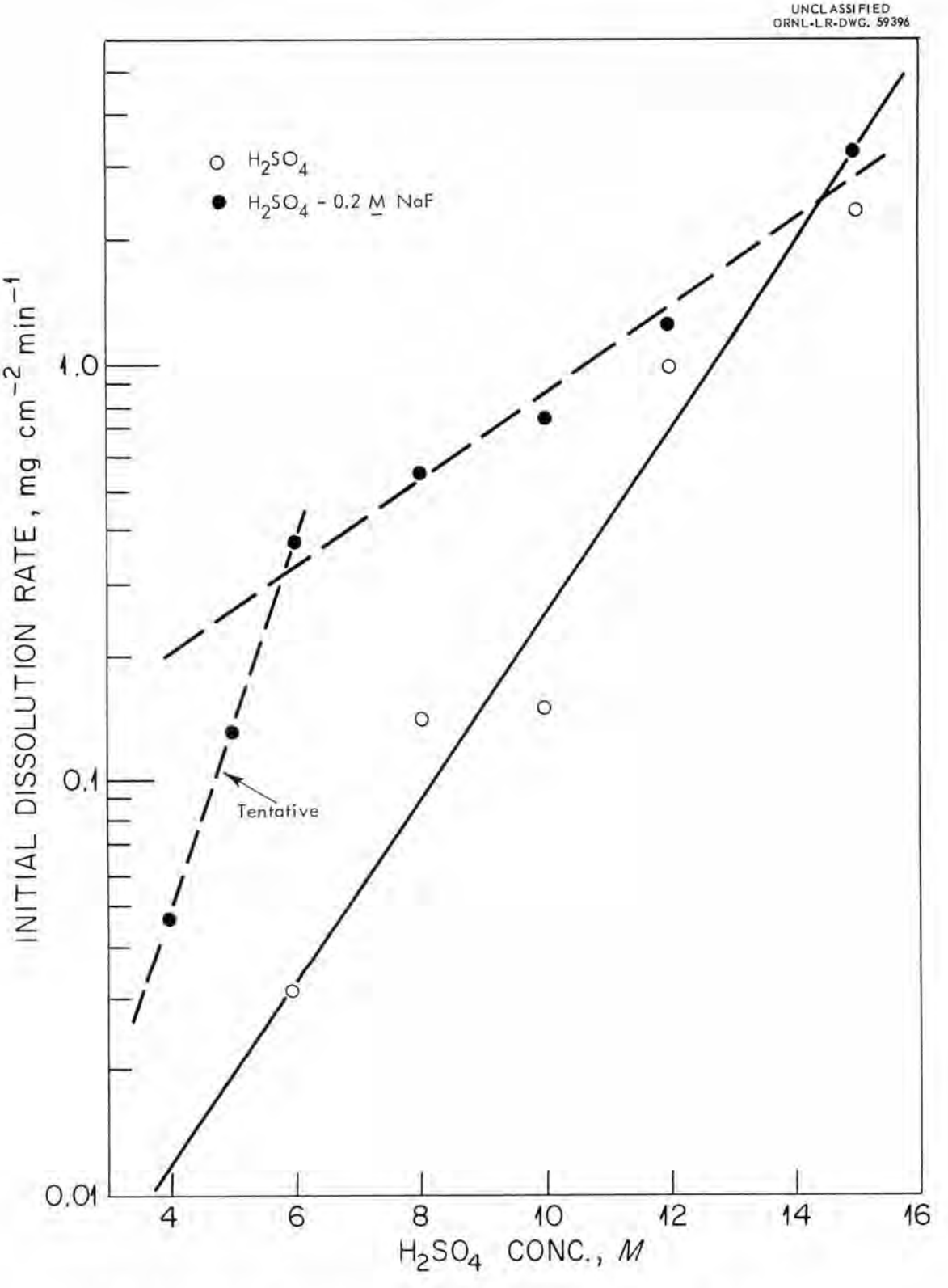

Fig. 3. Initial dissolution rates of BeO in boiling H_2SO_4 solutions.

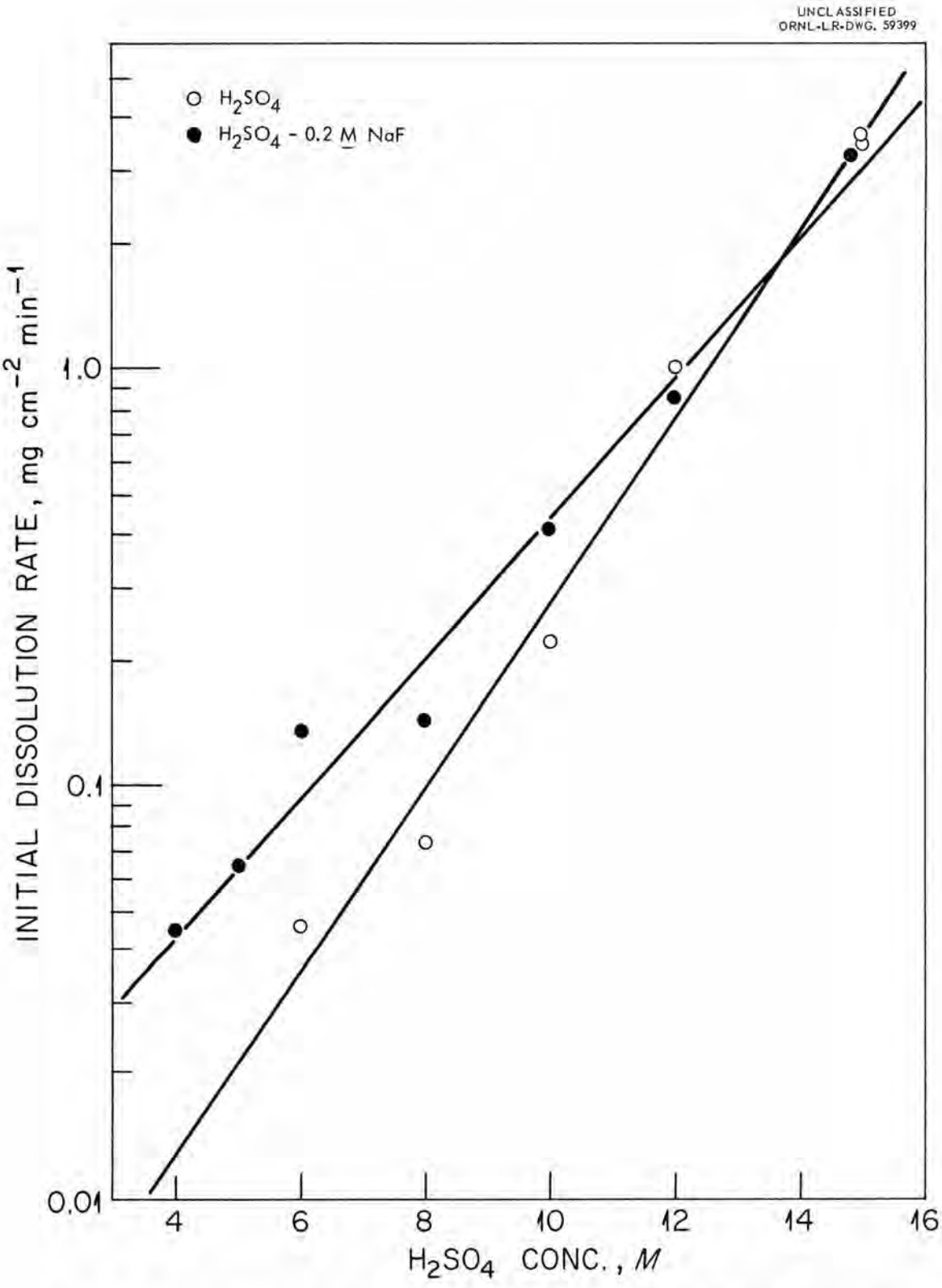

Fig. 4. Initial dissolution rates of BeO-5% UO_2 in boiling H_2SO_4 solutions.

The behavior of pure BeO in H_2SO_4--0.2 M NaF solutions was somewhat different. Two linear regions, intersecting at about 6 M H_2SO_4, were obtained when the data were plotted on semi-log paper (Fig. 3). This curve is "tentative" until verification.

Dissolution of BeO-5% UO_2 in boiling NH_4F--HF solutions was also studied. Initial dissolution rates in NH_4F solutions (up to 8 M) were 0.07 mg $min^{-1}cm^{-2}$ or less. In solutions containing HF, the rate increased with increasing HF concentration; e.g., in 5 M NH_4F--HF solutions the rate increased from about 0.07 to 3.5 mg $min^{-1}cm^{-2}$ as the HF concentration increased from 0 to 20 M (Fig. 5). In solutions of constant HF concentration, the rate increased with increasing NH_4F concentration up to about 8 M. In 5 to 10 M HF, the effect of NH_4F concentration on the rate was not nearly so marked as in solutions of higher HF concentration.

Dissolution rates in KF-HF solutions were lower than those in corresponding NH_4F-HF solutions. In 3.2 M KF the initial rate was 0.0061 mg $min^{-1}cm^{-2}$, and in 3.2 M KF-5 M HF it was 0.36 mg $min^{-1}cm^{-2}$, about one-fourth the corresponding values obtained with NH_4F.

One test was carried out with boiling 3 M HNO_3-0.5 M HBF_4-0.3 M $(NH_4)_2Cr_2O_7$, a solution which is being tested as a dissolvent for zirconium in titanium vessels. Beryllium oxide-5% UO_2 dissolved in this mixture at a rate of only 0.03 mg $min^{-1}cm^{-2}$. In 0.5 M HBF_4, the rate was 0.026 mg $min^{-1}cm^{-2}$, essentially the same as that obtained in the test solution.

Boiling 8 to 16 M HNO_3 was ineffective in dissolving BeO and BeO-5% UO_2. Rates ranged from 0.0054 to 0.016 mg $min^{-1}cm^{-2}$ (Table 4). Admixtures of sulfuric acid or hydrochloric acid with nitric acid did not appreciably enhance the rates, the highest being about 0.05 mg $min^{-1}cm^{-2}$ in 8.6 M HNO_3-4.3 M H_2SO_4. Mixtures such as these do not offer promise as dissolvents for high-fired beryllia-based fuels.

Scouting tests of beryllia dissolution were made in selected reagents. These included a number of oxy-acids, fluorine-containing materials, and two organic compounds (Table 5). None dissolved high-fired BeO rapidly enough to warrant further interest.

Low Beryllia Content Fuels

Studies were continued on the effect of additives such as sulfate ion, fluoride ion, and chloride ion on the dissolution of GCRE fuel pellets (70% UO_2-30% BeO) in boiling nitric acid solutions. In 6 to 8 M HNO_3, the presence of up to 2 M H_2SO_4 had no effect on the rate of leaching of the UO_2. In all cases, uranium was leached completely from the BeO matrix in 5 to 7 hr (Fig. 6). Complete dissolution of the pellets was achieved in about 24 hr. Although the initial rate of dissolution of the BeO matrix was higher in solutions containing sulfuric acid, the time required for total dissolution was not greatly affected (Fig. 6). The final solutions contained about 3.0 g of uranium per liter.

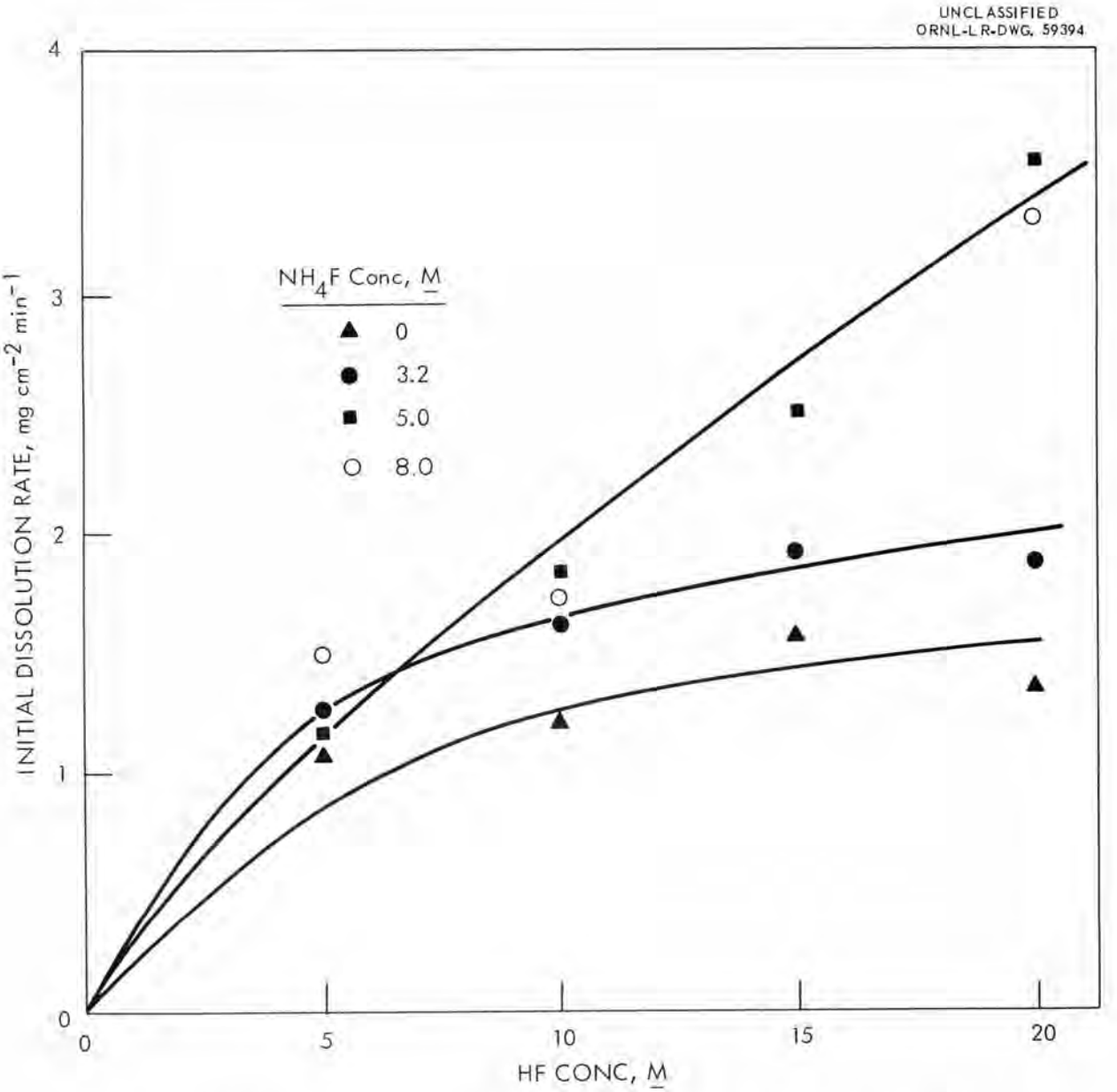

Fig. 5. Initial dissolution rates of BeO-5% UO_2 in boiling NH_4F-HF mixtures.

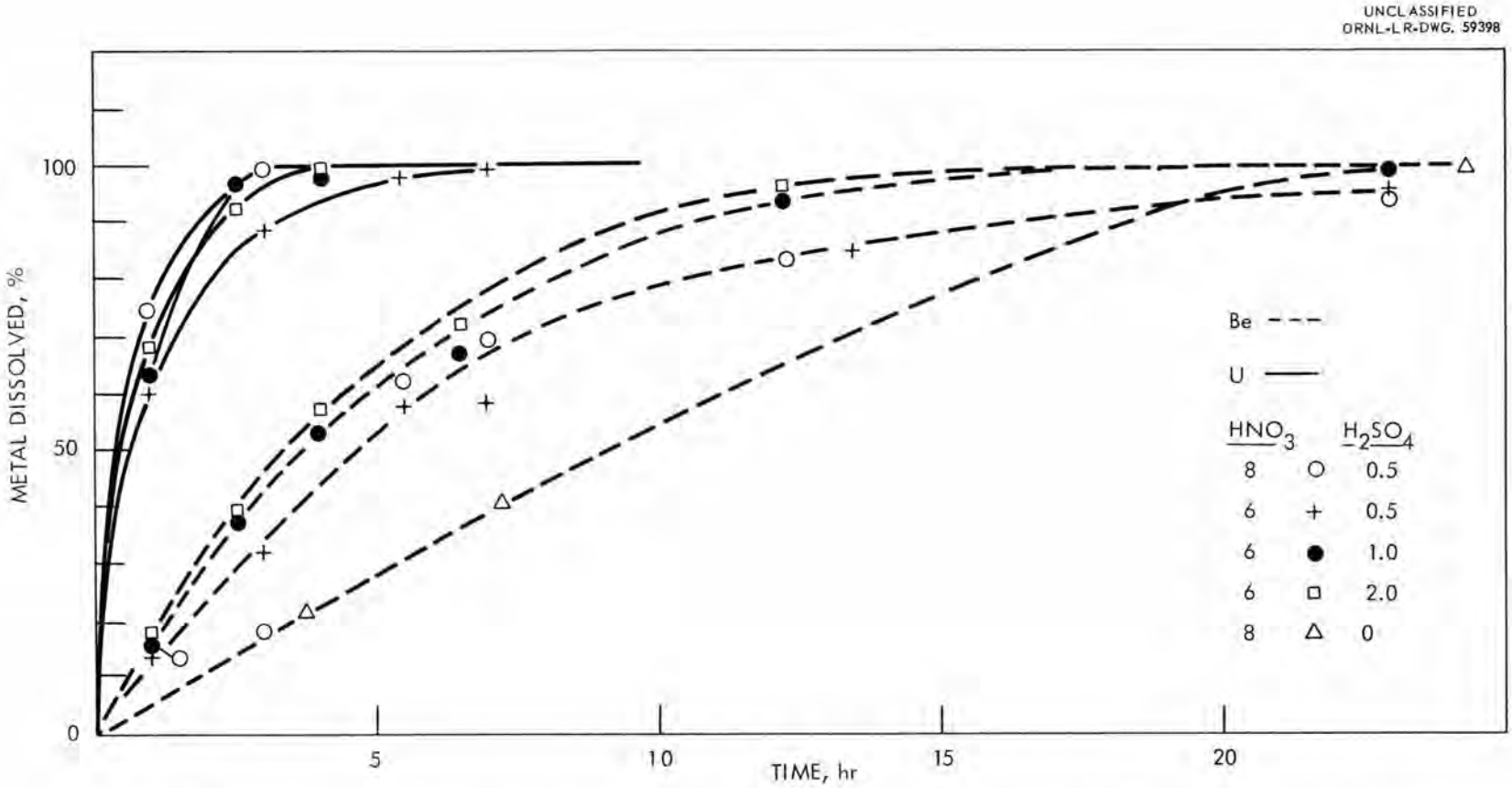

Fig. 6. Dissolution of GCRE fuel pellets (70% UO_2--30% BeO) in boiling HNO_3-H_2SO_4 solutions.

Table 4. Initial Dissolution Rates of BeO and BeO-5% UO_2 in Boiling Nitric Acid, HNO_3-H_2SO_4, and HNO_3-HCl Solutions

Acid Conc., M			Initial Dissolution Rate, mg $min^{-1}cm^{-2}$	
HNO_3	H_2SO_4	HCl	BeO	BeO-5% UO_2
8.0	0	0	0.0054	0.014
12.0	0	0	0.011	0.016
15.7	0	0	0.010	0.016
5.0	5.0	0	0.026	0.036
8.63	4.32	0	0.033	0.048
8.61	8.61	0	0.011	0.026
8.0	0	1.0	0.011	0.012
4.0	0	2.0	0.007	0.016
2.0	0	4.0	0.003	0.013
2.0		6.0	0.003	0.023

Table 5. Initial Dissolution Rate of High-fired BeO in Various Boiling Solutions

Solution	Rate, mg $min^{-1}cm^{-2}$
Fluosilicic acid, 30%	0.70
Ammonium Silicofluoride	0.0086
Phosphoric acid, 7.37 M	0.093
Phosphoric acid, 7.37 M-0.25 M NaF	0.18
Trichloracetic acid, 2.5 M	0.0024
Hypophosphorus acid, 31%	0.0094
Sulfuric acid, 30%, fuming	0.007
Dimethyl sulfoxide, 100%	0.000
Resorcinol, 100%	0.003

Similar results were obtained in 2 M HNO_3 solutions containing 2 to 6 M HCl. Uranium was completely leached in 5 to 7 hr with total dissolution of the pellets requiring at least 30 hr (Fig. 7). Traces of undissolved BeO remained after a 30-hr dissolution period. The rate at which the BeO matrix dissolved was not affected by the three-fold increase in HCL concentration (Fig. 7).

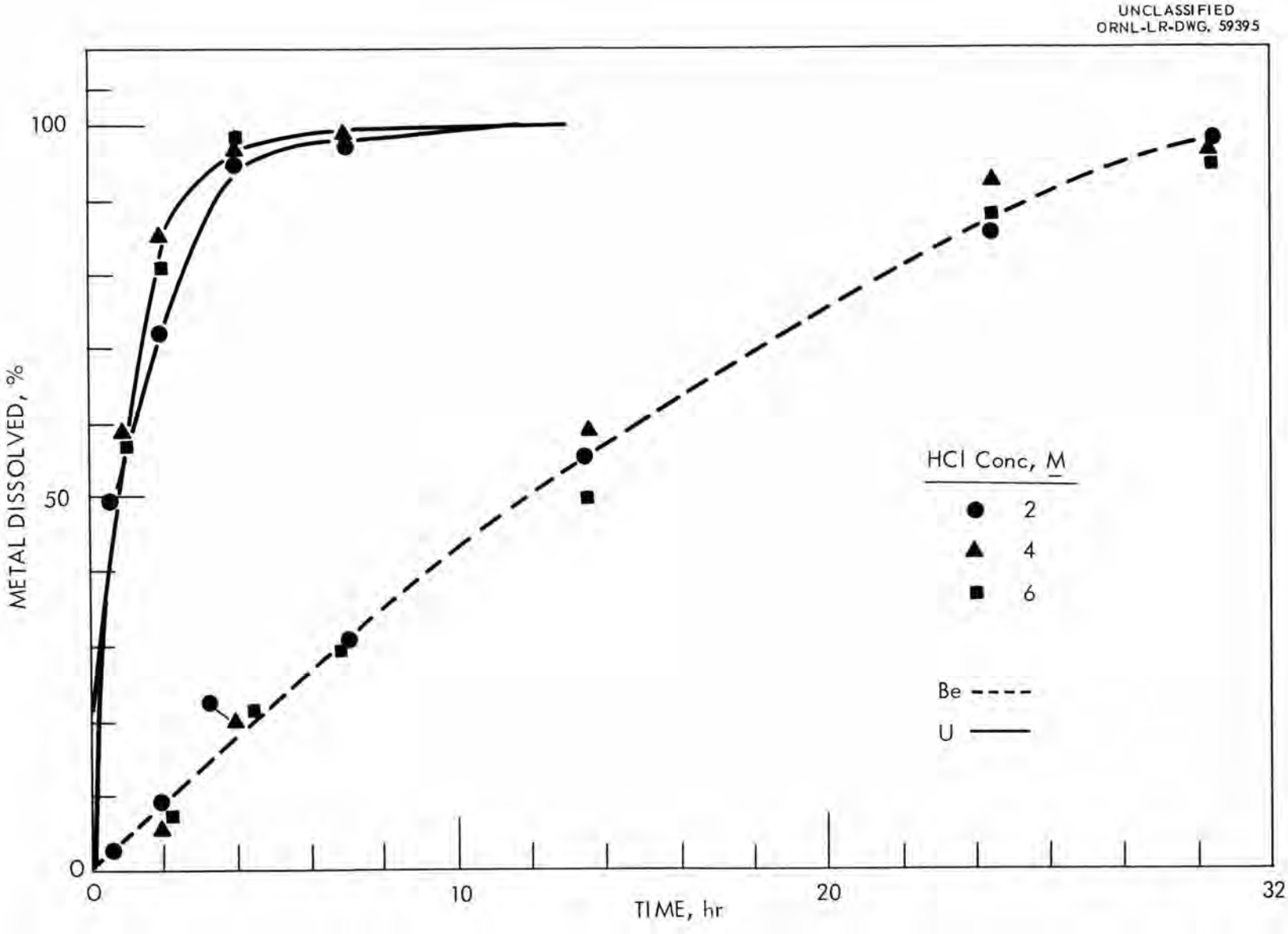

Fig. 7. Dissolution of GCRE fuel pellets (70% UO_2--30% BeO) in boiling HNO_3-HCl mixtures. HNO_3 concentration in each case was 2 M.

The effect of addition of NaF on GCRE pellet dissolution in nitric acid was also briefly investigated. At the end of 47 hr of reflux in 8 M HNO_3-0.1 M NaF, 85% of the BeO had dissolved although chemical analyses showed that the uranium had been completely dissolved during the first 6 to 8 hr of leaching (Fig. 8). No explanation is offered for the fact that the amount of beryllium dissolved reached its maximum value in 9 to 10 hr although ample nitric acid remained for complete dissolution. Similar results have recently been obtained in solutions containing 0.05 and 0.2 M NaF.

1.4 Volatilization of Chloride with Hydrogen Peroxide (T. A. Gens)

Several processes which yield chloride-containing uranium solutions from spent reactor fuels are being investigated, including the Darex (8) process (dissolution of iron alloys in aqua regia), the Zircex (9) process (high temperature hydrochlorination of zirconium alloys), and a oxyhydrochlorination (10) process for uranium-molybdenum alloys. Removal of chloride from these solutions is needed so that uranium may be recovered by solvent extraction and the wastes may be stored in conventional plant materials, such as stainless steel. Chloride removal by volatilization from concentrated nitric acid solution has been intensively investigated in the Darex process. Hydrogen peroxide addition is being investigated as an alternative method of volatilizing chloride.

One ml aliquots of 10 M H_2O_2 were repeatedly added to ten ml samples of 1.33 M $ZrOCl_2$- 8 M HCl at 75 and 99°C to evolve chlorine. This zirconyl chloride solution, which solidifies upon cooling to about 60°C, was prepared by diluting simulated Zircex waste, 2 M $ZrOCl_2$-12 M HCl, which solidifies at 85°C. Analysis of the product solutions after various numbers of peroxide additions showed that chloride was evolved according to the reaction

$$2\ HCl + H_2O_2 \longrightarrow Cl_{2(g)} + 2H_2O,$$

until the total chloride concentration was reduced to about 1 M (Fig. 9). Formation of a gelatinous solid, probably zirconium peroxide, prevented further chloride removal. Addition of a small amount of nitric acid prevented the solids formation and appeared to permit chloride removal to below 1 M Cl^-. The product was stable at room temperature. The reduction of chloride concentration to <1 M should result in a smaller volume of neutralized, radioactive zirconium waste solution.

The results of the above work disagree with the reported result (11) that addition of sodium and hydrogen peroxides did not reduce the chloride ion concentration in HNO_3-HCl-H_2O solutions. Dissolved metal may have caused the unfavorable result, although the presence of dissolved metal was not reported.

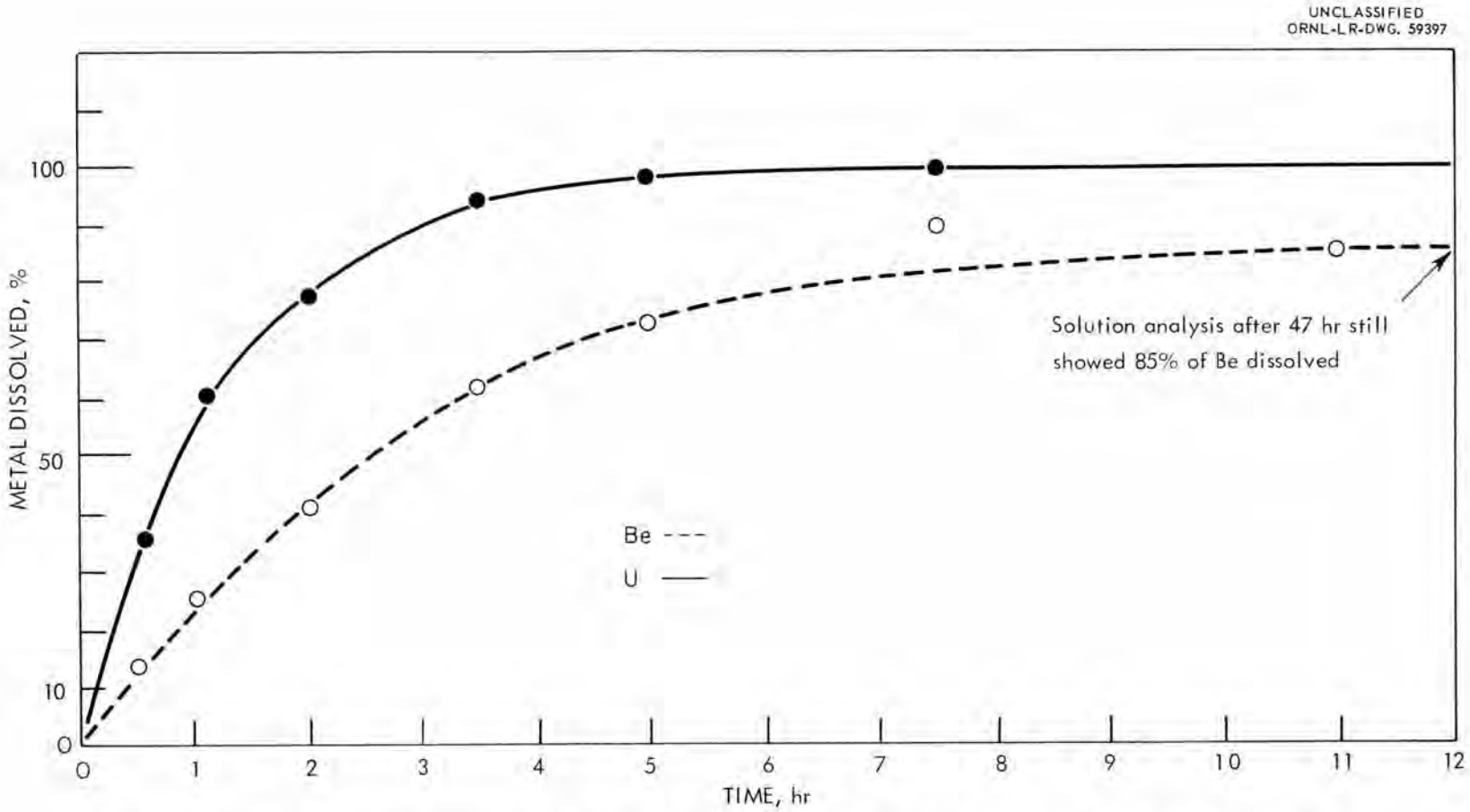

Fig. 8. Dissolution of GCRE fuel pellet (70% UO_2--30% BeO) in boiling 8 M HNO_3--0.1 M NaF.

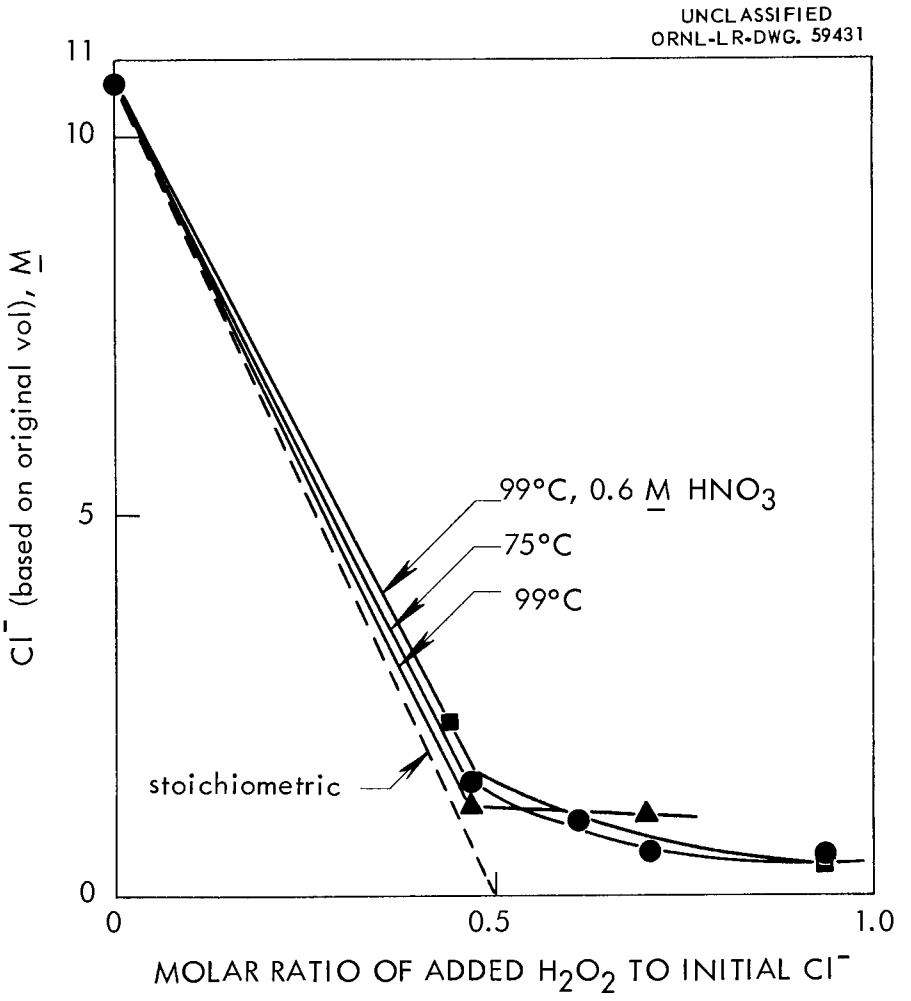

Fig. 9. Removal of chloride from Zircex waste (1.33 M $ZrOCl_2$-8 M HCl) by the reaction $2HCl + H_2O_2 \longrightarrow Cl_{2(g)} + 2H_2O$. Time, 0.2-1 hr.

2.0 SOLVENT EXTRACTION STUDIES
(R. H. Rainey)

2.1 Acid Thorex Process (R. H. Rainey)

Comparison of Amsco, Solvesso-100, and Sec-Butyl Benzene as Diluent for TBP in Acid Thorex Process

A series of countercurrent batch extraction experiments comparing Solvesso-100, sec-butyl benzene, and Amsco as diluents for the TBP in the Acid Thorex process (12) showed that TBP in sec-butyl benzene gave decontamination factors about 5 times larger than TBP in the other two diluents. These results are in agreement with the distribution coefficient data reported by Gresky et al (13). However, when the solvent were degraded the decontamination was twice as large with Amsco as with the other diluents. Treatment of the degraded solvents with carbonate did not effectively improve the decontamination (Table 6). When fresh solvent was used in the experiments the gross gamma decontamination factors using Amsco, Solvesso-100 and sec-butyl benzene were 7,500, 11,000, and 48,000, respectively. A sample of each of the solvents was then degraded by refluxing for 1 hr with 6 M HNO_3 and washing with water to remove the free acid. Corresponding decontamination factors using the degraded solvent were 7,000, 2,600, and 2,200, respectively. A portion of each of the degraded solvents was then washed 3 times with 1/5 volume of 5% Na_2CO_3 to remove degradation products. The countercurrent batch extraction now resulted in corresponding decontamination factors of 6,700, 2,700, and 3,300. The minimum, mean, and maximum decontamination values reported in Table 6 reflect the counting accuracy in the radiochemical analysis.

At the end of the series an additional experiment was made using undegraded Amsco as the diluent. A decontamination factor of 12,000 was obtained which showed that the lower decontamination factors were not the result of aging of the solutions during the experimentation period.

The average thorium loss with Amsco, Solvesso and sec-butyl benzene was 0.7, 2.1 and 1.2, respectively. These losses correspond to the thorium distribution coefficients which were observed at the feed stage in the experiments (Table 7).

Recycle of Darex Declad Solution to Acid Thorex Solvent Extraction Flowsheet

The solution obtained in decladding stainless steel jacketed thorium reactor fuel with the Darex process (14) may be used as the salting agent in the extraction section of the Acid Thorex Process (Fig. 10). Laboratory experiments using this process resulted in decontamination factors of 560, 9,000, and 2.5×10^5 from ruthenium, zirconium-niobium, and rare earths, respectively. Uranium and thorium losses were $<0.001\%$ and 0.4%. Although these decontamination factors are less than those resulting from the

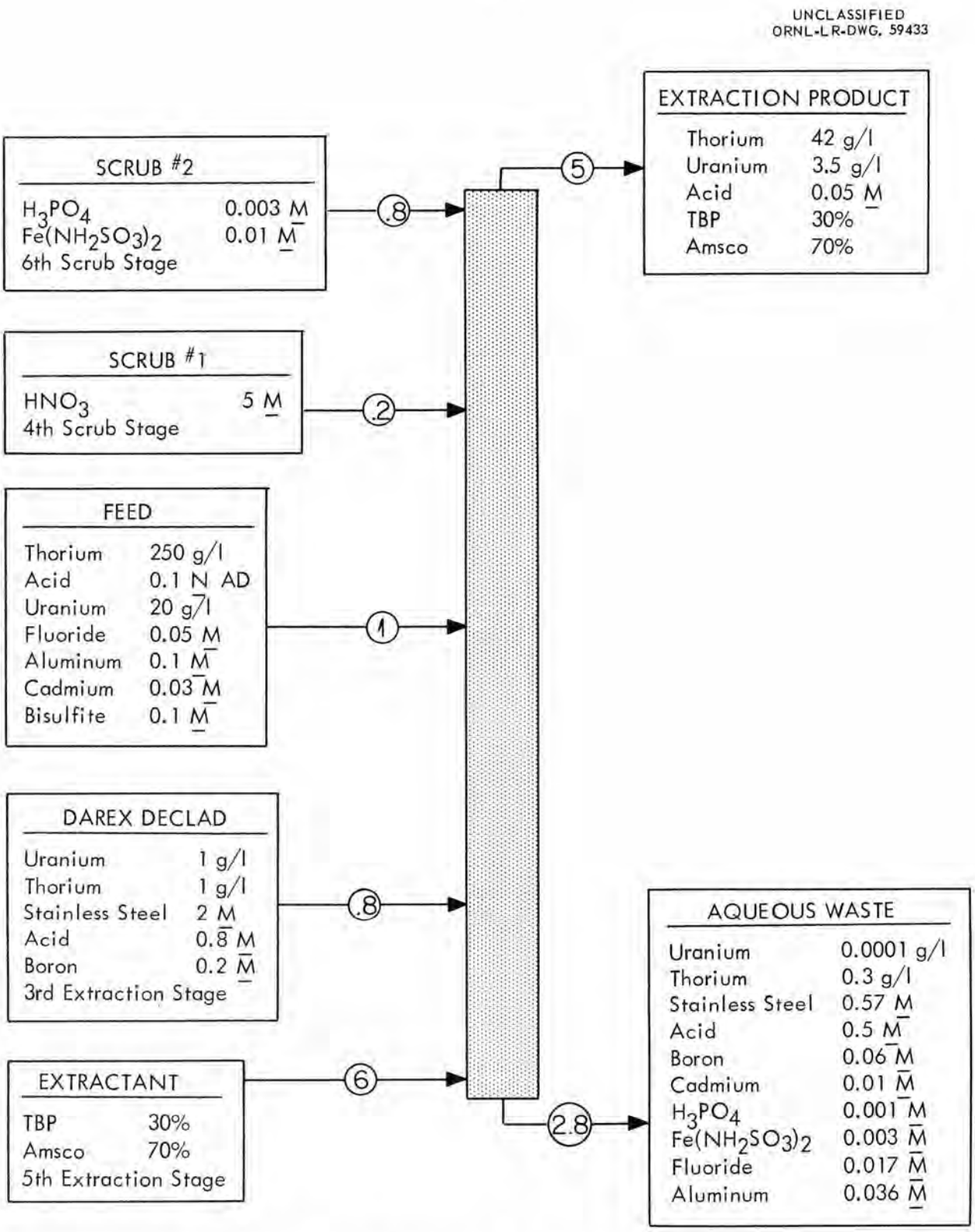

Fig. 10. Thorex flowsheet for Darex declad process.

Table 6. Comparison of Decontamination with Acid Thorex Flowsheet Using Varying Diluents for TBP

Solvent			Decontamination Factor				Thorium Loss, %
			Gr γ	Ru	Zr-Nb	TRE	
Amsco		min		18,500	5,120		0.55
	Fresh	mean	7,550	26,100	5,850	>54,000	
		max		44,000	6,820		
		min			5,240		0.8
	Degraded	mean	6,970	>5,120	5,720	89,400	
		max			6,360		
		min		2,330	2,280		0.64
	Recovered	mean	6,730	3,170	2,520	>136,000	
		max		5,010	2,800		
		min		7,650	8,590	68,200	0.80
	Fresh	mean	12,200	13,000	11,200	97,400	
		max		43,400	16,000	182,000	
Solvesso-100		min			7,320	62,500	1.28
	Fresh	mean	10,800	>8,320	9,460	87,200	
		max			13,300	145,000	
		min			15,920		3.4
	Degraded	mean	2,580	>5,990	17,460	109,000	
		max			19,300		
		min			1,430	132.000	1.7
	Recovered	mean	2,710	>12,600	1,690	205,000	
		max			2.070	434,000	
Sec-butyl Benzene		min		10,200	15,400		1.20
	Fresh	mean	48,000	12,200	21,200	>127,000	
		max		15,200	33,700		
		min		3,380	1,240	94,500	1.3
	Degraded	mean	2,170	6,290	1,360	147,000	
		max		41,900	1,650	335,000	
		min		4,930	2,030	64,600	1.2
	Recovered	mean	3,330	8,210	2,210	117,000	
		max		24,600	2,430	641,000	

Table 7. Feed Stage and Organic Product Conditions Using Various Diluents

Solvent		Feed Plate Conditions: Thorium Aq (g/l)	Thorium Org (g/l)	Thorium DC_a^o	Acid Aq (N)	Acid Org (N)	Acid DC_a^o	Organic Product: Th g/l	Organic Product: H^+ N
Amsco	Fresh	105	48.7	0.464	1.09	0.06	0.055	36.4	0.13
	Degraded	109	49.9	0.457	1.04	0.14	0.134	36.4	0.07
	Recovered	107	49	0.457	1.07	0.13	0.122	37	0.07
	Fresh	115	50	0.435	1.00	0.06	0.060	37	0.12
Solvesso-100	Fresh	114	49.1	0.431	1.05	0.16	0.154	35.5	0.09
	Degraded	140	51	0.364	1.41	0.18	0.128	34	0.14
	Recovered	116	49.5	0.427	0.99	0.15	0.152	35.8	0.09
Sec-butyl Benzene	Fresh	126	50.1	0.398	0.84	0.10	0.116	34.7	0.07
	Degraded	132	51.2	0.388	0.91	0.11	0.121	35.7	0.06
	Recovered	123	49.0	0.398	0.93	0.11	0.118	35.0	0.06

standard Acid Thorex process using nitric acid as the salting agent (12) they are much higher than those resulting from the extraction of uranium and thorium from fuel elements which had been totally dissolved in the Darex solution (15).

The Darex declad process consists of dissolving the stainless steel in dilute aqua regia followed by the dissolution of the thoria in nitric acid catalyzed by fluoride. Early data using unirradiated fuel pins indicated that the uranium loss to the declad solution would be less than 0.1%. Therefore after removal of the chloride to decrease corrosion, the solutions could be sent to waste storage. Additional data however, have indicated that the uranium and thorium loss increases with irradiation level. At high irradiation levels the uranium loss has been as much as 1 g/liter (16) and therefore must be recovered. Direct extraction of the uranium with TBP results in very low decontamination and would require additional facilities. An alternate recovery method previously investigated was the total dissolution of the fuel element by addition of fluoride catalyst to the aqua regia followed by extraction of the uranium and thorium with TBP. Total dissolution was demonstrated (17) but the highly salted acidic feed resulted in decontamination factors of only 20 and 500 from ruthenium, and zirconium-niobium compared with 1,000 and 5,000 when an acid deficient feed was processed with the Acid Thorex process. The total dissolution feed cannot be made acid deficient without precipitating the iron. In the present process the core solution is made acid deficient for a feed and the declad solution is substituted for the acid in the extraction section. Synthetic solutions containing tracer from the dissolution of thoria pellets were used in these solvent extraction experiments.

2.2 Extraction of Uranium from Zirconium Fuel Solution (R. H. Rainey and J. G. Moore)

Laboratory countercurrent batch extraction experiments have demonstrated no variation in fission product decontamination when using zirconium fuel solutions prepared by the Modified Zirflex instead of the Idaho hydrofluoric acid dissolution method. Modifications in the solvent extraction flowsheet resulted in at least a factor of 20 improvement in decontamination and may improve column operation as well.

The use of the Modified Zirflex rather than the hydrofluoric acid method for dissolving zirconium fuel results in a solvent extraction feed which contains ammonium ion and possibly more uranium (Table 8). As expected this small difference in feed composition did not make a detectable difference in the fission product decontamination factor (Table 9).

Table 8. Composition of Solvent Extraction Feed from Hydrofluoric Acid and Modified Zirflex Dissolution of Zirconium Fuel

		HF Dissolution	Modified Zirflex Dissolution
U	g/l	~1.2	3.3
Zr	M	0.5	0.44
F^-	M	3.3	3.3
H^+	N	~1.0	0.78
Al	M	0.78	0.78
NH_4	M	-	~1

Table 9. Comparison of Hydrofluoric Acid and Modified Zirflex Dissolved Zirconium Fuel in the ICPP Solvent Extraction Flowsheet

Flowsheet: Extraction Column
Feed - see Table 8
Extractant - 10% TBP in Amsco, 1 vol
Stages 7
Scrub Column
Feed - 1/2 g/l U, 10% TBP in Amsco, 1 vol
Scrub - 0.7 M $Al(NO_3)_3$, 0.5 vol
Extractant - 10% TBP in Amsco, 0.2 volume
Stages - 4 scrub, 4 extraction

Fuel Dissolution	Decontamination Factor: Extraction Column Only Gr γ	Ru	Zr-Nb	RE	Extraction-Scrub Gr γ	Ru	Zr-Nb	RE	Uranium Loss
HF	-	-	-	-	1300	72	940	$<3\times10^6$	.008
HF	250	21	850	370	330	24	2,100	2×10^5	.008
Modified Zirflex	270	18	1200	580	420	28	2,800	6×10^5	.008
Modified Zirflex	210	15	850	390	350	22	2,000	7×10^5	.008

Modification in flowsheet conditions, however, make large differences in the decontamination. The Idaho flowsheet (18) uses an extraction column and a separate scrub column containing a re-extraction section. Stream compositions are as follows:

Extraction column conditions:
Feed: 1.2 g/l U, 0.5 M Zr, 3.3 M F^-, 0.78 M Al, 1 vol
Extractant: 10% TBP in Amsco, 1 vol
Stages: 7

Scrub column conditions:
Feed: 1.2 g/l U, 10% TBP in Amsco, 1 vol
Scrub: 0.7 M $Al(NO_3)_3$, 0.5 vol
Extractant: 10% TBP in Amsco, 0.2 vol
Stages: 4 scrub, 4 extraction

This flowsheet results in two waste streams; a high activity zirconium fluoride waste, and low activity aluminum waste. Using these flowsheet conditions decontamination factors from ruthenium varied from 22 to 72 and from zirconium-niobium from 1,000 to 2,800. When the volume of the feed was doubled the corresponding decontamination factors were 130 and 11,000. The use of 4 N HNO_3 instead of 0.7 M $Al(NO_3)_3$ in the scrub gave decontamination factors of 240 and 39,000. The uranium loss in all experiments were $<0.008\%$ in the extraction column, and $<0.004\%$ in the scrub column (Table 10). The use of 5% TBP instead of 10% TBP and 4 M HNO_3 instead of 0.7 M $Al(NO_3)_3$ in the scrub, increased the decontamination factors to 3,800 and 1.6×10^5. The uranium loss in the scrub column was 0.15%.

However, there seems to be no advantage in having an extraction section in this column since the aqueous from the scrub column could be added to the extraction column feed where the uranium would be extracted.

The use of flowsheet conditions of the compound extraction scrub type with 5% TBP and an acid scrub resulted in ruthenium and zirconium niobium decontamination factors of 2,600 and greater than 2×10^5, respectively. Uranium loss in duplicate experiments were 0.015% and 0.004%. Flowsheet conditions were as follows:

Feed: 3.3 g/l U, 40 g/l Zr, 1 M NH_4^+, 0.78 M Al, 0.78 M H^+, 62 g/l F, 1 vol
Scrub: 1 M HNO_3, 0.2 vol
Solvent: 5% TBP in Amsco, 1 vol
Stages: 7 extraction, 6 scrub

Comparison of physical measurements for the various flowsheet conditions are given in Table 11.

Table 10. Modified Solvent Extraction Processes for the Recovery of Uranium from Zirconium Fuel

	Decontamination Factor								U Loss
	Extraction Only				Extraction-Scrub				
	Gr γ	Ru	Zr-Nb	RE	Gr γ	Ru	Zr-Nb	RE	%
Average of ICPP[a]	240	18	970	450	600	37	1,900	1×10^6	<0.008
Modification									
No. 1	740	58	2800	1300	1,800	130	11,000	4.8×10^5	<0.008
No. 2	190	10	81	270	4,800	240	39,000	$>2.1 \times 10^6$	<0.008
No. 3	2600	160	10,000	4200	59,000	3800	1.6×10^5	3.1×10^4	0.12
Compound	7000[b]	-	-	-	41,000	2700	2×10^5	1×10^7	0.015
Extraction-Scrub	4500[b]	-	-	-	37,000	2600	1×10^6	2×10^7	0.004

Modification No. 1 - 2 vol of feed
No. 2 - 4 N HNO_3 scrub without aluminum
No. 3 - 5% TBP in Amsco, 4 M HNO_3 scrub without aluminum

[a] Table 9.

[b] At feed plate.

Table 11. Physical Measurements for Zirconium-Solvent Extraction Flowsheet

	Density at 23°C	Viscosity Centipoise	Interfacial Tension dynes/cm	
			5% TBP	10% TBP
Feed only	1.2186	1.450	18.68	16.87
Feed + 0.2 Vol 4 N H^+ Scrub	1.1915	1.310	18.58	16.02
5% TBP in Amsco	0.7774	1.134	-	-
10% TBP in Amsco	0.7983	1.122	-	-

2.3 Extraction of Niobium-95 with Tributyl Phosphate (J. G. Moore)

Extraction of Niobium-95 from 2 M HNO_3

The distribution coefficient of niobium-95 between freshly purified 30% TBP in dodecane and an aqueous solution of niobium-95 in 2 M HNO_3 ranged from 0.003 to 0.01 for the aqueous to organic values and 0.2 to 1 for the organic or aqueous values. The coefficients were higher with organic solutions containing degraded TBP and/or degraded Amsco.

A series of experiments were made with 2 M HNO_3 solutions using the multiple contact technique previously used in the 4 M HNO_3 extraction tests (19). The distribution coefficients (Table 12) ranged from 0.003 to 34 depending on the organic used and whether the value was an organic to aqueous or aqueous to organic measurement. The maximum aqueous to organic coefficients were obtained in the tests using degraded TBP and/or Amsco. Organic solutions containing TBP and Amsco that had been degraded separately produced the highest coefficients. However, the organic to aqueous values were quite similar to the results obtained in tests using only degraded TBP. Much lower values were obtained using TBP and Amsco that had been degraded together. Similar results were obtained in the 4 M HNO_3 series (19).

Table 12. Extraction of Nb-95 from 2 N HNO_3 with Tributyl Phosphate

Organic	1	2	3	4	5[a]	6[b]
% Dodecane	70	70	63	63	63	63
% TBP	30	30	27	30	27	27
% Degraded TBP	-	-	3	-	3	3
% Amsco	-	-	7	-	-	-
% Degraded Amsco	-	-	-	7	7	7
	Distribution Coefficient DC_a^o					
0-4	0.0028	0.0027	0.12	0.014	0.20	0.11
0-3	0.0033	0.0040	0.14	0.014	0.24	0.12
0-2	0.0044	0.0041	0.15	0.015	0.27	0.14
0-1	0.0057	0.0066	0.16	0.018	0.31	0.17
Feed Point	0.011	0.010	0.43	0.021	0.61	0.31
A-1	0.26[c]	0.22[c]	2.37	0.23	1.95	0.55
A-2	0.92[d]	0.83[d]	11.9	0.80[d]	5.65	0.90
A-3	0.77[d]	0.85[d]	35.9	0.76[d]	16.0	0.87
A-4	1.10[d]	0.71[d]	34.4	0.79[d]	33.6	0.87[c]

Aqueous - 1.4×10^5 c/m/ml Nb-95; 2 M HNO_3
Degraded reagents were degraded by refluxing with 6 M HNO_3 for 6 hr.
The error in the material balance was $<\pm 10\%$ unless specified.

[a] TBP and Amsco degraded separately.

[b] TBP and Amsco degraded together as a 30% TBP in Amsco solution.

[c] Error in material balance of activity $>+10< + 20\%$.

[d] Error in material balance of activity $>+60\%$.

Extraction of Niobium-95 from 4 M HNO_3

The distribution coefficient of niobium-95 between an organic phase consisting of 63% dodecane, 27% freshly purified TBP, 3% degraded TBP, and 7% degraded Amsco and an aqueous solution of niobium-95 in 4 M HNO_3 was 0.8 with 20% of the niobium-95 in an unextractable form. The organic to aqueous value for the same system was 1.8 with ~0.7% of the niobium retained by the organic. A comparable aqueous to organic distribution coefficient with freshly purified 30% TBP in dodecane was ~0.01 with ~40% of the niobium unextractable. The degraded reagents were prepared by refluxing a 30% TBP-Amsco solution with 6 M HNO_3 for 6 hr. This solution was then diluted with 30% TBP in N-dodecane. The N-dodecane was used as the reference diluent since it may be obtained in reproducible quality whereas Amsco cannot.

The distribution coefficients and the amounts of unextractable or retainable niobium were determined using the Martin technique (20). The aqueous niobium solutions and organic solutions which had been pre-equilibrated with nitric acid solution containing no niobium were contacted using varying ratios of solvent volume to aqueous volume. After contact, the niobium-95 content was determined for both phases and plotted with the niobium-95 concentration in the organic phase as the ordinate and the niobium in aqueous phase as the abscissa. For solutions containing extractable species in equilibrium together with nonextractable species, a straight line is obtained which intercepts the abscissa. This intercept indicates the proportion of the unextractable species. A similar treatment was made of the organic to aqueous results. Organic solutions containing niobium-95 were contacted with nitric acid solutions containing no niobium. The phases were analyzed for niobium-95 and the values plotted as above. For organic solutions containing extractable species in equilibrium together with species that are not removable from the organic, a straight line is obtained which intercepts the ordinate. This intercept indicates the percentage of niobium retained by the organic and the slope of the line, the distribution coefficient. The method of least squares was used to determine the best straight line fit for the data. In cases where visual inspection of the data indicated a straight line followed by a curved section in the higher niobium concentrations, only the data for the straight line portion was used.

The results of three experiments are shown in Fig. 11. The organic to aqueous phase ratio varied from 0.5 to 8 and the contact time was five minutes. The mathematical expression for the straight line using this data is $y = 0.80x - 2.74 \times 10^4$ indicating a slope (DC_a^o) of 0.80 and an intercept at $x = 3.42 \times 10^4$ c/m/ml Nb-95. Since the initial solution contained 1.70×10^5 c/m/ml Nb-95, 20% of the material is unextractable.

The distribution coefficient for the same system obtained by contacting a similar organic solution containing niobium-95 with 4 M HNO_3 was 1.77 with 0.7% of the niobium retained. The organic solution containing ~8×10^4 c/m/ml Nb-95 was contacted for 5 min with aqueous to organic

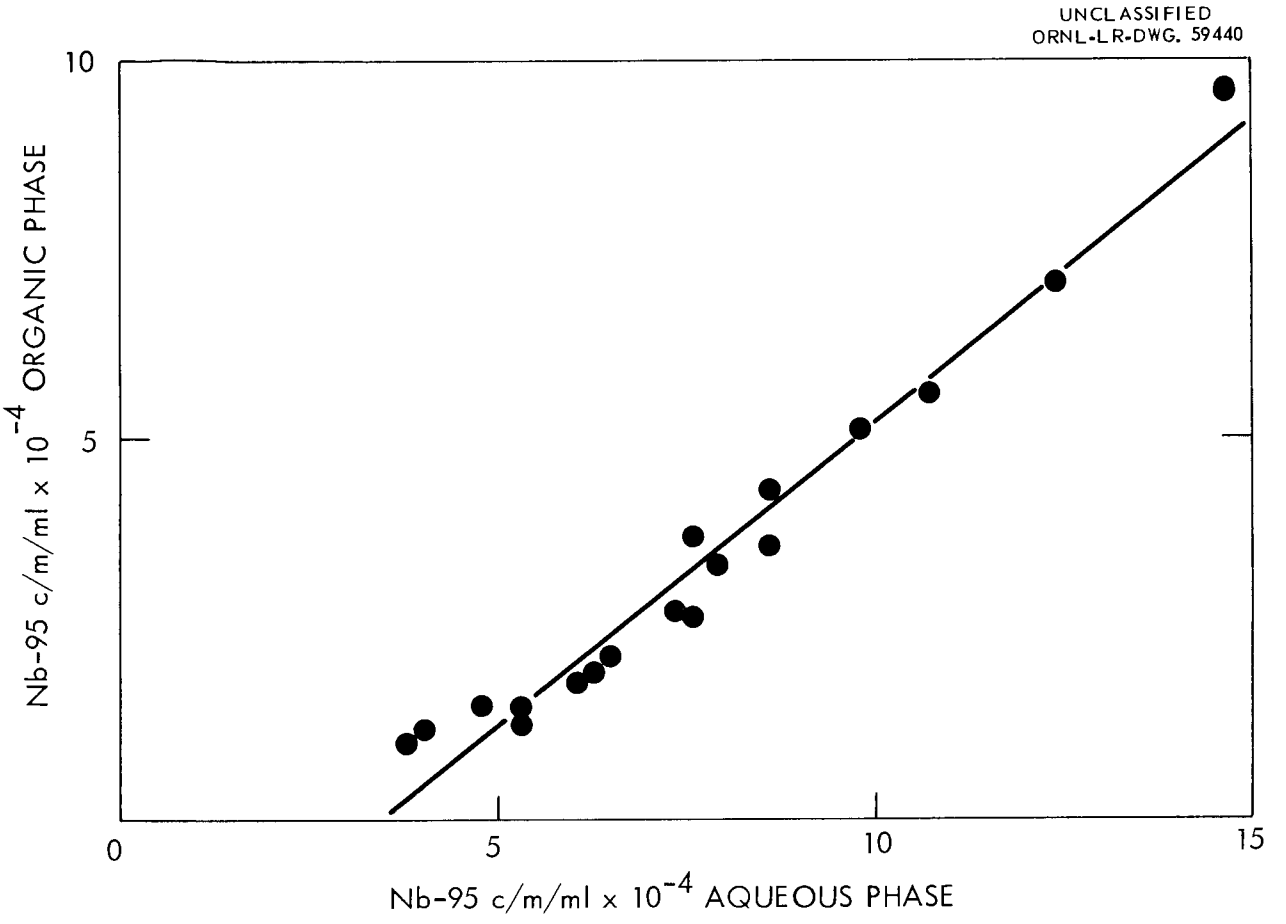

Fig. 11. Distribution of niobium between 4 M HNO_3 and a solvent containing 63% dodecane, 27% purified TBP, 3% degraded TBP, and 7% degraded amsco. Feed solution: 1.7×10^5 c/m/ml Nb-95, 4 M HNO_3. TBP and amsco were degraded together.

ratios varying from 0.25 to 20 (Fig. 12). Three experiments were made. The results were combined and a line derived for the straight line portion of the data.

Similar experiments have been made with freshly purified 30% TBP in dodecane. Although the data were very scattered and must be repeated, they indicated a distribution coefficient of ~0.01 with 40% of the niobium unextractable.

Results of batch shakeouts showed very little effect of contact time on the extraction of niobium-95 with purified 30% TBP-dodecane or solvents containing degraded TBP and Amsco (Table 13). Equal volumes of 4 M HNO_3 and the TBP solutions were contacted for a total of 360 min and the niobium-95 content of each phase determined after various time intervals. The material balance of the activity was ±20% and probably accounts for the small random variation observed in the distribution coefficients.

The niobium distribution coefficient between 4 M HNO_3 and an organic consisting of 63% dodecane, 27% TBP, 3% degraded TBP and 7% degraded Amsco using the Martin technique with 30 min contact times was 0.95 with 23% of the niobium unextractable. As shown above, the value obtained using a 5-min contact time was 0.80 with 20% of the niobium unextractable. Both of these values are from aqueous to organic experiments. Two 30-min runs were made to determine the organic to aqueous coefficient. The first was made about 15 min after the niobium-95 was extracted into the organic solvent and the second was made 3 hr after the niobium was put in the solvent. These data were found by visual inspection to fit curves rather than straight lines (Fig. 13). The distribution coefficient at the lower concentration of niobium was ~3.5 for the test using fresh organic and ~2.0 for the 3-hr organic. This experiment should be repeated using organic solutions aged for different times before definite conclusions are made.

Extraction of Niobium-95 with Degraded TBP in Dodecane

The distribution coefficient of niobium-95 between nitric acid and an organic solution consisting of 70% Dodecane, 27% freshly purified TBP plus 3% degraded TBP ranged from 0.2 to 0.6 for nitric acid concentrations of 0.2 N AD to 4.1 M. Results from organic to aqueous experiments for the same nitric acid concentrations ranged from 0.3 to 1.6. In both cases the minimum value was obtained with 2.0 M HNO_3. The aqueous to organic value for acid deficient solutions could not be accurately measured but was ~10^{-4}.

The Martin technique described above was used to determine the distribution coefficient in these experiments. Plastic equipment was used throughout. There was so little niobium extracted from the acid deficient solution that the distribution coefficient could not be measured accurately. The coefficients ranged from 0.2 to 0.7 for the acid solutions (Table 14a). The amount of unextractable niobium ranged from <0 to 12% and did not follow any definite pattern.

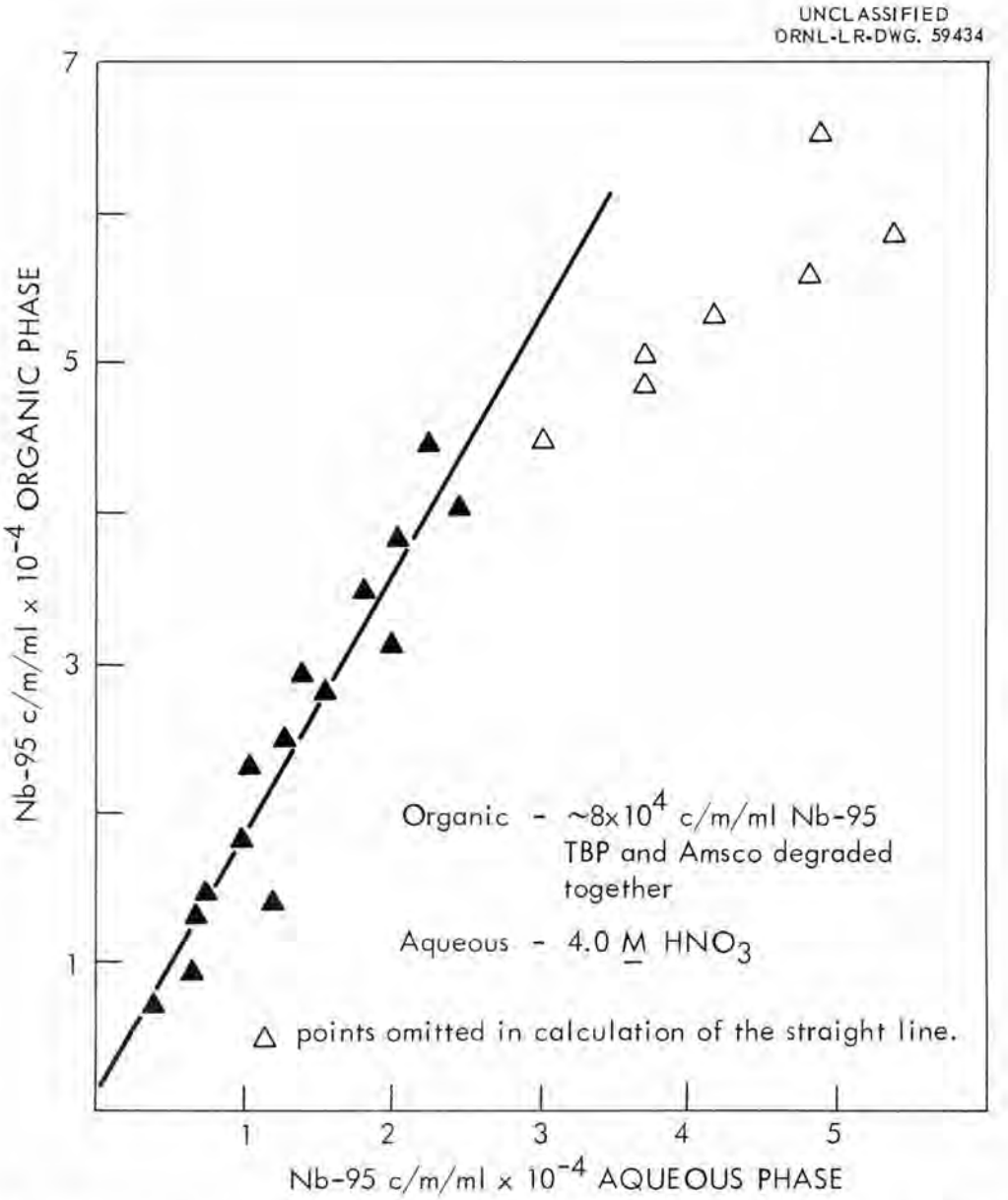

Fig. 12. Organic to aqueous distribution of niobium between 4 M HNO_3 and a solvent containing 63% Dodecane, 27% purified TBP , 3% degraded TBP and 7% degraded Amsco.

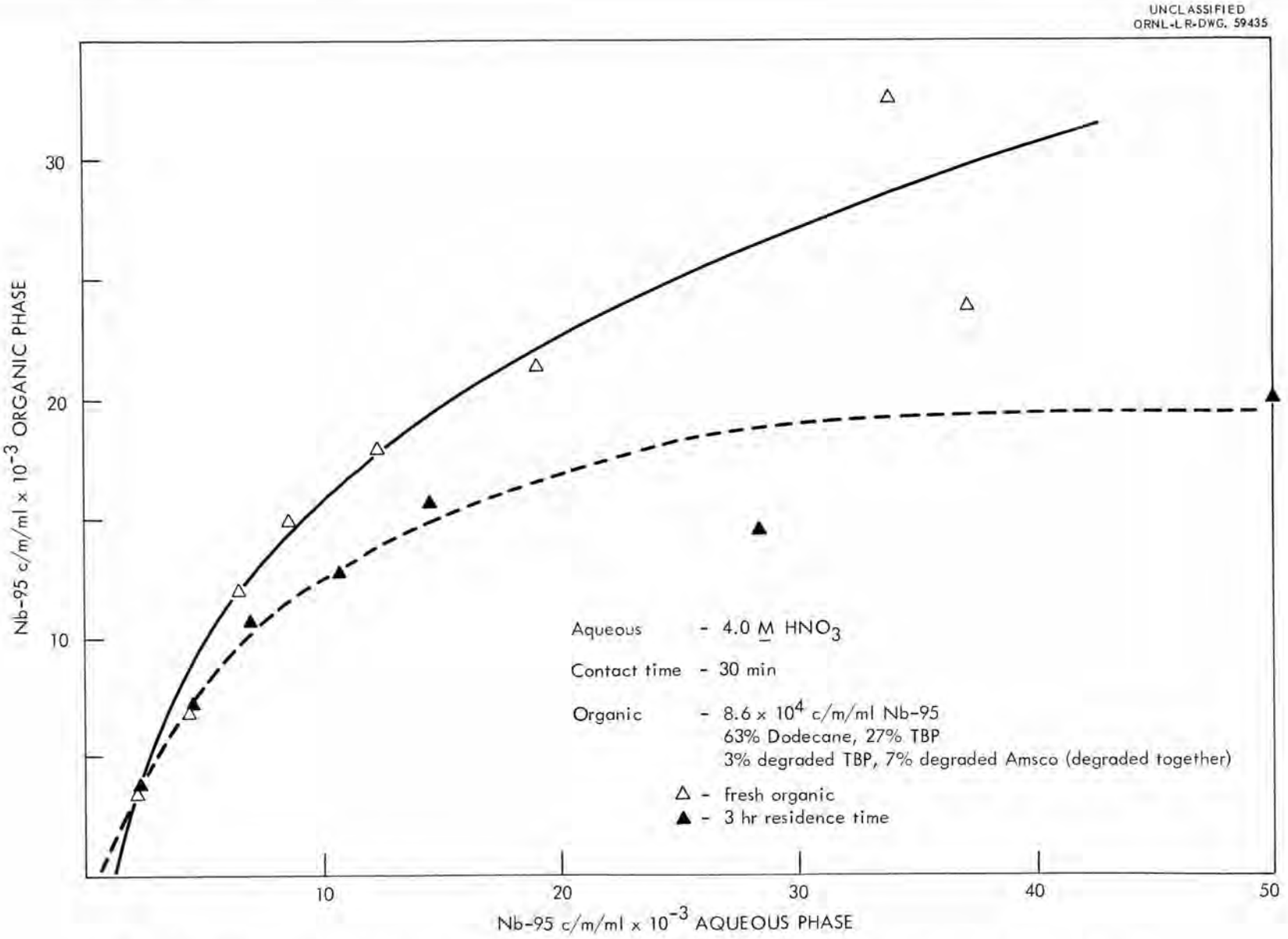

Fig. 13. Effect of the niobium residence time in the organic phase on the distribution of niobium.

Table 13. Effect of Contact Time on the Extraction of Nb-95 from 4 M HNO_3

Organic				
% Dodecane	70	70	63	63
% TBP	30	30	27	27
% Degraded TBP	-	-	3	3
% Degraded Amsco	-	-	7	7
	Distribution Coefficient DC_a^o			
	Aq to Org	Org to Aq	Aq to Org	Org to As
Contact time, (min)				
5	0.050	0.31	0.39	0.92
15	0.054	0.26	0.30	0.78
30	0.053	0.22	0.44	0.64
60	0.061	0.22	0.48	0.58
120	0.061	0.27	0.50	0.76
180	0.062	0.25	0.50	0.82
240	0.053	0.24	0.30	0.78
300	0.061	0.23	0.27	0.64
360	0.059	0.25	0.26	0.61

With the exception of the 0.55 M HNO_3 experiment, very little difference was observed in coefficients obtained with fresh feed solutions and solution that had been allowed to age 24 hr. The coefficient changed from 0.35 to 0.66 in the 0.55 M HNO_3 test and probably indicates the degree of scatter of the data (Table 14a). A graph made of the combined data shows a distribution coefficient of 0.48 with none of the niobium in an unextractable form (Fig. 14).

One explanation for the deviation of the data from a straight line in the higher concentrations (Fig. 14), is the solubility of the degraded organic extractant in the aqueous phase. Any effect of aqueous solubility should be seen in this region since the concentration of the extractant in the organic phase would decrease as the aqueous to organic ratio increased. Such a solubility effect was seen in an experiment in which a degraded organic solution was washed with equal volumes of 0.5 M HNO_3 several times prior to equilibration with a 0.5 M HNO_3 feed solution containing ~2 x 10^5 c/m/ml Nb-95. The distribution coefficient was found to be dependent on the amount of washing the organic had received (Table 15). One feed solution that had already been equilibrated with an organic phase was re-equilibrated with another organic solution that had received the same washing as the first. The distribution coefficient was higher the second time indicating a larger amount of the extractant in the system, i.e., the feed solution had not removed as much extractant from the second organic phase.

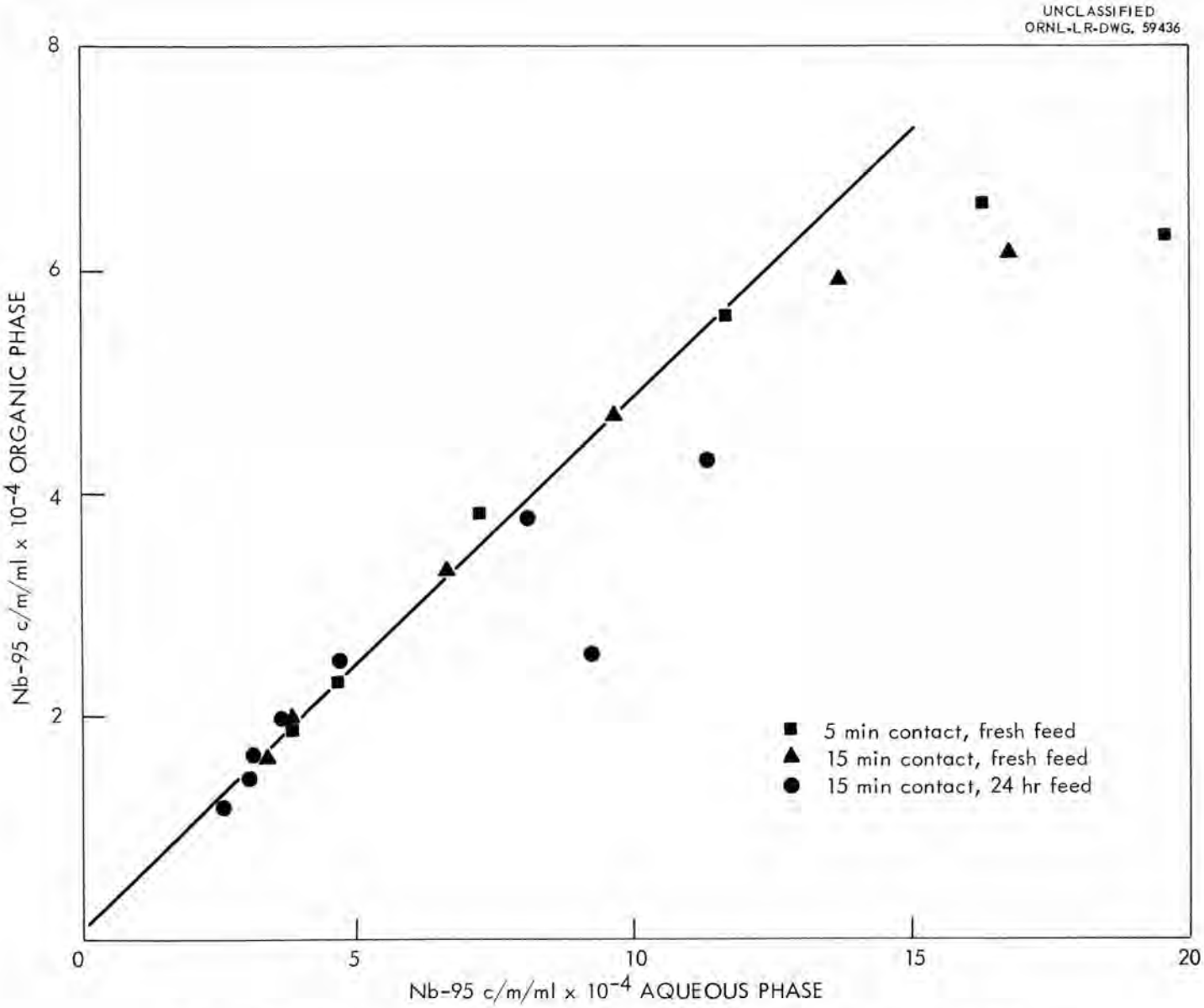

Fig. 14. Extraction of niobium-95 from 0.55 M HNO_3 with degraded TBP.

Table 14. Extraction of Niobium-95 with Degraded TBP

A. Aqueous to Organic

HNO_3, M	0.04	0.09			0.4	0.55			1.1		2.0				4.1	
Contact time, min	5	15	15	60	60	5	15	15	5	15	5	15	15	30	15	15
Age of Feed, hr	<.2	<.2	24	<.2	<.2	<.2	<.2	24	<.2	24	<.2	<.2	73	<.2	<.2	24
DC_a^o at O/A Ratio of:																
0.5	0.12	-	-	0.63[b]	0.16	0.32	0.37	-	0.29	-	0.26	0.22	0.24	0.23	-	-
1	0.21	-	-	0.10	0.21	0.41	0.44	-	0.32	-	0.27	0.25	0.26	0.25[a]	-	-
2	0.22[b]	0.20	0.18	0.15	0.29	0.48	0.48	0.38	0.34	0.29	0.29	0.25	0.26	0.25	0.47	0.45
3	0.22[b]	0.32	0.23	0.17	0.32	-	-	0.47	-	0.33	-	-	-	-	0.46	0.43
4	0.35[b]	0.36	0.13	0.20	0.32	0.52	0.50	0.27	0.34	0.25	0.28	0.24	0.25	0.25	0.43[a]	0.38
6	0.42[b]	0.46	0.26	0.20	0.29	-	-	0.53	-	0.36	-	-	-	-	0.43	0.35
8	-	0.43	0.22	0.19	0.27	0.50	0.52	0.54	0.33	0.25	0.27	0.25	0.26	0.26	0.40	0.33
10	-	0.41	0.20	0.20	0.25	0.49	0.49	0.51	0.32	0.35	0.27	0.24	0.25	0.25	0.37	0.31
12	-	0.42	0.18	-	-	-	-	0.46	-	0.32	-	-	-	-	0.31	0.29
15	-	0.39	0.17	-	-	-	-	0.44	-	0.31	-	-	-	-	0.34	0.25
Calculated DC_a^o	-	0.53	0.42	0.22	0.43	0.31	0.35	0.66	0.29	0.42	0.26	0.22	0.25	0.23	0.53	0.56
inextractable[a] Nb,%	-	3.8	6.0	3.8	12	<0	<0	4	<0	4.5	<0	<0	<0	<0	6	11

B. Organic to Aqueous

HNO_3, M	0.06				0.5				1.0		2.0				4.2	
Contact time, min	5	15	15	60	5	15	15	60	5	15	5	15	15	30	15	15
Age of aqueous feed (c), hr	<.2	<.2	24	<.2	<.2	<.2	24	<.2	<.2	24	<.2	<.2	73	<.2	<.2	24
DC_a^o at A/O Ratio of:																
0.5	0.65	0.67	0.74	0.40[b]	0.47	0.45	0.62	-	0.34	0.45[b]	0.33	0.27	0.30	0.29	0.77	0.80
1	1.09	0.91	1.17	0.61[b]	0.54	0.48	0.70	0.49	0.40	0.49	0.32[b]	0.30	0.31	0.30	0.75	0.79
2	1.21[b]	1.18	1.41	0.83[c]	0.54	0.50	0.73	0.60	0.40	0.48	0.33	0.32	0.32	0.32[b]	0.72	0.75
3	-	1.2	1.44	1.04[c]	-	-	0.72	0.65	-	0.45	-	-	-	-	0.67[b]	0.69
4	1.72	1.21	1.41	1.20[b]	0.59	0.51	0.67	0.68	0.39	0.47	0.34	0.34[b]	0.32	0.32	0.67	0.66
6	-	1.03	1.17	1.63[b]	-	-	0.57	0.74	-	0.38	-	-	-	-	0.58	0.63
8	1.90	-	-	1.81[b]	0.64	0.52	-	0.79	0.49	-	0.32	0.40	0.36	0.38[b]	-	-
10	1.80[b]	0.90	1.09	-	0.64	0.52[b]	0.51	0.84	0.47	0.36[b]	0.31	0.42	0.36	0.39[b]	0.49	0.5
Calculated DC_a^o	0.84	1.55	1.60	0.32	0.46	0.45	0.76	0.53	0.33	0.52	0.33	0.26	0.30	0.28	0.82	0.85
Retained Nb, %	5	<0	<0	15	2.6	1.2	2.1	3.0	2.0	<0	<0	2.0	0.6	1.3	<0	<0

The organic consisted of 70% dodecane, 27% TBP, and 3% TBP that had been degraded by refluxing with 6 M HNO_3 for 6 hr. The initial concentration of niobium-95 in the aqueous was ~2 x 10^5 c/m/ml and the organic ranged from 2 x 10^4 to 6 x 10^4 c/m/ml. The error in the material balance of the activity is $<\pm 5\%$ unless specified.

(a) Error in the material balance of activity $>\pm 5\%$ $<\pm 10\%$.
(b) Error in the material balance of activity $>\pm 10\%$.
(c) Age of the aqueous feed used in the initial aqueous organic equilibration.

Table 15. Effect of Multiple Washing on the Extraction of Niobium with Degraded TBP

Experiment No.	1	2	3	4	5
Number of Washes	3	4	5	7	-[a]
DC_a^o	0.17	0.14	0.12	0.085	0.107

[a]The aqueous from experiment No. 4 was equilibrated again with organic that had been prewashed 7 times.

The distribution coefficients from organic to aqueous experiments were higher than the corresponding aqueous to organic tests (Table 14b). These coefficients ranged from 0.3 to 1.6. The minimum coefficient was observed in the 2 M HNO_3 test in both series (Figs. 15a and b). The percent of the niobium that was retained by the organic varied from 0 to 15% and did not follow any definite pattern.

With the exception of the 60 min contact using 0.1 M acid, coefficients obtained from organics that had been equilibrated with fresh solutions were approximately the same as those obtained from experiments which used 24 hr aqueous feed solutions. There is no explanation for the results obtained with the 60 min, 0.1 M acid experiment.

2.4 Separation of Thorium from Uranium-233 Product by Ion Exchange (R. H. Rainey)

Laboratory experiments have demonstrated that thorium may be effectively removed from U-233 product by passage through a Dowex 50W ion exchange resin. Passing a solution containing 25 g/l U, 0.25 g/l Th and 0.25 M HNO_3 through the resin results in the adsorption of 99% of the thorium and 1% of the uranium (19). Additional studies have demonstrated that more than 99% of the uranium and less than 3% of the thorium which adsorbed on the resin may be eluted with 0.5 N HNO_3. The thorium can be eluted with Acetate-Citrate. A combination adsorption and elution cycle therefore results in 99% of the uranium in a product which contains about 1% of its original thorium concentration, 1% of the uranium containing twice the concentration of thorium as the feed, and 99% of the thorium nearly free of uranium. About 8 grams of uranium per batch may be processed per milliliter of resin.

The laboratory experiments used synthetic U-233 product solutions and an ion exchange column 24 cm long containing 5 ml of 8% cross-linked, 50-100 mesh, Dowex 50W resin.

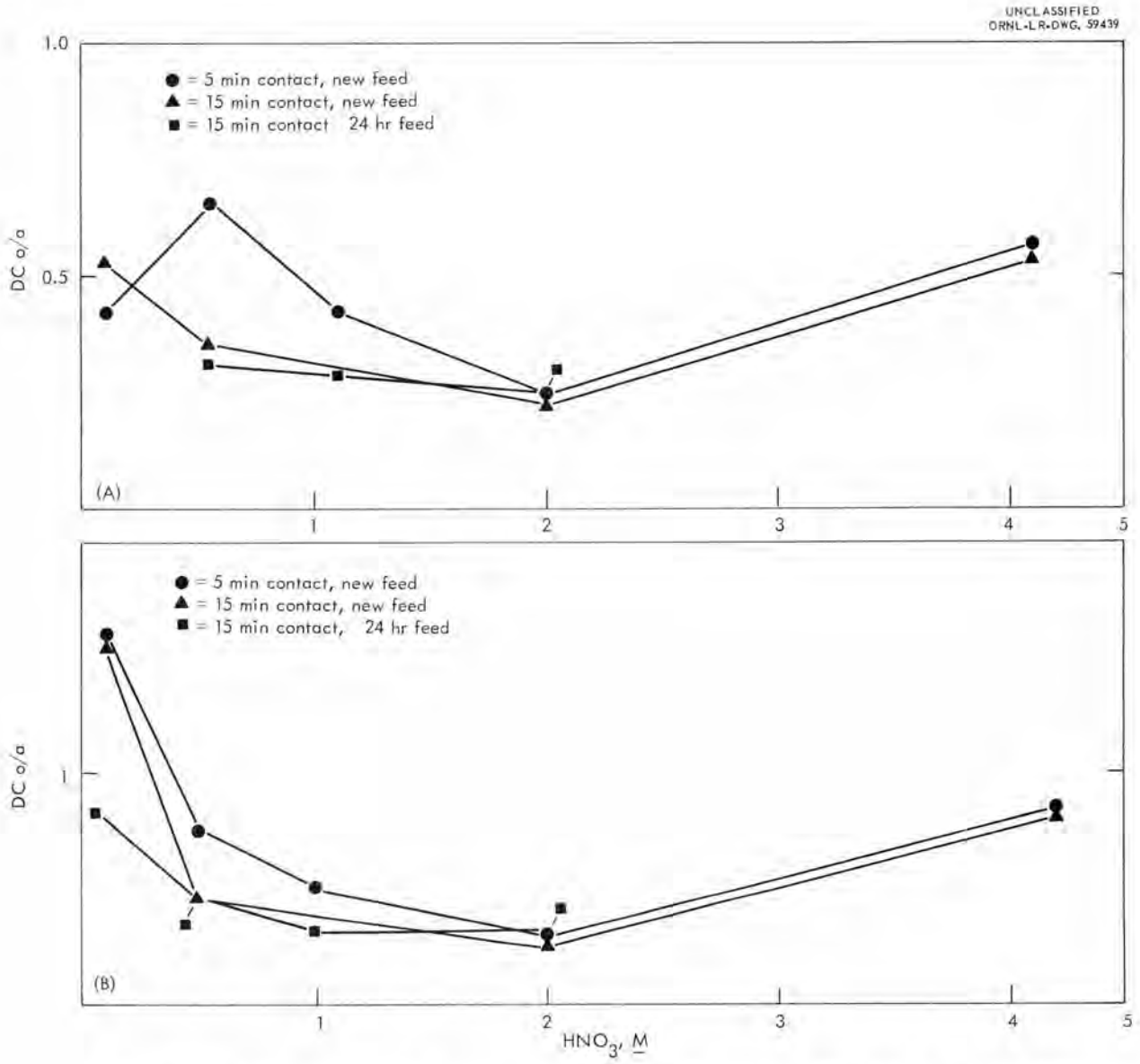

Fig. 15. Effect of acidity on the extraction of niobium-95 with degraded TBP (A) aqueous to organic and (B) organic to aqueous.

A conservative separation process consists of the following steps:

1) The U-233 product presently in storage would be diluted to 25 g/l U, 0.25 g/l Th, and 0.25 M HNO_3 by the addition of three volumes of water.
2) About 350 column volumes of the diluted solution would be passed through a Dowex 50W ion exchange column at about 0.7 ml $min^{-1}cm^{-2}$ (Table 16). About 99% of the uranium passes through the column.
3) Uranium which adsorbed on the column is eluted with about 20 column volumes of 0.5 M HNO_3 at about 1 ml $min^{-1}cm^{-2}$ (Table 17).
4) Thorium is then eluted with about 20 column volumes of 3 M NH_4Ac, 1.5 M HAc at about 1 ml $min^{-1}cm^{-2}$ (Table 18).

2.5 Separation of Aqueous from Organic Solutions (R. H. Rainey)

A series of experiments designed to determine the fission product decontamination by removing aqueous from organic solutions have given inconclusive results. The organic product from an extraction-scrub bank and the organic from the solvent recovery system was passed through an electrostatic precipitator by the Petrolite Co. Analyses by centrifuging the samples illustrated that the water content of the organic stream was reduced during the treatment; however, there was no noticeable improvement in fission product decontamination or solvent quality. The use of limited volume of the extraction-scrub product from a laboratory countercurrent batch extraction experiment and synthetically degraded solvent, gave results which would not necessarily be typical of plant application.

Table 16. Separation of Thorium from U-233 Product by Ion Exchange: Adsorption Cycle

Resin: Dowex 50W

Feed: 25 g/l U, 0.25 g/l Th, 0.25 N HNO_3

Column Volumes	Flow Rate ml $min^{-1}cm^{-2}$	Thorium in Effluent g/l	Total Thorium Adsorbed mg Th/ml Resin
160	1.4	<0.002	38
200	0.9	<0.002	48
240	0.8	<0.002	58
280	0.7	<0.002	67
320	0.7	<0.002	77
360	0.6	<0.002	87
400	0.8	0.20	97

Table 17. Separation of Thorium from U-233 Product by Ion Exchange: Uranium Elution Cycle

Uranium and Thorium on column (from elution material balance): 81.1 mg U per ml resin, 75.2 mg Th per ml resin
Eluting agent: 0.5 M HNO_3

Column Volumes of Eluant	Uranium Aliquot Conc, g/l	Uranium Amount Eluted % of Total	Thorium Aliquot Conc, g/l	Thorium Amount Eluted % of Total
1	3.4	4.2	0.026	0.03
2	33.1	45	1.78	2.39
3	18.6	68	0.06	2.47
4	9.21	79	0.011	2.49
5	5.55	86	0.007	2.50
6	3.71	91	0.005	2.50
7	2.53	94	0.004	2.51
8	1.84	96	0.004	2.51
9	1.36[a]	98	<0.002	2.52
10	0.93	99.3	0.0024	2.52
12	0.48	99.85	0.014	2.54
14	0.029	99.90	0.008	2.55
16	0.074[a]	99.98	0.004	2.55
18	0.0056	99.99	0.003	2.56
20	0.009	99.99	0.003	2.56

[a]Solution set overnight in resin.

Table 18. Separation of Thorium from U-233 Product by Ion Exchange: Thorium Elution Cycle

Uranium and Thorium on Resin:[a] Uranium trace, 73.3 mg Th per ml resin
Eluting agent: 3 M NH_4Ac, 1.5 M HAc

Column Volumes of Eluant	Uranium Aliquot Conc, g/l	Thorium Aliquot Conc, g/l	Thorium Amount Eluted % of Total
1	0.001	6.96	9.50
2	0.003	21.5	38.8
3	0.002	13.1	56.7
4	0.001	8.96	69.0
5	0.001	6.55	77.9
6	0.001	4.70	84.3
8	0.001	2.72	91.7
10	<0.001	2.69	99.1
12	<0.001	0.18	99.6
14	<0.001	0.078	99.8
16	<0.001	0.071	99.98
18	<0.001	<0.005	99.99
20	<0.001	0.002	100

[a]Uranium previously eluted from resin as described above.

3.0 IMMI MIXER-SETTLER STUDIES
(J. R. Flanary and J. H. Goode)

Performance studies have been continued with the intermediate-scale mixer-settlers, the solvent extraction contactors intended for installation in the IMMI facility, Cell 1, Bldg. 4507. Initial tests have shown stage efficiencies for uranium extraction and stripping of only 40 to 50%, and low volumetric throughputs. The study was limited to the standard Purex flowsheet, Table 19. Over-all objectives of the study are to: (a) define the variables which affect mixer-settler performance, (b) improve performance by mechanical alterations, (c) establish optimum operating conditions and collect performance data for typical concentrated and dilute TBP flowsheets, and (d) train technicians in the basic mechanics and chemistry of the operation.

Table 19. Standard Purex Flowsheet - First Cycle[a]

Stream	Composition	Relative Flow
	Extraction-Scrub	
Aqueous Feed, AF	324 g U/liter, 2 M HNO_3	100
Aqueous Scrub, AS	3 M HNO_3	67
Solvent, AX	30% TBP in Amsco	333
Aqueous Waste, AW	2.2 M HNO_3	145
Solvent, AP	90.6 g U/liter, 0.2 M HNO_3 30% TBP in Amsco	355
	Back Extraction - Parition	
Solvent, AP	91 g U/liter, 0.2 M HNO_3 30% TBP in Amsco	355
Aqueous Partition, BX	0.1 M HNO_3	45
Solvent, BS	30% TBP in Amsco	89
Aqueous Partition, BP	0.94 M HNO_3	45
Solvent, BU	73 g U/liter, 0.03 M HNO_3, 30% TBP in Amsco	444
	Strip	
Solvent, BU	73 g U/liter, 0.03 M HNO_3, 30% TBP in Amsco	444
Aqueous Strip, CX	0.03 M HNO_3	666
Aqueous Product, CU	47 g U/liter, 0.05 M HNO_3	688
Solvent, CW	30% TBP in Amsco	422

[a]When the Purex first cycle is operated without plutonium partitioning the AP stream, relative flow: 355, is stripped with CX, relative flow: 666, to produce the CU stream whose HNO_3 concentration increases to 0.13 M.

Previously (21,22), 33 runs have been conducted in a 5-stage mockup of the IMMI contactors, using the mockup alternatively as an extraction bank and a strip bank. The results showed that uranium extraction and stripping stage efficiencies up to 92% could be attained with modified impellers operated at speeds up to 1100 rpm and 1600 rpm, respectively. Aqueous throughputs up to 92 ml/min and 550 ml/min were predicted for the IMMI extraction-scrub and stripping contactors.

The IMMI mixer-settler assembly fabricated mainly from 304L stainless steel, consists of "A" bank, a 17-stage extraction-scrub unit, "B" bank, a 17-stage partition unit, and "C" bank, a 11-stage strip unit, racked vertically for gravity flow of the solvent effluent from "A" to "B" to "C", or from "A" to "C". "A" and "B" banks are identical in size; each mixing chamber is 1 in. x 1 in. x 2-1/2 in. deep and each settling chamber is 1 in. x 4 in. x 3-1/8 in. deep. With proper control of the interfaces, aqueous holdup in the mixing and adjacent settling chamber is 20 and 120 ml, respectively. Corresponding organic holdup is 20 ml and 80 ml. "C" bank is oversized by a volumetric factor of 2.25, compared to "A" and "B" banks.

Aqueous flow through the contactors is governed by the pump action of the impellers which pull aqueous into the bottom of each mixing chamber, and discharge the organic/aqueous emulsion through the mixed phase discharge port into each settling chamber. The organic stream moves countercurrently from settling chamber to mixing chamber via overflow ports (Fig. 16).

Recently, a series of 15 runs have been completed. Optimum operating conditions for "A" bank were established at a total volumetric throughput of 284 ml/min (92 ml/min of total aqueous) with impeller speed of 1200 rpm "Reverse". "Reverse" impeller direction of rotation means that the organic/aqueous emulsion is thrown against the louvers located behind the mixed phase discharge ports. This arrangement provides some recirculation of the mixed phase and also restricts the aqueous stage-to-stage pumping. Further restriction of aqueous stage-to-stage pumping is provided by stainless steel discs attached to the bottom of each impeller in "A" and "B" banks. Previous studies (21,22) with the 5-stage mockup had shown that the discs restrict the impeller pump action which is produced by the vortex forcing aqueous upward between the rotating impeller and the square walls of the mixing chamber. The discs are provided for both "A" and "B" banks since, with the Purex flowsheet, these contactors must accomodate a relatively small flow of aqueous compared to the organic flow. Otherwise, it would be impossible to maintain organic/aqueous interfaces throughout the banks at the impeller speeds required for high stage efficiencies.

Table 20 shows the operating conditions for "A" bank using the Purex flowsheet, and uranium distribution across seven extraction stages and at the first scrub stage. Uranium analyses of the organic and aqueous stage samples, before and after equilibration, provided sufficient data to

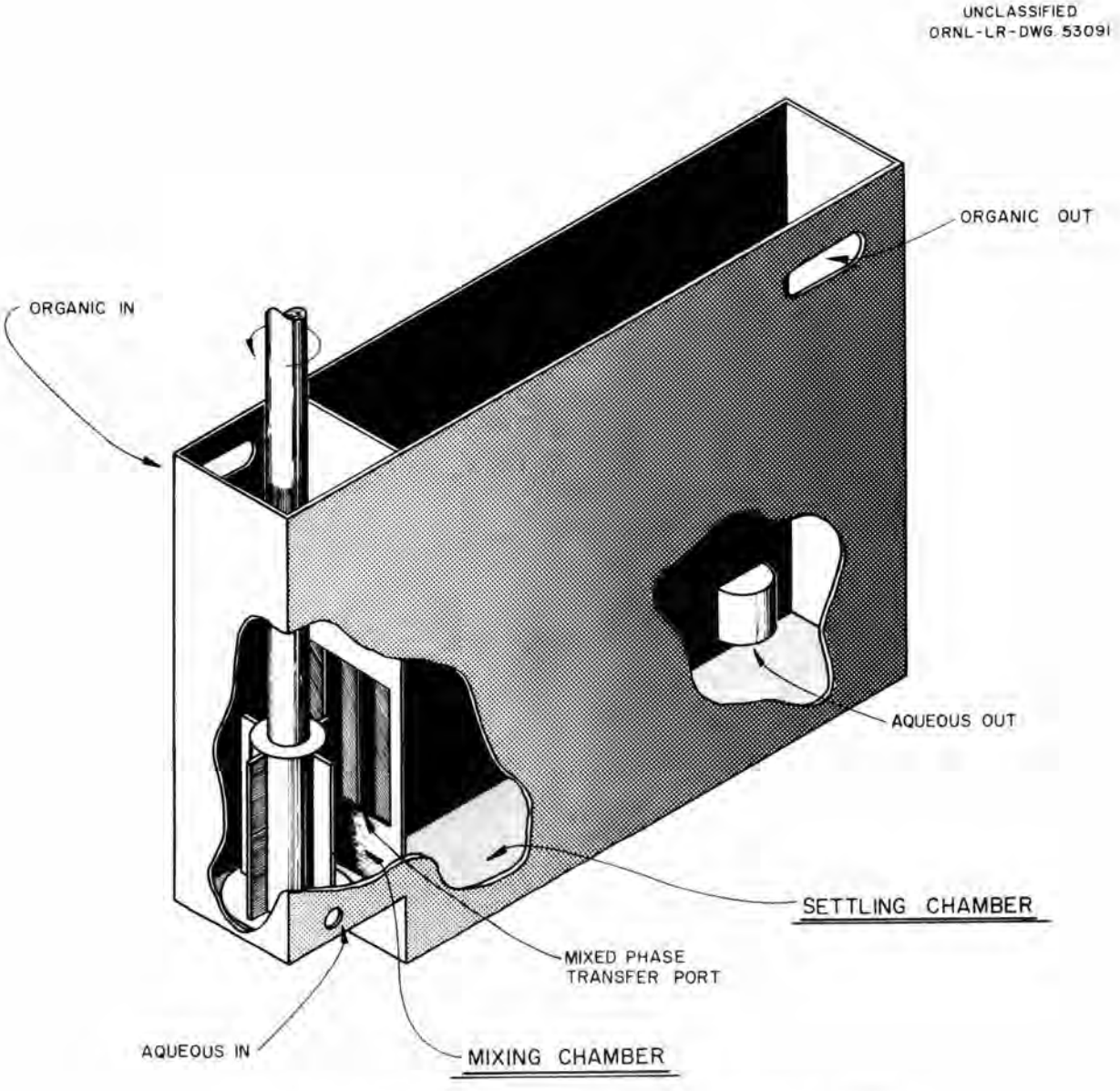

Fig. 16. IMMI mockup individual mixer-settler stage.

Table 20. Stage Efficiency for Uranium Extraction in the IMMI Mixer-Settler "A" Bank with the Standard Purex Flowsheet Operated at 85% Flooding

Extraction stages: 7; Scrub stages: 10

Flow Rates

AF: 55 ml/min	AF: 320 g U/liter, 2 M HNO_3
AS: 37	AS: 3 M HNO_3
AX: 180	AX: 30% TBP in Amsco 125-82

Impeller Speed: 1200 rpm "Reverse" (against louvers)

	Mixer-Settler Samples		Mixer-Settler Samples, Equil.		Mixer-Settler Stage Efficiency[a]
Stage No.	Org, g U/l	Aq, g U/l	Org, g U/l	Aq, g U/l	%
Scrub 10	88.9				
Scrub 1	98.9	89.5	107	58.6	
Ext 1	101	47.8	103	37.4	94
2	29.3	2.46	33.6	1.37	97
3	4.41	0.20	4.51	0.011	92
4	0.011	0.014	0.025	0.0006	93
5	0.003	0.002	0.009	0.0006	90
6	0.002	0.0006	0.004	0.0004	88
7	0.004	0.0018	0.019	0.005	-

[a] Stage efficiency = $\frac{X_{In} - X_{Out}}{X_{In} - X_{Eq\ Out}}$ where X is the uranium concentration in the aqueous phase.

calculate individual stage efficiencies for uranium extraction. Across seven actual extraction stages, uranium extraction efficiency varied from 88 to 97% with an overall average of 92%. Uranium loss to the aqueous waste was less than 0.01% with four actual stages, 0.001% with five actual stages. Accidental cross-contamination during sampling caused the slight rise in uranium concentration at the seventh stage.

Table 21 shows the operating conditions established for "B" bank using the Purex flowsheet. Eleven partition and six back extraction stages were used; uranium distribution across the six back extraction stages is shown. The solvent effluent stream from "A" bank (AP) was higher in uranium, 97.2 g/l, than nominal flowsheet value; therefore, the solvent effluent from "B" bank (BU) is also higher in uranium, 80.1 g/l, than flowsheet value. Across the back extraction section, uranium extraction efficiency varied from 78 to 100% with an overall average of 93%. Uranium loss to the aqueous stream was less than 0.001% with five actual stages.

Table 21. Stage Efficiency for Uranium Extraction in the IMMI Mixer-Settler "B" Bank with the Standard Purex Flowsheet Operated at 23% Flooding

Back Extraction stages: 6; Partition stages: 11

	Flows	Composition
AP:	200 ml/min	30% TBP in Amsco, 97.2 g U/liter, 0.2 M HNO_3
BX:	25	0.1 M HNO_3
BS:	50	30% TBP in Amsco

Impeller Speed: 950 rpm "Reverse" (against louvers)

Stage	Mixer-Settler Samples Org, g U/l	Mixer-Settler Samples Aq, g U/l	Mixer-Settler Samples, Equil. Org, g U/l	Mixer-Settler Samples, Equil. Aq, g U/l	Mixer-Settler Stage Efficiency[a] %
11th Partition	80.1				
1st Partition		34.2			
1st Extraction	68.1	13.9	66.8	12.3	93
2	50.7	8.56	50.7	7.08	78
3	5.61	0.74	5.48	0.37	96
4	0.48	0.058	0.47	0.052	100
5	0.040	0.006	0.035	0.005	98
6	0.018	0.007	0.016	0.006	-
					Avg. 93%

[a] Stage efficiency = $\frac{X_{In} - X_{Out}}{X_{In} - X_{Eq\ Out}}$ where X is the uranium concentration in the aqueous phase.

Optimum operating conditions for "C" bank, Table 22, were determined after certain mechanical alterations were made to improve the aqueous stage-to-stage pumping action. These included: 1) removal of the stainless steel discs previously attached to the bottom of the impellers, 2) reduction of impeller vane height and thickness to 7/8 in. and 1/16 in., respectively, to permit higher pumping speed without overmixing, and 3) enlargement of the mixed phase discharge ports to lower resistance to flow. It was established that, with the impeller direction of rotation "Forward" which flings the mixed phase directly through the louvers behind the mixed phase transfer ports, intermittent flooding occurred at an aqueous throughput of 375 ml/min. The flooding is a gradual buildup and backout of aqueous via the solvent effluent line.

At an aqueous throughput of 350 ml/min, and impeller speed of 950 rpm, "Forward" stable operation is realized. Stage efficiencies for uranium stripping varied from 91 to 100% across eight stages in the 11-stage bank, Table 22. Overall average stage efficiency was 95%. Uranium loss was ~0.001% with seven actual stages.

Table 22. Stage Efficiency for Uranium Stripping in the IMMI Mixer-Settler "C" Bank with the Standard Purex Flowsheet Operated at 90% Flooding

Strip stages: 11

Flows		Composition
AP:	180 ml/min	30% TBP in Amsco, 91.4 g U/liter, 0.2 M HNO_3
CX:	350	0.03 M HNO_3

Impeller Speed: 950 rpm, "Forward" (through louvers)

Stage	Mixer-Settler Samples Org, g U/l	Mixer-Settler Samples, Equil. Org, g U/l	Mixer-Settler Stage Efficiency,[a] %
1st Strip	56.8	56.8	100
2	32.4	29.8	91
3	9.2	8.38	96
4	1.96	1.15	93
5	0.17	0.078	93
6	0.021	0.006	91
7	0.001	0.0004	97
8	0.0001	0.0001	100
9[b]	-	-	
			Avg. 95%
10	-	-	
11	-	-	

[a] Stage Efficiency = $\frac{Y_{In} - Y_{Out}}{Y_{In} - Y_{Eq\ Out}}$ where Y is the uranium concentration in the organic phase.

After several runs, it was evident that stable operation of the "C" bank with the Purex flowsheet is greatly dependent on the selection of the proper impeller speed. The solvent effluent from "A" bank entering "C" bank has a specific gravity of 0.95 which reduces to 0.82 as it leaves the bank. The aqueous strip entering the bank has a specific gravity of 1.00 which increases to 1.07 as it leaves the bank. Thus, the specific gravity difference is small between the phases particularly at the product end, and the system is rather easily emulsified. Too great an impeller speed can cause overmixing, i.e., a highly emulsified condition in the mixing chambers, which seems to resist flow through the mixed phase discharge ports. With such resistance to flow out of the mixing chamber, the flow of aqueous into the mixing chamber created by the vortex action of the impeller, i.e., the pumping action, is reduced and eventually the flooded condition is reached.

Flooding was also encountered as stable emulsification of phases with excessive coalescence time for the limited capacity of the settling chambers. This condition was attributed to TBP degradation when solvent and nitric acid solution remained in the banks during several days shutdown. When such

flooding is encountered, stable operation can be restored by vacuuming all solution from the banks and restarting the run.

Flooding caused by overmixing can be eliminated by stopping the impellers and pumps feeding solutions to the machine long enough for complete separation of phases. Then, the run is resumed with a reduced impeller speed.

4.0 CORROSION STUDIES

(Work performed by members of the Reactor Chemistry Division, ORNL) (W. E. Clark)

During the past quarter the corrosion systems investigated included Modified Zirflex dissolvent and proposed solvent extraction environments; proposed gas-solid PRFR processing environments; stainless steel nitrate waste storage tests and tests in miscellaneous aqueous systems, principally those required for dissolution of UO_2 from decladding processes and "ashes" from gas-solid reaction processing schemes.

4.1 Modified Zirflex System

In the Modified Zirflex process, zirconium alloy fuels are dissolved in boiling NH_4F-NH_4NO_3-H_2O_2 and the uranium recovered from the resulting solution by solvent extraction. Aluminum nitrate is added to the dissolver solution to allow the solvent extraction to be carried out in equipment constructed of more or less conventional alloys.

Welded specimens of Type 347 stainless steel and of Haynes alloy 6B and unwelded specimens of rolled Haynes 21 were exposed in flowing 5.4 M NH_4F-0.33 M NH_4NO_3-0.003 M H_2O_2 at the boiling point. The data (Table 23) indicate the clear superiority of Haynes 21 ($\leq$ 1 mil/mo maximum) over the other alloys tested, both of which underwent localized attack and showed overall rates in excess of 6 mils/mo.

Welded specimens of Types 304L and 309 SCb stainless steel were exposed in Modified Zirflex solution approximately 0.7 M in dissolved Zr^{+4} and 0.001 M in H_2O_2. Maximum rates obtained for 48 hr exposures were 24 and 4.0 mils/mo, respectively (Table 24) which are higher by factors of 2-3 than those observed for similar exposures in the initial dissolver solution containing no Zr^{+4} (23). Whether these higher rates are due to the presence of dissolved Zr^{+4} or to the lowered concentration of H_2O_2 is not clear. Surfaces of both alloys had a pickled appearance and the 304L had suffered edge corrosion and pitting attack.

Types 304L and 347 stainless steels, Carpenter 20 SCb and LCNA were exposed for 336 hr in a number of fluoride-nitrate-aluminum solutions representing different possible solvent extraction compositions which might be encountered in the Modified Zirflex process. The solutions studied (Table 25) vary in composition from 0.75 to 1.5 M in HNO_3, 0.6 to 1.0 M in

Table 23. Corrosion of Various Alloys in Flowing Modified Zirflex Dissolver Solution[a] at the Boiling Point

Alloy	Specimen Position	Corrosion Rate (mils/mo) 24-36 hr	96-108 hr	186-216 hr	304-330 hr	402-423 hr	490-500 hr	689 hr
Type 347[b] stainless steel (welded)	V	0.83	0.44	0.80-0.97[c]	0.72-0.77	0.54-0.80	0.46-0.88	
	I	3.9-4.6	3.9-4.1	5.7-5.7[c]	5.8-5.9	6.2-6.2	6.4-6.4	
	S	4.1-4.3	3.9-4.0	5.5-5.5[c]	5.6-5.7	5.9-6.1	6.2-6.3	
Haynes 21 (unwelded)	V	0	0.01	0.01	0.02	0.03	0.04	0.06
	I	0.45	0.46	0.69	0.63	0.65	0.67	0.75
	S	1.01	0.43	0.66	0.60	0.61	0.62	0.68
Haynes 6B (as-welded)	V	0.36	0.58	1.2	-	-	-	-
	I[d]	3.5	2.4	3.2	-	-	-	-
	S[d]	3.3	3.0	3.6	-	-	-	-
Haynes 6B (solution annealed)	V	0.45	0.14	1.0	-	-	-	-
	I[d]	3.5	5.9	7.7	-	-	-	-
	S[d]	3.6	7.0	9.6	-	-	-	-

[a] Solution composition: 5.4 M NH_4F-0.33 M NH_4NO_3-0.003 M H_2O_2.
[b] Interface and solution specimens suffered extensive edge corrosion and pitting attack.
[c] These data and those for longer exposure times were obtained using different specimens from those for which data are reported for 108 hr and less exposure.
[d] Specimens suffered weld decay and general intergranular attack.

Table 24. Corrosion of Various Alloys in Modified Zirflex Solutions[a] Containing Dissolved Zirconium

Test Period (hr)	Alloy	Corrosion Rate (mpm) V	I	S
24	304L	0.16, 0.47	13.33, 13.52	14.34, 14.14
	309SCb	0.46, 0.26	3.71, 3.64	3.46, 3,70
48	304L	1.53, 0.46	19.74, 19.81	23.92, 24.03
	309SCb	0.44, 0.29	4.56, 4.40	3.92, 3.97

[a] Solutions prepared by dissolving 61 g of Zircaloy-2 in one liter of 5.4 M NH_4F-0.33 M NH_4NO_3 solution. Solutions were ~0.001 M in H_2O_2.

Table 25. Corrosion of Various Alloys in Possible Modified Zirflex Solvent Extraction Solutions at 50°C

Solution Composition (M)				Specimen Position	Corrosion Rate (mils/mo)							
					Type 304L		Type 347		LCNA[a]		Carpenter 20SCb	
HNO_3	Al	Zr	F		168 hr	336 hr	168 hr	336 hr	168 hr	336 hr	168 hr	336 hr
0.75	0.6	0.49	3.33	V	0.10	0.07	0.09	0.07	0.08	0.08	0.10	0.10
				I	0.67	0.43	0.19	0.13	0.12	0.10	0.27	0.25
				S	1.26	0.74	0.22	0.16	0.20	0.15	0.28	0.26
0.75	0.6	0.40	2.72	V	0.06	0.05	0.06	0.06	0.03	0.04	0.03	0.05
				I	0.19	0.12	0.11	0.07	0.09	0.08	0.15	0.13
				S	0.49	0.30	0.18	0.12	0.15	0.11	0.23	0.21
0.75	0.8	0.49	3.33	V	0.04	0.04	0.05	0.05	0.04	0.05	0.04	0.05
				I	0.10	0.06	0.10	0.06	0.09	0.09	0.17	0.15
				S	0.24	0.13	0.19	0.10	0.10	0.10	0.20	0.18
0.75	0.8	0.40	2.72	V	0.03	0.03	0.02	0.02	0.05	0.03	0.05	0.04
				I	0.08	0.05	0.10	0.05	0.08	0.07	0.15	0.12
				S	0.11	0.06	0.12	0.07	0.09	0.09	0.16	0.15
0.75	1.0	0.40	2.72	V	0.04	0.06	0.04	0.03	0.04	0.03	0.05	0.05
				I	0.03	0.03	0.07	0.04	0.06	0.05	0.11	0.09
				S	0.07	0.02	0.11	0.05	0.12	0.09	0.12	0.09
0.75	1.0	0.36	2.44	V	0.05	0.03	0.03	0.03	0.03	0.02	0.04	0.04
				I	0.04	0.03	0.06	0.04	0.05	0.04	0.08	0.05
				S	0.06	0.03	0.08	0.06	0.04	0.04	0.11	0.08
1.5	0.6	0.45	3.04	V	0.19	0.14	0.17	0.17	0.17	0.18	0.25	0.21
				I	0.83	0.55	0.24	0.23	0.25	0.22	0.39	0.27
				S	2.12	1.27	0.36	0.26	0.35	0.25	0.46	0.31
1.5	0.6	0.36	2.44	V	0.14	0.11	0.12	0.11	0.13	0.11	-	0.02
				I	0.21	0.15	0.18	0.15	0.16	0.13	0.27	0.20
				S	1.21	0.82	0.36	0.24	0.22	0.17	0.55	0.56
1.5	0.8	0.45	3.04	V	0.14	0.14	0.15	0.15	0.20	0.17	0.19	0.18
				I	0.17	0.14	0.20	0.17	0.16	0.14	0.31	0.28
				S	0.21	0.19	0.32	0.22	0.19	0.15	0.49	0.46
1.5	0.8	0.36	2.44	V	0.09	0.09	0.05	0.07	0.08	0.08	0.09	0.09
				I	0.13	0.11	0.13	0.11	0.10	0.09	0.16	0.14
				S	0.15	0.13	0.22	0.14	0.15	0.12	0.31	0.27
1.5	1.0	0.36	2.44	V	0.06	0.07	0.07	0.06	0.05	0.05	0.07	0.08
				I	0.09	0.08	0.13	0.10	0.11	0.10	0.16	0.14
				S	0.15	0.11	0.23	0.15	0.15	0.12	0.25	0.22

[a]Low carbon nickel alloy approximately the composition of Ni-o-nel.

Al^{+3}, 0.36 to 0.49 M in Zr^{+4} and 2.44 to 3.33 M in F^-. Rates were lowest ($\leq$0.26 mil/mo) for Type 347 and LCNA. The following corrosion generalizations can be made:

1) In otherwise similar solutions doubling the acid concentration more than doubled the corrosion rate.
2) Little if any corrosion advantage can be gained by increasing the aluminum concentration above 0.8 M.

The specimens of Type 304L experienced grain-boundary attack plus some localized etching. The appearance of the 347 was that of a light pickle. The LCNA showed some local etching and the Carpenter 20 SCb suffered some intergranular attack in the heat-affected zone of the welds, particularly in the high-acid solutions. It appears that either Type 347 or LCNA can be employed for construction of the solvent extraction equipment but that storage of acid waste solutions approximating these compositions will probably not be safe at temperatures as high as 50°C in tanks constructed of these alloys.

Prior to dissolution of the TRIGA core alloy in NH_4F-NH_4NO_3-H_2O_2 solution it is necessary to decompose the graphite plugs in the fuel assembly. One proposal for doing this consists of treatment with a mixture of 90% fuming HNO_3-10% fuming H_2SO_4 (volume percentage) at relatively low temperatures. LCNA, and CD4M Cu* were tested in this environment for periods of a week or longer, and shorter tests were run on several other alloys. The results (Table 26) show that with all alloys tested except Nichrome V and INOR-8 the corrosion is far more aggressive in the vapor than in the liquid or at the interface. Sweeping the vapor region of the test vessel with dry air to remove the corrosive vapor lowered the overall corrosion rate of LCNA from 0.90 to 0.03 mil/mo for 336 hr exposure but did not eliminate weld decay and grain boundary attack in the vapor phase. Of the alloys tested only INOR-8 and Nichrome V could be considered as candidate materials and the former can be eliminated for a general Modified Zirflex dissolver because of its poor resistance to relatively dilute HNO_3 (vide infra).

4.2 Acid Waste Storage Tests

Exposures of Types 304L and 347 stainless steel specimens in simulated Darex-Purex waste solution (24,25) at 80°C has continued for 6036 hr in low (1-2 M) acid waste solutions both with and without the addition of polyethylene chips and for 4082 hr in the high (5 M) acid solution. The data (Tables 27-29; Fig. 17) show that 1) increasing the free nitric acid content of the waste solution from 2 to 5 M resulted in an overall rate increase of from 0.36 to 0.75 mil/mo for Type 304L and 4052-4082 hr exposure (Tables 27 and 28) and that 2) the presence of polyethylene chips decreased the overall rate from 0.36 to 0.02 mil/mo in the low acid waste (Tables 28 and 29). The latter effect is almost certainly due to some material leached from the polyethylene, possibly a plasticizer. Attempts are being made to identify this material.

* Nominal composition (%): Cr, 25-27; Ni-4.75-6.00, Mo, 1.75-2.25, Cu, 2.75-3.25; C, 0.04 max, Si, 1.0 max; Mn, 1.0 max; fe, bal.

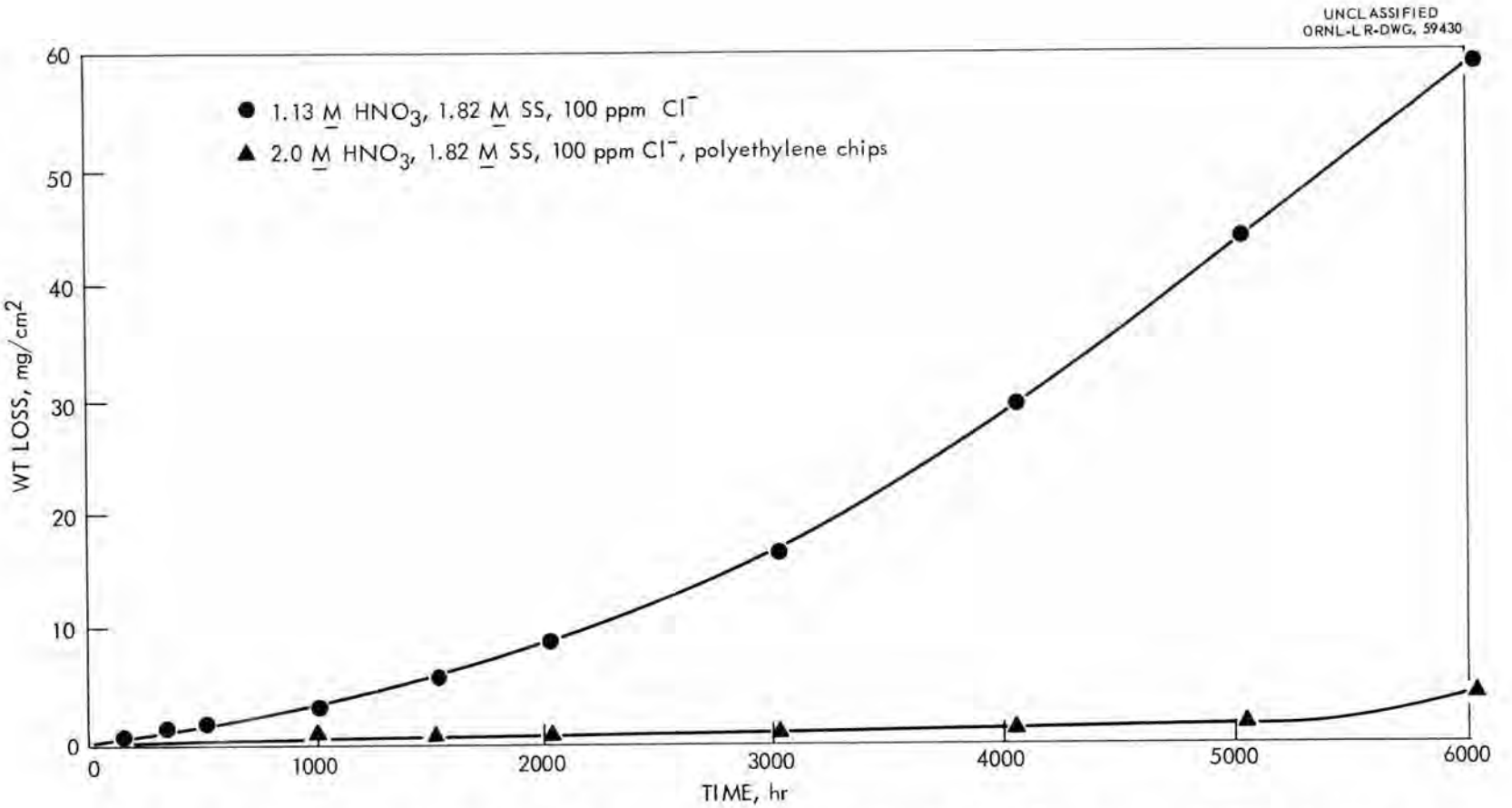

Fig. 17. Corrosion of welded type 304L stainless steel in simulated Darex-Purex type solutions at 80°C.

Table 26. Corrosion of Various Alloys in 90 Vol % 21 N HNO_3 - 10 vol % 40 N H_2SO_4 at 50°C

Alloy	Specimen Position	Corrosion Rate (mils/mo) 24 hr	96 hr	168 hr	336 hr	504 hr	672 hr
LCNA[a]	V			0.57-0.57	0.90-0.90		
	I			0.03-0.03	0.03-0.03		
	S			0.06-0.06	0.06-0.06		
LCNA (air swept)[b]	V			0.09-0.10	0.30-0.30	0.42-0.45	0.48-0.52
	S			0.05-0.04	0.05-0.06	0.06-0.06	0.06-0.06
INOR-8 (unwelded)	V			0.18-0.17	0.16-0.15	0.16-0.17	0.17-0.16
	S			0.25-0.26	0.15-0.17	0.13-0.12	0.11-0.10
CD4MCu (wrought)	V			1.74			
	S			0.02			
CD4MCu (cost)	V			1.41			
	S			0.03			
Nichrome V	V	0.14					
	I	0.19					
	S	0.20					
Carpenter 20 SCb	V	2.6					
	I	0.18					
	S	0.23					
Type 347 SS	V		4.1				
	I		0.06				
	S		0.07				
Type 304L SS	V		3.1				
	I		0.03				
	S		0.11				
Type[a] 309 SCb SS	V			1.7-1.9	2.8-2.9		
	I			0.3-0.17	0.03-0.10		
	S			0.03-0.02	0.04-0.03		

[a] These data were reported in the monthly progress report for Chemical Development Section B, March, 1961.

[b] Dry air was passed over the test solution to remove corrosive vapor.

Table 27. Corrosion of Welded Types 347 and 304L Stainless Steel Specimens in Simulated High-Acid Darex-Purex Waste Solutions[a] at 80°C

Test Period (hr)	Corrosion Rate (mpm)					
	347 SS			304L SS		
	V	I	S	V	I	S
168	0.01	0.17	0.29	0.02	0.18	0.29
336	0.01	0.18	0.32	0.01	0.17	0.27
570	0.01	0.22	0.43	0.01	0.17	0.29
739[b]	0.01	0.25	0.52	0.01	0.17	0.31
906	0.01	0.28	0.58	0.01	0.18	0.34
1074	0.01	0.30	0.63	0.01	0.19	0.36
1574	0.01	0.35	0.70	0.01	0.21	0.43
2074	0.01	0.41	0.78	0.01	0.25	0.51
3082	0.01	0.45	0.81	0.01	0.29	0.61
4082	0.01	0.51	0.90	0.01	0.36	0.75

[a] 5.0 M HNO_3, 1.82 M stainless steel, 100 ppm Cl^-.

[b] Onset of intergranular attack.

Table 28. Corrosion of Type 304L Stainless Steel in Simulated Darex-Purex Low-Acid Waste Solution[a] at 80°C

Test Period (hr)	Corrosion Rate (mpm)		
	V	I	S
168	0.03, 0.03	0.07, 0.07	0.09, 0.10
504	0.02, 0.02	0.08, 0.07	0.11, 0.11
1008	0.01, 0.01	0.08, 0.08	0.12, 0.12
1536	0.01, 0.01	0.09, 0.07	0.14, 0.14
2040	0.01, 0.01	0.09, 0.10	0.15, 0.16
3040	0.02, 0.01	0.11, 0.11	0.19, 0.20
4052	0.01, 0.01	0.13, 0.15	0.26, 0.27
5052	0.01, 0.01	0.16, 0.18	0.31, 0.32
6036	0.01, 0.01	0.17, 0.19	0.35, 0.36

[a] 1.13 M HNO_3, 1.82 M stainless steel, 100 ppm Cl^-.

Table 29. Corrosion of Type 304L Stainless Steel in Simulated Low-Acid Waste Solution[a] Containing Polyethylene Chips at 80°C

Test Period (hr)	Corrosion Rate (mpm)		
	V	I	S
168	0.02, 0.02	0.01, 0.01	0.01, 0.01
336	0.01, 0.01	0.01, 0.01	0.01, 0.01
504	0.01, 0.01	0.01, 0.01	0.01, 0.01
1008	0.01, 0.01	0.01, 0.01	0.01, 0.01
1536	0.01, 0.01	0.01, 0.01	0.01, 0.01
2040	0.01, 0.01	0.01, 0.01	0.01, 0.01
3040	0.01, 0.01	0.01, 0.01	0.01, 0.01
4052	0.01, 0.01	0.01, 0.01	0.01, 0.01
5052	0.01, 0.01	0.01, 0.01	0.01, 0.01
6036	0.01, 0.01	0.02, 0.02	0.02, 0.02

[a] 2.0 M HNO_3, 1.82 M stainless steel, 100 ppm Cl^-.

The intergranular attack characteristic of this solution on stainless steel is, if not eliminated, at least greatly postposed by the presence of the polyethlene.

4.3 Chloride Volatility System

Reaction of zirconium alloy fuels with gaseous HCl at elevated temperatures (Zircex) has been proposed and the corrosion encountered during cycling between the high temperature dry HCl and various concentrations of nitric acid has been investigated in some detail for various nickel and high cobalt alloys, particularly Haynes 25 and S-816 (26,27). This type of processing can in principle be utilized for processing other types of fuels by using other reactive gases. Thus graphite fuels can be burned in oxygen and ZrO_2 and certain other oxides can be volatilized by treatment with CCl_4 carried in an inert gas such as nitrogen. It would, of course, be desirable to find a material of construction which would be resistant to all of the gaseous reagents proposed plus the nitric acid solutions which would be used to remove the chloride and/or oxide "ashes" remaining after completion of the gas-solid reaction.

Haynes 25, Nichrome V, INOR-8 and Pyroceram 9608 were exposed to anhydrous HCl at temperatures of 200°, 350°, and 600°C. At 200°C none of these materials corroded at rates greater than 0.01 mil/mo; at 350°C at rates no greater than 0.25 mil/mo; but at 600°C maximum rates were 5.30, 5.36, 16.4, and 1.2 mils/mo, respectively (Tables 30 and 31). It was observed that the specimen of each alloy exposed in the "downstream" position of the gas stream corroded at a rate 1.5 to 3.5 times greater than the duplicate "upstream" specimen. The reason for this effect is not clear nor is the

Table 30. Corrosion Rates of Various Materials in Anhydrous HCl at 350°C

Test Period (hr)	Corrosion Rate (mpm) Material			
	Haynes 25	Nichrome V	INOR-8	Pyroceram
24	0.05, 0.23	0.06, 0.54	0.05, 0.09	<0.04
48	0.05, 0.13	0.09, 0.35	0.10, 0.12	<0.01
72	0.05, 0.20	0.02, 0.21	0.03, 0.07	<0.01
144	0.02, 0.20	0.02, 0.33	0.02, 0.06	<0.01
360	0.08, 0.25	0.05, 0.16	0.02, 0.03	<0.01

Table 31. Corrosion of Various Materials in Anhydrous HCl at 200 and 600°C

Test Period (hr)	Temperature (°C)	Corrosion Rate (mpm)[a]			
		Haynes 25	Nichrome V	INOR-8	Pyroceram 9608
192	200	0.01, 0.01	0.01, 0.01	0.01, 0.01	<0.01
34	600	5.30, 2.14	5.63, 1.52	10.8, 16.4	1.2[b]

[a]In every case the lower rate observed on duplicate specimens was an upstream specimen.
[b]Possibly reflects weight change due to chipping of edge.

increase in overall rate for Haynes 25 compared to the BMI results (26,27) entirely clear, though the BMI experiment employed an approximately equi-molar mixture of H_2-HCl with a slight amount of $ZrCl_4$ contamination vs the pure HCl used in these experiments.

Nickel, Haynes 25, Nichrome V, INOR-8, and Pyroceram 9608 corroded at maximum rates of 11.4, 35.2, 8.79, 27.1 and 0 when exposed for 24 hr in dry Cl_2 at 600°C (Table 32). In this case the differences between behavior of "upstream" and "downstream" alloy specimens were even more sharply marked than in the HCl case, the rate of the upstream specimens varying between 10 and 60 times that of those located downstream. At temperatures of 350°C and below, rates of all materials tested were less than 0.1 mil/mo. When these same materials were exposed to oxygen at 725°C for 188 hr all materials showed rates $\leq$0.1 mil/mo (Table 33).

Haynes 25, Nichrome V, INOR-8, and Pyroceram 9608 were exposed in a stream of nitrogen saturated (at room temperature) with CCl_4. Exposure temperatures were 300°, 450°, and 600°C. "Downstream" specimens of all materials failed (rates $\geq$100 mils/mo) at 600°C (Table 34). At 450°C maximum

Table 32. Corrosion of Various Materials in Dry Cl_2 at 200, 350, and 600°C for 24-hr Test Periods

Temperature (°C)	Corrosion Rate (mpm)[a]				
	Nickel	Haynes 25	Nichrome V	INOR-8	Pyroceram 9608
200	Weight Gain	Weight Gain	Weight Gain	Weight Gain	No change
350	0.04, 0.06	0.06, 0.08	<0.01,<0.01	0.03, 0.08	No change
600	1.08, 11.37	0.60, 35.20	0.38, 8.79	2.31, 27.14	No change

[a]In every case the lower rate was an upstream specimen.

Table 33. Corrosion of Various Materials in Oxygen at 725°C

Test Period (hr)	Corrosion Rate (mpm)[a]				
	Nickel	Haynes 25	Nichrome V	INOR-8	Pyroceram 9608
24	0.38, 0.18	0.10, 0.10	0.08, 0.12	0.06, 0.11	0
188	0.10, 0.02	0.02, 0.02	0.01, 0.01	0.01, 0.01	0

[a]All corrosion rates were calculated from weight-gain data.

Table 34. Corrosion of Various Materials in a Mixture of Nitrogen and Carbon Tetrachloride at 300, 450, and 600°C

(24-hr tests except as indicated)

Material	Test Temperature (°C)	Corrosion Rate (mpm)	
		Upstream	Downstream
Haynes 25	300	(+), 0.05	0, 0.12
	450	3.89, 1.86	7.33, 5.52
	600	1.20, a	5.89, a
Nichrome V	300	(+), 0.12	0, 0.11
	450	0.27, 0.35	0.95, 1.13
	600	0.07, a	1.51, a
INOR-8	300	0.03, 0.08	0.04, 0.07
	450	0.19, 0.24	1.16, 1.13
	600	0.13, a	2.57, a
Pyroceram 9608	300	b	(+), 0.01
	450	b	(+), 0.02
	600	b	0.42,107.6[c]

[a]Specimen consumed during 18 hr in test.
[b]Only one downstream specimen exposed during each run.
[c]18-hr test.

rates for these materials were 7.33, 1.13, 1.16, and 0.02, mils/mo, respectively. Again there was a tremendous increase in the corrosion rates of the "downstream" compared with the "upstream" specimens for exposures at 600°C.

Welded specimens of INOR-8 and Nichrome V were exposed in boiling 4 M HNO_3 to test their resistance during the "ashes dissolution" part of the fuel cycle (Table 35). INOR-8 failed immediately (rate ≥200 mils/mo) but Nichrome V showed a relatively steady maximum rate (vapor phase) of 0.22 mil/mo for 336 hr exposure. No localized attack was observed on the Nichrome V specimens.

Table 35. Corrosion of Welded INOR-8 and of Unwelded Nichrome V in Boiling 4.0 M HNO_3

Test Period (hr)	Alloy	Corrosion Rate (mpm) V	I	S
1.5[a]	INOR-8	16.5, 14.2	242,161	375, 235
168	Nichrome V	0.25, 0.04	0.10, 0.13	0.17, 0.15
336	Nichrome V	0.22, 0.11	0.11, 0.11	0.14, 0.13

[a]Solution had not reached reflux temperature; test terminated after 1.5 hr.

4.4 Multipurpose Aqueous PRFR Studies

Welded specimens of Haynes Alloy 6B were exposed to boiling initial Darex dissolver solution. Maximum rates for 72 hr exposures were 305, 26.5, and 10.6 mils/mo in vapor, interface, and solution phases, respectively, for the as-welded alloy (Table 36). This alloy obviously cannot be considered as a candidate material for construction of a Darex dissolver.

The solutions used for simulating pregnant UO_2 core dissolvent in multipurpose PRFR centrifuge tests at 35°C (23,28,29) were found to be unstable as prepared and to vary considerably in composition. Specifically the uranium concentration was found to vary from 1.04 to 1.34 M, the fluoride concentration from 2 x 10^{-4} to 1 x 10^{-2} M and the F/Zr mole ratio from 6.3 to 200. The variable corrosion results obtained, particularly with titanium are, therefore, not surprising, particularly in view of the wide range in the F/Zr ratio. Exposure of titanium in a solution of this general composition containing no fluoride resulted in a maximum corrosion rate of 0.03 mil/mo vs 1.0 mils/mo for one in which F^- = 0.063 M, Zr^{+4} = 0.01 M and Fe^{+3} = 0.06 M and vs 8.5 mils/mo for another in which F^- = 0.04 M and Zr^{+4} = 2 x 10^{-4} M.

Table 36. Corrosion of Haynes Stellite Alloy No. 6B in Refluxing Initial Darex Solution[a]

Test Period (hr)	Alloy Condition	Corrosion Rate (mpm) V	I	S
24	As-welded	49.36	30.06	10.14
	Solution-annealed	46.10	54.49	32.31
72	As-welded	304.75	26.47	10.63
	Solution-annealed	26.46	74.28	69.21

[a] 5.0 M HNO_3 - 2.0 M HCl.

5.0 MECHANISMS OF SEPARATIONS METHODS
(W. Davis, Jr.)

5.1 Radiation Damage to TBP--Amsco 125-82 Systems (Work performed at Stanford Research Institute on Contract AT(04-3)-115, Project Agreement No. 25) (W. Davis, Jr.)

Studies of the decomposition of ~1 M solutions of TBP in Amsco 125-82 by nominal 1 Mev electrons were continued using apparatus (30) in which the organic solution is recirculated through an external, aqueous nitric acid solution. This procedure maintains the organic acidity nearly constant whereas in previous studies (31) of the radiolysis of static solutions, much or all of the nitric acid was decomposed, thereby rendering calculated yields, such as G(-HNO_3) and G(HDBP), very uncertain. Even under these improved experimental conditions, considerable variations in yields of G(-HNO_3) and G(HDBP) were obtained in some cases (Table 37).

Radiolytic yields of dibutyl phosphoric acid formation, G(HDBP), Table 37, increase from ~1 to ~3 molecules/100 ev at a dose of 45 w-hr/liter as the nitric acid concentration in the organic phase increases from ~0.1 to ~0.7 M. At a constant acidity, the value of G(HDBP) at a dose of 135 w-hr/liter is only 60 to 80% of its value at 45 w-hr/liter. Yields of nitric acid decomposed, G(-HNO_3), are also dependent on the nitric acid concentration, increasing from 4-5 molecules/100 ev at an organic acidity of 0.1 M, to ~10 molecules/100 ev at an acidity of 0.7 M, all at a dose of 45 w-hr/liter. Within the limits of uncertainty of the present results (Table 37), which include a range of radiation power densities of 153-347 w/liter, G(-HNO_3) is independent of total dose.

Burger (32) has summarized data on the rates of thermal decomposition of TBP in diluent containing dissolved HNO_3 and H_2O. Although he does not have data for 1 M TBP in Amsco 125-82, he does present data for 20% TBP in kerosene (0.75 M) containing 0.14 M HNO_3, conditions close enough to those

Table 37. Electron Radiolysis Yields of Solutions of 1 M TBP in Amsco 125-82 Containing H_2O and HNO_3

HNO_3 Conc, M,		Dose Rate,	Dose	Yields, molecules/100 ev,		
Aqueous Phase	Organic Phase	w/l	w hr/l	G(-HNO_3)	G(HDBP)	G(H_2MBP)
0.796	0.126	167.3	45	5.55	1.18	0.076
0.772	0.116	220.2	45	4.82	1.16	0.12
0.776	0.116	220.2	45	4.00	1.21	0.10
0.865	0.0640	165.5	135	3.74	0.761	0.048
0.867	0.0645	165.5	135	3.73	0.806	0.038
0.874	0.0629	165.5	135	3.70	0.593	0.026
0.674	0.177	220.2	135	3.55	0.98	-
1.62	0.312	153.1	45	5.71	2.18	0.124
1.63	0.321	153.1	45	4.40	1.86	0.005
1.74	0.339	153.1	135	6.98	1.53	0.066
1.74	0.329	153.1	135	6.17	1.48	0.075
2.42	0.452	178.3	45	5.86	2.31	0.07
2.44	0.447	178.3	45	5.25	2.52	0.07
2.61	0.510	153.1	135	8.46	1.62	0.093
2.59	0.490	153.1	135	9.43	1.71	0.059
4.21	0.706	178.3	11.9	6.86	6.33	-
4.15	0.679	220.2	45	12.22	3.15	0.24
4.22	0.654	220.2	45	10.91	2.97	0.06
4.13	0.691	347.1	45	10.93	2.87	0.39
4.13	0.709	347.1	45	7.85	2.95	0.12
4.46	0.734	17.83	135	9.98	1.76	0.11
3.84	0.618	220.2	135	8.00	2.13	0.25
3.85	0.632	220.2	135	7.89	1.86	0.13
4.38	0.718	178.3	221	7.23	1.42	0.07
4.28	0.431	165.5	405	7.59	0.80	0.047

of the first 7 experiments in Table 37 to warrant comparison. At 21°, 30°, 50°, and 70°C, the first order TBP decomposition rate constants given by Burger are 0.058×10^{-5}, 0.11×10^{-5}, 0.48×10^{-5} and 2.3×10^{-5} hr^{-1}, respectively. At an organic phase electron power density of 1 w/liter, which is greater than that prevalent in present Purex operations but less than the 6.5 w/liter of Thorex short decay runs (33), the radiolytic decomposition of HNO_3, for $G(-HNO_3) = 5$ molecules/100 ev, occurs at the rate 1.8×10^{-3} moles HNO_3/l hr or 1.3×10^{-2} hr^{-1}; the corresponding yield of dibutyl phosphoric acid, for G(HDBP) = 1 molecule/100 ev, is $3.7 \times 0.75 \times 10^{-4}$, or 2.8×10^{-4} moles HDBP/l hr. This also corresponds to a TBP decomposition rate $>4 \times 10^{-4}$ hr^{-1}. Thus, the radiolytic decomposition of 1 M TBP containing ~0.1 M dissolved HNO_3 at 1 w/liter is approximately the same as that obtained by heating the solution to 100°C in the absence of radiation. Similarly, 0.01 w/liter corresponds to ~50°C in terms of TBP decomposition.

5.2 Foam Separation (E. Schonfeld at ORNL, on Subcontract 2024 with Radiation Applications, Inc.)

5.2.1 Distribution Coefficient of Ca-RWA-100 by Surface Counting. Variation of the distribution coefficient of calcium, $(\Gamma/c)_{Ca}$, with surfactant concentration in solutions of the surfactant RWA-100, a phenyl phenol sodium sulfonate, was determined by use of surface radioactivity measurements with Ca-45 tracer, as described previously (34). At a calcium concentration of 5×10^{-7} M, pH 7, and a RWA-100 concentration of 0.04-0.07 g/l, $(\Gamma/c)_{Ca}$ attained the very high value of 1.4×10^{-2} cm. However, a solution with concentrations such as these would not produce much foam and would be impractical in decontamination or metal recovery operations. At surfactant concentrations corresponding to ~50% of the critical micelle concentration of 2 g RWA-100/liter, $(\Gamma/c)_{Ca}$ is $\sim 4 \times 10^{-3}$ cm.

5.2.2 Surface Tension Measurements. Surface tensions of two series of 15 concentrations of cerous nitrate in RWA-100 were measured to compare the tendency of the Ce-RWA-100 complex to concentrate at the surface with similar tendencies of the H^+, Na^+, and Ca^{++} complexes, as previously reported (35). The sequestering tendency of the cerous complex, expressed as the constant α in equation 1, was the same as those for other complexes within experimental error. Values of α for the undissociated components of cation-sulfonate complexes determined from experimental data are as follows: H-RWA-100, $\alpha = 1.5 \times 10^6$ liter/mole; Na-RWA-100, $\alpha = 1.3 \times 10^6$ liter/mole; Ca-RWA-100, 1.6×10^6 liter/mole; Ce-RWA-100, $\alpha = 1.3 \times 10^6$ liter/mole.

$$\gamma_o - \gamma = b \log (1 + \alpha c) \qquad (1)$$

where γ_o and γ are surface tension of water and solution containing c moles of surfactant per liter, respectively, α and b are constants.

The fact that γ is essentially independent of cation, at least for the surfactant RWA-100, shows that if the concentrations, c's, of all complexes are equal, no cationic separation could be achieved by the foam process.

However, the concentrations of complexes, at constant cation concentration, vary greatly with cation valence. Thus, Na or Cs complexes are more than 90% dissociated into ions in the range of concentrations applicable to the foam process, while Ca, Sr, and Ce complexes are mostly undissociated. Therefore, separation of the latter three elements from Na or Cs is very efficient.

5.2.3 Foam Density Studies. A limited study of the effect of linear foam flow rate on foam density was initiated since the specific foam density is an important parameter in the foam column separation equation, expressed for a single stage column by equation 2,

$$\frac{\Gamma}{c} = k(E-1)\ lD, \qquad (2)$$

where Γ/c is the separation factor, cm,
k is a constant, 1/6 for spherical bubbles,
E is the enrichment ratio, i.e., (concentration of component in the foam condensate)/c,
l is the ratio of foam density to foam condensate density, and has dimensions ml condensed foam/ml foam or ml liquid product/ml foam,
D is the average equivalent bubble diameter, cm.

In this study three gas dispersion units were used, namely a capillary tube, a Spinarette cup with 50 micron holes, and an extra coarse sintered glass disc. Approximate diameters of bubbles in the foam produced by these units were 3.4, 0.75, and 0.37 mm, respectively.

From the data, Fig. 18, it can be seen that the foam density is very dependent on bubble size at high linear foam flow rates; as the linear rates decrease to 1 cm/min, or less, the foam density becomes essentially independent of bubble size. From photographs of the foam it was also concluded that as the linear rate decreases there is a growth in average bubble diameter up the column. Large bubbles grow at the expense of small ones, but mainly by a process that reduces the size of the small bubbles rather than by completely eliminating the small bubbles. The bubble growth rate decreases as the initial bubble uniformity increases. Values of foam specific surface area ranged up to 3×10^5 cm^2/cm^3 foam condensate, which corresponded to a very dry foam.

5.2.4 Removal of Cesium from Synthetic Hanford 1WW-NS. Cesium can be precipitated from the neutralized supernatant liquid of Hanford 1WW, i.e., from 1WW-NS, as a ferrocyanide (36). However, colloid formation causes difficulties. Since removal of Illite clay solids (37) improved as the particle size decreased, in the 200 mesh range, several tests were performed to determine whether the presence of colloidal or very small particles of the ferrocyanide could be converted to an advantage. For this purpose, to 80 ml of solution containing 6 M $NaNO_3$, 10^{-5} M $CsNO_3$,

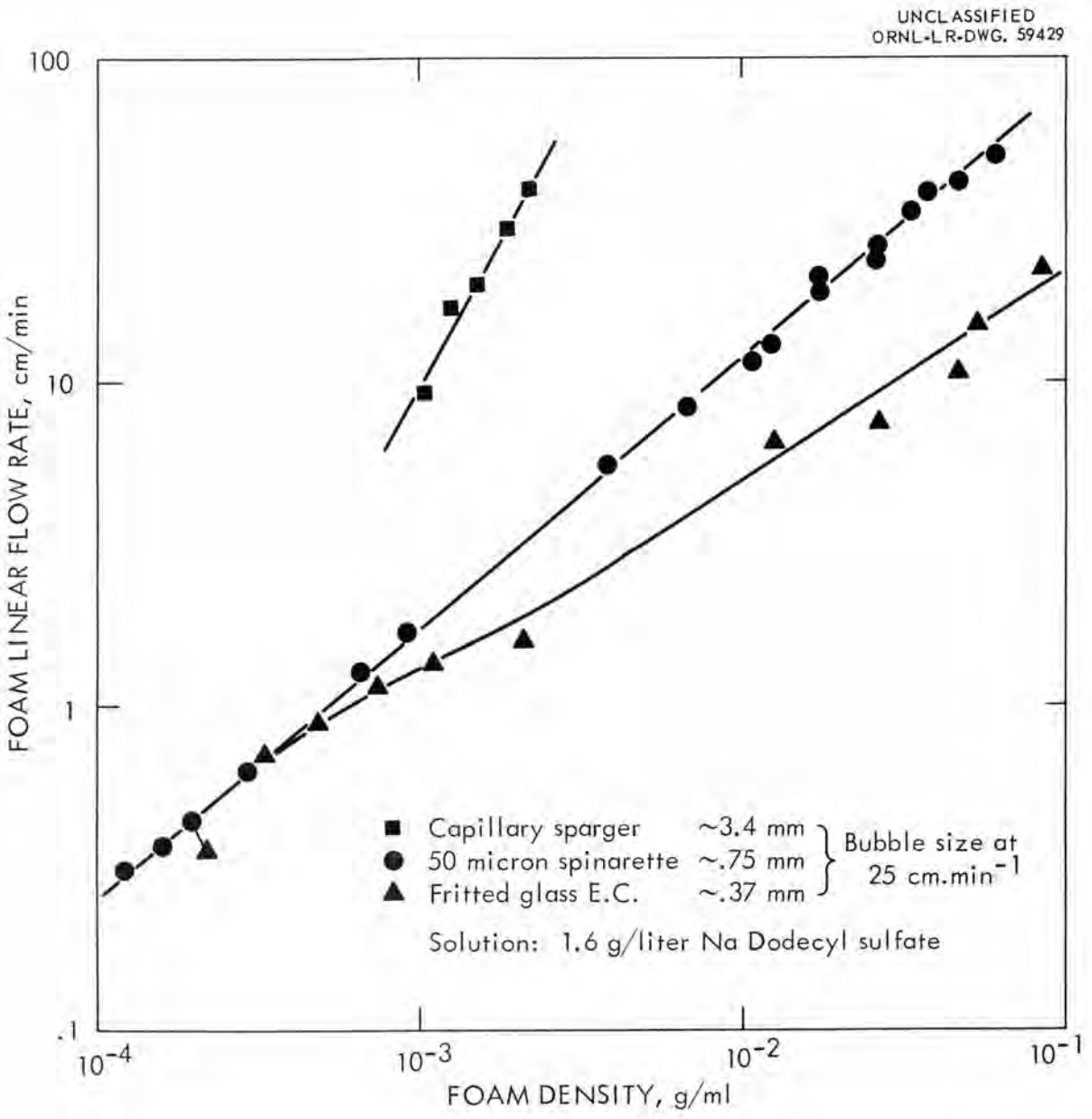

Fig. 18. Effect of foam linear flow rate on foam density.

and 1.92×10^{-4} M $K_4Fe(CN)_6$ was added during a 5-min interval 2.5×10^{-4} moles of $CuSO_4$ to produce 60 ppm of purple, solid $K_2Cu_3[Fe(CN)_6]_2$. After the addition of 65 ppm gelatin, which is a surfactant, the solution-suspension was sparged with nitrogen through a sintered glass dispersion tube. After 30 sec of sparging all visible color had been transferred from the liquid phase to the foam. After 3 min of sparging, the foam was allowed to collapse, thereby depositing the solid ferrocyanide on the glass wall, from which it was washed--without peptization--after removal of the bulk solution. Analyses of solution and solid for Cs-137 in four runs showed an average of 95% of the cesium in the solid, corresponding to a distribution coefficient, $K_D = 3 \times 10^5$ ml/g, or 3×10^5 counts $min^{-1}g^{-1}/(1 \text{ count } min^{-1}ml^{-1})$. The volume reduction factor was > 200. Cesium was subsequently converted to a nearly sodium-free, carrier-free solution by dissolving the precipitate in triethanolamine, sorption from the amine solution on Duolite S-30 ion exchange resin, and elution with 6.5×10^{-3} M HCl solution.

5.3 Distribution of Nitric Acid Between Aqueous and TBP-Amsco 125-82 Solutions (W. Davis, Jr.)

It was reported previously (38) that the extraction of 0-5 M HNO_3 from aqueous solutions by 5, 10, 15, 30, 65, and 100% TBP in Amsco 125-82 is accurately defined by equation (38), where square brackets refer to molal activities, parentheses to molal concentrations, and the subscripts org and aq to organic and aqueous phases, respectively. The constants a and b are functions of the ratio TBP/Amsco.

$$\log \frac{(HNO_3)_{org}}{[HNO_3]_{aq}\,(3.75493-(HNO)_{org})} = a + b\,(HNO_3)_{org} \qquad (1)$$

From analyses of the organic phases for water and nitric acid it is probable that the complexes $TBP \cdot H_2O$, $TBP \cdot HNO_3$, and $TBP \cdot HNO_3 \cdot H_2O$ are present, in addition to uncomplexed TBP, at lower acidities (0-2 M in the aqueous phase) and that $TBP \cdot 2HNO_3$ is present in significant quantities when the aqueous acidity is in the range 3-5 M. From these and material balance considerations, the quantity $(HNO_3)_{org}$ in equation 1 is described by equation 2, while the second significant term of equation 1, namely $(3.75493 - (HNO_3)_{org})$, is defined by equation 3 for the restricted nitric acid concentrations of these studies, (38) namely 0-5 M.

$$(HNO_3)_{org} = (TBP \cdot HNO_3)_{org} + (TBP \cdot HNO_3 \cdot H_2O)_{org} + 2(TBP \cdot 2HNO_3)_{org} \qquad (2)$$

$$(3.75493 - (HNO_3)_{org}) = (TBP)_{org} + (TBP \cdot H_2O)_{org} - (TBP \cdot 2HNO_3)_{org} \qquad (3)$$

Therefore, equation 1 is representative, at the lower acidities, of an overall equilibrium, such as equation 4, rather than representative of a single reaction between two separate species, as in equation 5.

$$\left.\begin{matrix} TBP_{org} \\ + \\ TBP{\cdot}H_2O_{org} \end{matrix}\right\} + HNO_{3\ aq} \rightleftharpoons \left\{\begin{matrix} TBP{\cdot}HNO_{3\ org} \\ + \\ TBP{\cdot}HNO_3{\cdot}H_2O_{org} \end{matrix}\right. \qquad (4)$$

$$TBP_{org} + HNO_{3\ aq} \rightleftharpoons TBP{\cdot}HNO_{3\ org} \qquad (5)$$

On the basis of this interpretation, the quantity a of equation 1 may be identified as $K_1^m\gamma_T$, when K_1^m is the overall equilibrium constant for reaction 4 and γ_T is the mean activity coefficient of TBP and TBP·H_2O in a water-saturated TBP-Amsco-H_2O solution. The quantity $K_1^m\gamma_T$ has values ranging from 0.27 to 1.51 kg H_2O/mole "TBP" as the TBP concentration in diluent increases from 5 to 100 vol %. The term "TBP" is used to refer to the sum of both species, TBP and TBP·H_2O, in TBP-Amsco-H_2O solutions.

5.4 Vapor Pressure of Tributyl Phosphate (A. Faure)

Measurements of the vapor pressure of nearly anhydrous TBP and of water-saturated TBP were attempted using two different techniques in order to obtain an estimate of the mean activity coefficient, γ_T, of TBP and TBP·H_2O in a water-saturated TBP solution (Sect. 5.3). The first method, involving measuring the gas phase beta activity of P-32 labelled TBP at 90-120°C, was abandoned because suitable corrections for the adsorption of TBP on the vessel and Geiger-Muller counter walls could not be determined. The second method, namely the transpiration method, involved saturating a known volume of air with vapor over the TBP or TBP-H_2O solution, condensing the TBP and water from the air stream by use of a dry ice trap, and then determining the quantity of TBP transported by standard, P-32 counting techniques. In each experiment the air volume was 10 liters, the specific activity 20 to 50 μc P-32/ml TBP, and the weight of TBP transported about 80 μg.

The measured vapor pressures of TBP at ~25°C over the nearly anhydrous (0.2 wt % H_2) or water saturated solution (Table 38) are lower by a factor of ~10 than the value of 6.7 microns calculated from the equation of Evans, Davis, and Jones (39). However, since this calculation involved extrapolation of the data of these authors from 150°C, and higher, down to 25°C, the calculated value is not considered reliable.

Since the solubility of water in TBP corresponds to a solution of ~50 mole % TBP, then the activity coefficient of TBP in the water-saturated

solution, i.e., γ_T, is approximately that given in equation 6, wherein the activity coefficient of anhydrous TBP is set equal to unity.

$$\gamma_T \simeq \frac{0.51}{0.80 \times 0.5} \simeq 1.3 \qquad (6)$$

Table 38. Vapor Pressures of TBP Over TBP-H_2O Solutions

System	Temp, °C	Vapor Pressure of TBP, microns
TBP-0.2 wt % H_2O	25.0	0.82
"	25.5	0.80
"	25.8	0.77
TBP sat'd with H_2O	25.0	0.515
"	25.2	0.509
"	25.1	0.513
"	25.0	0.512

6.0 WASTE TREATMENT
(W. E. Clark)

6.1 Waste Fixation in Borate and Phosphate Glasses (H. W. Godbee, K. L. Servis)

A series of glassy products were prepared from simulated high sulfate Purex waste (Table 39) with borate and phosphate fluxing agents. These solids melted, or softened, between 825 and 950°C depending upon the additives. They had densities ranging from 2.6 g/ml to 2.8 g/ml, representing between 4.9 and 6.9 gal of final solid per ton of uranium processed (40). Calcium and magnesium, as the oxides, were added to prevent sulfate volatility. In general, the magnesium mixtures melted lower (825-875°C) than the calcium mixtures (~950°C).

One of the more satisfactory products with borate and phosphate contained 21.5, 29.0, 6.4, and 8.7 wt %, respectively, of SO_3, P_2O_5, B_2O_3, and MgO (40). One of the better products with a phosphate flux contained 23.7, 31.9, and 9.5 wt %, respectively, of SO_3, P_2O_5, and MgO (40). A borate-phosphate glass was produced from TBP-25 waste (Table 39). The mixture softened at ~900°C and was prepared by adding 1.52, 0.13, and 1.58 moles, respectively, of H_3PO_3, borax, and NaOH to 1 liter of waste.

Table 39. Composition of Simulated High-Activity Wastes

Component (moles/liter)	Purex	TBP-25
Al^{3+}	0.1	1.6
Fe^{3+}	0.5	0.002
Cr^{3+}	0.01	
Hg^{++}		0.01
Ni^{++}	0.01	
NH_4^+		0.07
H^+	5.6	0.5
Na^+	0.6	
Ru	0.002	
NO_3^-	6.1	5.35
$SO_4^=$	1.0	0.026

Leach tests in distilled water were made on a borate-phosphate glass* containing Purex waste oxides. The leach rate for this glass decreased from an initial rate of 3.2×10^{-2} g $cm^{-2}day^{-1}$ to 6.6×10^{-5} g $cm^{-2}day^{-1}$ at the end of 37 days. The leach rate was determined by gamma counting of the Cs-137 in the leachate.

6.2 Ruthenium Volatility (H. W. Godbee, K. L. Servis)

Experiments were carried out in small glass equipment (40) at temperatures up to 500°C to study the effect of phosphite addition on ruthenium volatility.

Orthophosphorous acid (H_3PO_3) was added to the system to decrease ruthenium volatility; MgO or $Ca(OH)_2$ was added to decrease sulfate volatility. Monobasic sodium phosphate ($NaH_2PO_4 \cdot H_2O$) and borax ($Na_2B_4O_7 \cdot 10H_2O$) were added as fluxing agents. The solution fed to the evaporator was Purex waste (Table 39) containing the various additives (Table 40).

Two different modes of adding the H_3PO_3 were used. In three experiments (Expts. 1,6, and 7, Table 40) all of the H_3PO_3 was added to the feed solution previous to evaporation. In four experiments (Expts. 2,3,4, and 5, Table 40) a portion of the H_3PO_3 was added to the feed solution before evaporation

*One liter of Purex plus 1.52, 0.80, 0.26, and 1.84 moles, respectively, of H_3PO_3, MgO, borax, and NaOH.

Table 40. Ruthenium Volatility from Simulated Purex Waste[a]

Expt. No.	Additives, moles/liter							Ru Material Balance, %					% NO_3^- in Pot When H_3PO_3 Added	% NO_3^- in Residue (Calc'd)
	Initial H_2PO_3	H_3PO_3 After Feed	$Na_2B_4O_7 \cdot 10H_2O$	$NaH_2PO_4 \cdot H_2O$	NaOH	MgO	$Ca(OH)_2$	Condensate	Bubblers	HNO_3 Wash	Residue	Total		
1	0.40	-	0.13	1.12	0.46	0.80	-	4.92	6.00	8.56	85.47	98.95	-	42
2	0.10	0.30	0.13	1.12	0.46	0.80	-	1.38	0.00	Flask containing residue broke			60	35
3	0.05	0.35	0.13	1.12	0.46	0.80	-	9.41	0.09	12.76	74.01	96.27	-	-
4	0.05	0.35	0.13	1.12	0.46	0.80	-	12.23	0.17	8.68	79.79	100.87	72	30
5	0.05	0.35	0.13	1.12	0.46	-	0.80	7.77	0.28	7.63	73.78	93.46	73	44
6	0.60	-	0.13	0.92	0.67	-	0.80	4.03	0.35	13.11	63.1	80.59	-	52
7	0.80	-	0.13	0.72	0.87	-	0.80	1.31	0.09	12.20	87.29	100.89	-	30

[a]Purex composition (M): 6.1 NO_3^-, 5.1 H^+, 1.0 SO_4^{2-}, 0.6 Na^+, 0.5 Fe^{3+}, 0.1 Al^{3+}, 0.01 Cr^{3+}, 0.01 Ni^{2+}, 0.002 Ru, with 0.1 μc Ru-106 per ml.

and the remainder added at the end of the feeding period. The results, 1.31-12.23% Ru volatilized, indicate that ruthenium volatilization depends not only on the total H_3PO_3 added but also on when during the evaporation the H_3PO_3 is added. The bulk of the ruthenium is volatilized at the higher temperatures, 150-500°C, when the nitrate salts in the waste begin to decompose. The substitution of $Ca(OH)_2$ for MgO as an addition compound in the mix appeared to produce no significant change in the Ru volatility.

6.3 Low Level Waste Treatment (R. R. Holcomb)

A small pilot plant (Fig. 19) was constructed at the site of the present ORNL low-level waste treatment plant for demonstrating the phenolic ion-exchange process. Operation of this unit has successfully demonstrated reduction of radioactivity in ORNL wastes to less than 10% of MPC_w of individual isotopes studied for 168 hr week (Table 41).

The units of the semi-pilot plant in sequence are a flash mixer, flocculator, sludge-blanket clarifier, anthracite filter, polishing filter, and ion exchange column. The ion exchange resin was Duolite CS-100, a carboxylic-phenolic resin. The waste water was made 0.01 M in NaOH and 5 ppm in iron to provide a scavenging precipitation. After precipitation, feed clarification was excellent. An effluent with 3 ppm turbidity and 8 ppm total hardness as $CaCO_3$ was produced. Decontamination factors were equal to or better than design specifications and confirmed laboratory-scale results, i.e., decontamination factor for strontium >1000 and cesium >100 for an overall volume reduction of ~3000. Gross β activity in effluent was 54% of the MPC_w, assuming 100% Sr-90, for 168 hr week and strontium and cesium 1% or less of the MPC_w for a 168 hr week.

7.0 ION EXCHANGE
(W. Davis, Jr.)

7.1 Fission Product Recovery by Ion Exchange (W. C. Yee)

The presence of 1 M $SO_4^=$ in 1WW Purex waste solution interferes with a direct recovery of strontium by precipitation at 80-85% nitric acid as predicted for an all-nitrate system (41). Excess ferric ion was added to the synthetically prepared waste solution to precipitate >85% of the sulfate at 50-55% HNO_3 as iron sulfate (Table 42a). Analyses of the experiments which included the radioactive tracers Ce^{144}-Pr^{144}, Fe^{59} and Sr^{85} indicated that >90% of the strontium and >50% of the rare earths remained in solution (Table 42b). Ferric ion was added in the form of freshly precipitated $Fe_2O_3 \cdot xH_2O$. An alternative method involves dehydration of $Fe(NO_3)_3 \cdot 9H_2O$ to a boiling temperature of 130-140°C. This dehydrated ferric nitrate can be added directly to the 1WW Purex.

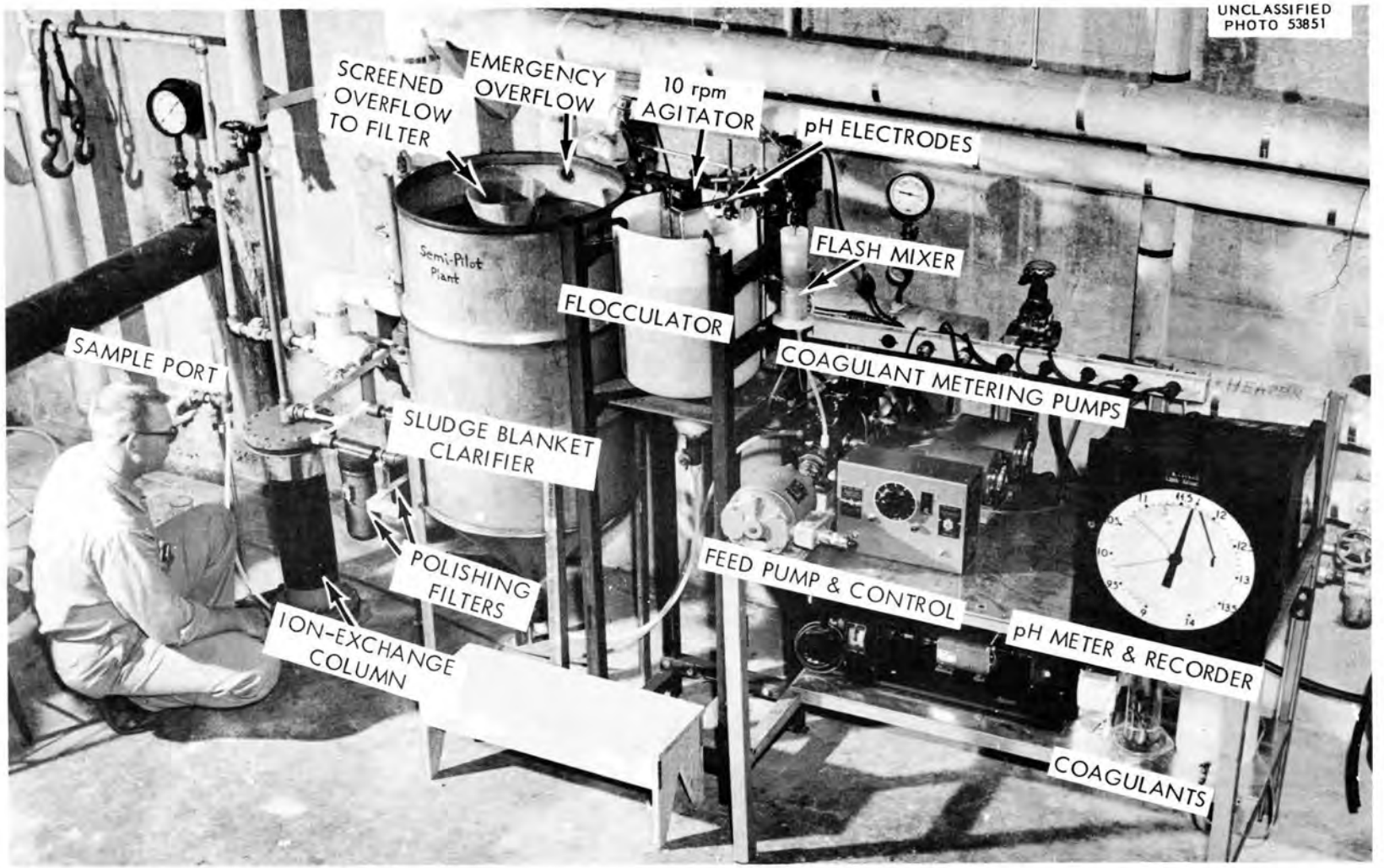

Fig. 19. Semi-pilot plant for demonstration of ion-exchange treatment of low level process waste water.

Table 41. Decontamination of ORNL Low-Level Waste by the Scavenging-Ion Exchange Process: 60 liters/hr Pilot Plant Tests

Code	Radiochemical			Gamma Spectrometry ($d\ ml^{-1}min^{-1}$)				
	Gr β ($c\ ml^{-1}min^{-1}$) (96% geometry)	TRE β ($c\ ml^{-1}min^{-1}$) (22.3% geometry)	Sr β ($d\ ml^{-1}min^{-1}$)	Ru-106	Cs-137	Zn-65	Co-60	Zr-Nb-95
SPP Run 1								
Feed	28	27	92	6.6	20	7.4	5.4	
Effluent (300 bed vol)	1.1	0.17	0.02	2.1	None detected	None detected	2.1	
SPP Run 2								
Feed	35.3	32	94	6.5	21	Trace	4.6	10
Effluent (1398 bed vol)	1.3	0.3	0.04	1.8	None detected	None detected	2.4	None detected
SPP Run 3								
Feed	46.0	4.50	123.20	6.24	22.14	Trace	6.74	
Effluent (1587 bed vol)	6.1	0.185	0.07	1.97	0.24	Trace	2.94	

Table 42. Sulfate Precipitation from 1WW Purex-Nitric Acid Solutions[a]

A. Sulfate Distribution - Wet Analysis

HNO_3 Conc. (Wt %)	$SO_4^=$ in Synthetic 1WW (moles/liter)	$SO_4^=$ in Products by Wet Analysis		
		Solution (moles/liter)	Precipitate (% Total)	Material Balance (Wt %)
46.6	0.987	8.31×10^{-2}	42[b]	71
50.9	0.987	2.22×10^{-2}	85	93
54.1	0.987	2.16×10^{-2}	88	97
54.8	0.987	1.73×10^{-2}	89	96

B. Strontium and Iron Distribution - Radioactive Trace Analysis

HNO_3 Conc. (Wt %)	Total Activity in Synthetic 1WW (cpm)	Cation in Products by Tracer Analysis		
		Total Activity in Solution (%)	Total Activity in Precipitate (%)	Material Balance (%)
		Strontium - Sr^{85}		
46.6	4.35×10^7	114	4[b]	118
50.9	4.31×10^7	102	6	108
54.1	4.54×10^7	99	8	107
54.8	4.21×10^7	105	9	114
		Iron - Fe^{59}		
46.6	1.09×10^7	91	17[b]	108
50.9	1.14×10^7	81	29	110
54.1	1.29×10^7	83	32	115
54.8	1.11×10^7	80	31	111

[a] Each solution was prepared by (1) adding ~90 g freshly prepared $Fe_2O_3 \cdot xH_2O$ to 100 ml of synthetic 1WW, (2) stirring for 24 hr to insure the presence of excess Fe^{+3}, (3) diluting with enough fuming nitric acid to the indicated HNO_3 concentrations, and (4) stirring for at least 48 hr to approach equilibrium conditions.

[b] Precipitate was only partially recovered.

The nearly-sulfate-free filtrate for the run, containing 54.1% HNO_3, was reduced to the point of nitrate decomposition (residue temperature of ~130°C) and diluted with 90% nitric acid to 63% HNO_3. By heating the precipitated solution to 65-70°C, it was possible to achieve separation of strontium from the major cationic impurities, iron and aluminum (42). Radiochemical analyses indicated that about 85% of the strontium precipitated with <10% of the original iron in the product. Wet chemical analyses showed that ~30% of the original aluminum was present in the strontium nitrate precipitate. At >80% HNO_3, it should be possible to obtain a strontium product with <10% aluminum (42).

Dissolution of the precipitate in 6 M HNO_3, gives a solution which can be processed by conventional ion exchange techniques to separate strontium from the remaining cationic impurities.

7.2 Radiation Damage to Ion Exchange Resins (W. C. Yee)

Strong Acid Resin-Amberlite 200 (16-50 mesh)

A relatively new, strongly acidic, cation exchange resin, Amberlite 200, was tested for radiation stability. Some of the merits claimed (43) for the resin by its manufacturer, Rohm and Haas Company, include 1) highly crosslinked yet porous bead structure, which gives a higher rate of ionic diffusion (or exchange) than other comparable and commercially available sulfonated styrene-divinylbenzene co-polymers, 2) good resistance of particles to oxidative attack, and 3) good bead integrity. Reported sodium form capacity of the highly crosslinked Amberlite 200 was 4.3 meq/gram of dry resin, which is almost equal to the capacity of an 8% crosslinked resin, Amberlite IR-120 (4.4 meq/gram of dry resin). Reported increase in moisture content (a measure of oxidative attack on the resin particle) of commercially available standard and highly crosslinked premium grade resins was 5.0 and 2.3 times greater, respectively, than Amberlite 200 after contacting each of these resins with 3% hydrogen peroxide at 45°C for 72 hr. Reported particle breakdown of these resins was 6-15 and 2-4 times greater, respectively, than Amberlite 200 after a number of drying and rewetting cycles. If the above claimed properties contribute to increased stability to radiation, such a resin could probably be quite useful in radiochemical processing.

Prior to irradiation, Amberlite 200 was treated with 1 M NaOH, ethyl alcohol, and 1.36 M (5%) HCl, with water rinses after each of these. Demineralized water, of specific resistance >1 meg ohm-cm, was circulated through a fixed bed of the resin at a rate of ~4 ml/min during irradiation in the 10,000 curie cobalt-60 source. The effluent solution was passed through a sintered glass disk to filter out particulate matter, through a series of conductivity cells which continuously monitored the concentration of ionic radiation degradation products in the stream (Fig. 20), and through a column of dyed anion exchange resin which was changed at various intervals to obtain rate data on the formation of these resin decomposition products. The pH of the effluent was recorded continuously by allowing a side stream to flow through a teflon cell (~0.1 ml/min) containing miniature glass and calomel electrodes (Fig. 20).

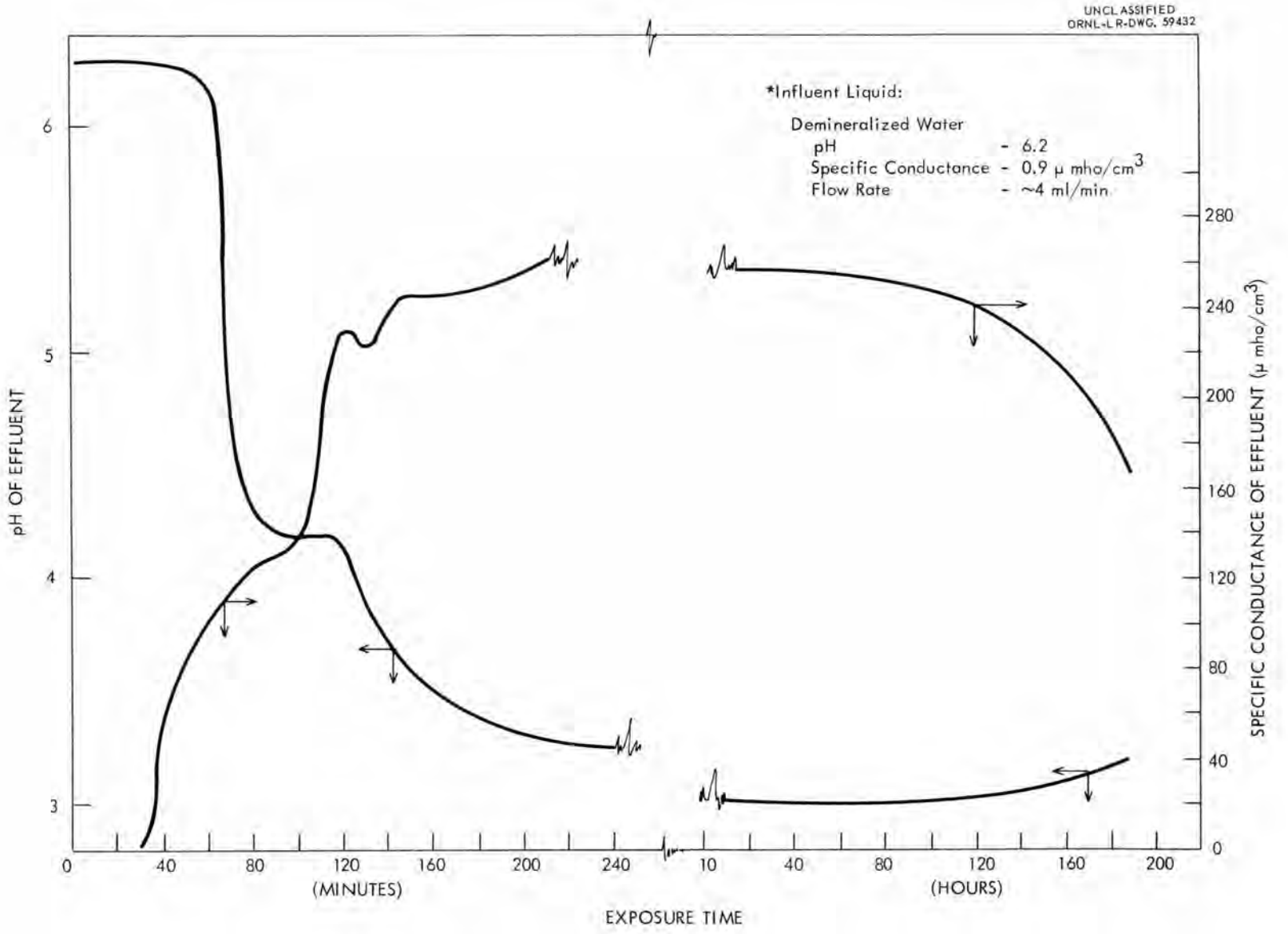

Fig. 20. Resin radiation experiment - flowing system. pH and specific conductance of effluent* from Amberlite 200 being exposed to gamma-radiation.

After an exposure of 0.82×10^9 r (2.2 watt hr/gram of dry resin), only 2 vol % of the highly crosslinked Amberlite 200 was lost. As a comparison, the lower crosslinked Dowex 50W X-8 resin lost 20 vol % (Table 43) after an exposure of 0.85×10^9 r (2.3 watt hr/gram of dry resin). Analyses are being made to determine the changes in the properties of the exposed resin and the types and amounts of radiation degradation products in the effluent collected.

Strong Acid Resin - Dowex 50W X-8 (20-50 mesh)

Analyses were made on Dowex 50W X-8 (20-50 M) resin which had been exposed, as described in the previous section, to γ-radiation doses of 0.85×10^9 and 3.9×10^9 r (2.3 and 10.6 watt-hr/gram of dry resin, respectively). Quantitative results of resin moisture content, capacity, sulfur analysis and sulfur sorbed on the anion resin column as $SO_4^=$ are summarized in Table 43. Qualitative analyses of the effluent stream prior to entering the anion resin column indicated the presence of $SO_4^=$ and polybasic organic acids.

Discrepancies exist between capacity and moisture content analyses of the Dowex 50W X-8 (20-50 mesh) resin exposed in the cobalt-60 source and Dowex 50W X-12 (100-200 mesh) resin used by Isotopes Division (44) to recover Pm^{147} — a beta emitter—from a mixture of rare earths. The 12%

Table 43. Summary of Data on Irradiated Dowex 50W X-8 (20-50 mesh) Resin[a]

	Original Resin	After One Week Irradiation	After One Month Irradiation
Radiation dose, r	-	0.85×10^9	3.9×10^9
watt-hr/g dry resin	-	2.3	10.6
Resin density, g dry resin/ml wet resin	0.386	0.418	0.25
Weight loss (dry basis), %	-	12	95.7
Moisture content, wt %	42.7	38.6	55.1
Sulfur content, wt %	15.7	12.9	7.0
Capacity, meq/g dry resin			
by titration	4.96	2.89	1.89
by sulfur analysis	4.90	4.03	2.18
Resin volume lost, vol %	-	20	85
Sulfur recovered as $SO_4^=$ from anion resin, meq	-	4.9	17.8
Sulfur recovery, %	-	80	64

[a]Radiation density 0.014 watt/g dry resin.

crosslinked irradiated resin, whose complete history is not known, was exposed to a calculated dose of 12-13 watt-hr/gram of dry resin. Its total capacity was found to be about 5 meq/gram of dry resin— unchanged from the original resin. Its moisture content increased from ~40% to ~70%, indicating a decrease in resin crosslinkage from 12% to 4%. The 8% crosslinked resin, exposed under known conditions to 10.6 watt hr/gram of dry resin, lost capacity, from 4.9 to 1.9 meq/gram of dry resin and increased in moisture content from 43% to 55%. The differences between the properties of the two irradiated resins remains to be resolved.

8.0 CHEMICAL APPLICATIONS OF NUCLEAR EXPLOSIONS (CANE)
(W. D. Bond)

This program is concerned with utilizing contained thermonuclear explosives for the production of desirable isotopes. Laboratory work has been confined to chemical and isotopic exchange studies of the isotope,tritium. Rock salt is considered the best containment medium for isotope production. The major impurities in the medium are sulfates of calcium, magnesium and potassium.

Work has continued on studies of tritium exchange in the reaction, $HTO + H_2 \longrightarrow H_2O + HT$, with $CaSO_4$ catalyst. The exchange studies under diffusion controlled conditions were completed and have been extended to forced flow of reactants through fixed beds of $CaSO_4$. The exchange is being studied by the two methods so that, at least, qualitative numbers may be obtained for conditions of poor contacting and of very good contacting of reactants with catalysts. Apparatus has been designed for a study of exchange in the D_2-H_2O system in a plasma jet. Plasma jets produce temperatures of 10-15,000°K which is sufficient to simulate temperatures that effect chemical changes in nuclear explosions. An apparatus for studying the D_2-H_2O system is being designed so that it may be of general utility for studying chemical reactions in plasma jets and thereby will contribute to the technology of plasma jet chemistry.

8.1 Diffusion Controlled Exchange of Tritium

The exchange of tritium was diffusion controlled when a gaseous mixture of HTO-H_2-H_2O was passed over layers of $CaSO_4$. The experimental equipment has been described in detail previously (45). The exchange increased with increasing temperature and with increasing mass of $CaSO_4$ (Table 44). The exchange was independent of $CaSO_4$ surface area and practically independent of reaction tube volume. The effect of increasing the mass of $CaSO_4$ is equivalent to decreasing the distance between the reactant gas entry point and the surface of the $CaSO_4$ layer (Table 45). The apparent activation energy calculated from the Arrhenius equation is 8.8 ±1.0 kcal. These data show that the reaction is undoubtedly controlled by rate of diffusion in the gas phase when the HTO-H_2-H_2O mixture is passed over layers of $CaSO_4$.

Table 44. Exchange for the Reaction, $HTO + H_2 \longrightarrow HT + H_2O$, Using $CaSO_4$ Catalyst

Initial flow rates, moles/min: $H_2 = 6.5 \times 10^{-3}$, $H_2O = 4.5 \times 10^{-4}$, $HTO = 4.1 \times 10^{-11}$, $He = 9.0 \times 10^{-3}$

Temp, °C	Mass of $CaSO_4$ g	Surface Area m^2/g	Furnace Tube Vol[a] cc	Steady State Exchange $\frac{\text{moles of } (H_2O + HTO)}{\text{min}} \times 10^5$	Percentage Exchanged at Steady State mole %
600	1.00	0.82	35	3.14	6.98
600	1.00	0.82	35	3.23	7.18
600	1.00	10.0	35	2.65	5.89
600	3.03	0.82	35	6.01	13.35
600	3.03	10.0	35	5.13	11.40
600	3.03	0.82	315	6.11	13.55
600	3.03	10.0	315	7.30	16.22
600	6.03	10.0	35	7.38	16.40
600	6.03	10.0	315	10.52	23.38
600	8.25	0.82	315	8.84	19.64
600	12.03	10.0	315	11.59	25.75
700	1.00	0.82	35	5.75	12.78
700	1.00	10.0	35	5.88	13.07
700	3.03	0.82	315	9.82	21.82
380	3.03	0.82	315	0.93	2.07

[a]Tube 35 cc volume = 2.0 cm ID, 315 cc tube = 4.0 cm ID.

Table 45. Effect of Distance of Entrance Gas Line to Edge of Sample

Initial flow rates, moles/min: $H_2 = 6.5 \times 10^{-3}$, $HTO = 4.1 \times 10^{-11}$
S.A. = 10.0 m^2/gm, $H_2O = 4.5 \times 10^{-4}$, He = 9.0

Distance of Gas Entry Tube to Sample, cm	Mass of $CaSO_4$ g	Steady State Exchange $\frac{\text{moles } (HTO + H_2O)}{\text{min}} \times 10^5$	Percentage Exchanged at Steady State mole %
3.0	6.03	5.39	12.0
3.0	3.03	5.13	11.4
1.3	6.03	7.38	16.4
4.0	1.00	2.65	5.9

8.2 Exchange Studies with Forced Flow

Tritium exchange was greatly increased when the reactant gases are allowed to flow through fixed beds of $CaSO_4$ (Table 46). The $CaSO_4$ used was technical grade but was pretreated with hydrogen prior to the exchange experiments. The surface area of the material was not measured. Steady state exchange was achieved in about 40 min. The theoretical equilibrium exchange was not achieved in any of the experiments (Fig. 21). On the basis of these preliminary experiments, it appears that increasing the bed length above 3 in. does not appreciably increase the exchange.

Table 46. Exchange for Reaction, $HTO + H_2 \longrightarrow HT + H_2O$, Over Fixed Beds of $CaSO_4$

Bed dia = 1 in.
Flow rates, moles/min: $H_2 = 6.5 \times 10^{-3}$
$H_2O = 4.5 \times 10^{-4}$
$HTO = 4.1 \times 10^{-11}$
$He = 9.0 \times 10^{-3}$

Bed Length in.	Mesh Size[a]	Steady State Exchange $\frac{\text{moles}(H_2O + HTO)}{\text{min}} \times 10^4$	Percentage Exchange at Steady State mole %
12	10-20	2.54	56.5
12	10-20	2.52	56.0
12	20-30	3.16	70.2
6	20-30	3.23	71.7
6	20-30	3.23	71.7
3	20-30	2.96	65.8

[a] 10-20 mesh = .84 50 2.0 mm particles.
20-30 mesh = .59 50 .84 mm particles.

Future work will be concerned with a systematic study of beds of $CaSO_4$ powders of known surface area to determine the exchange kinetics.

8.3 Plasma Jet Experiments

The isotopic exchange of deuterium in the D_2-H_2O system will be studied in an argon plasma jet temperature of 10-15,000°K. The parameters are to be concentration, temperature and residence time. However, before actual experimentation with the exchange system, apparatus and techniques for injection of reactants into the plasma and the collection of products must be developed. The apparatus is shown schematically in Fig. 22. Deuterium

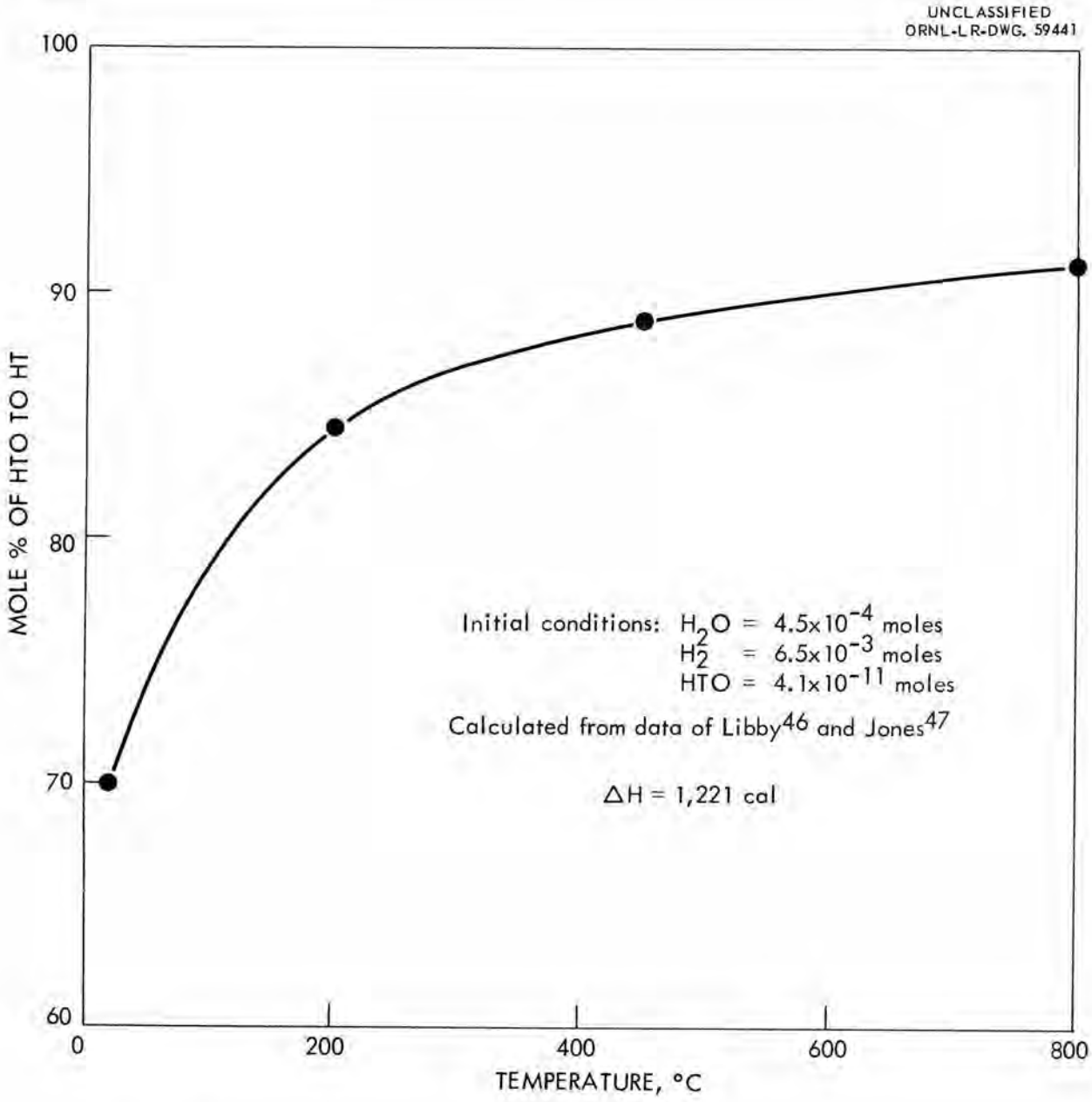

Fig. 21. Theoretical exchange in the reaction, $HTO + H_2 \longrightarrow HT + H_2O$.

and ordinary water are introduced into an argon plasma at 10-15,000°K, and the plasma is then cooled by a cooling chamber so that the water may be completely recovered by a condenser. The water is then analyzed for deuterium content. Equipment has been designed by A. M. Rom and is now being constructed (Fig. 23). The plasma jet nozzle is connected to the quartz tube via a water-cooled brass adaptor and o-ring seal. The quartz tube is utilized to cool the plasma and is able to exchange the heat to the surrounding atmosphere effectively. The inside wall temperature at a point >4 ft from the nozzle should be cooled sufficiently to collect products in receivers such as cold traps (Table 47).

Table 47. Inside Wall Temperature of Quartz Argon

Flow rate = 5 SCFH
Low momentum nozzle
F-40 torch

Power kw	Time min	Thermocouple Used	Temp, °F
150	6	2	70
15	9	2	70
15	12	2	70
15	3	1	210
15	6	1	240
15	9	1	280
15	12	1	280
15	15	1	290
21.5	1	1	200
21.5	3	1	240

Teflon or Neoprene o-rings at the quartz-brass connection failed because of the impinging radiant energy from the jet. Severe thermal decomposition was observed after 15 min operation at 15 kw. The brass adaptor is being modified such that a radiant shield of metal protects the o-ring.

It appears that a leak-tight system for studying gaseous reactions with a plasma jet can be made. Such apparatus alone will be a significant contribution to plasma jet chemistry.

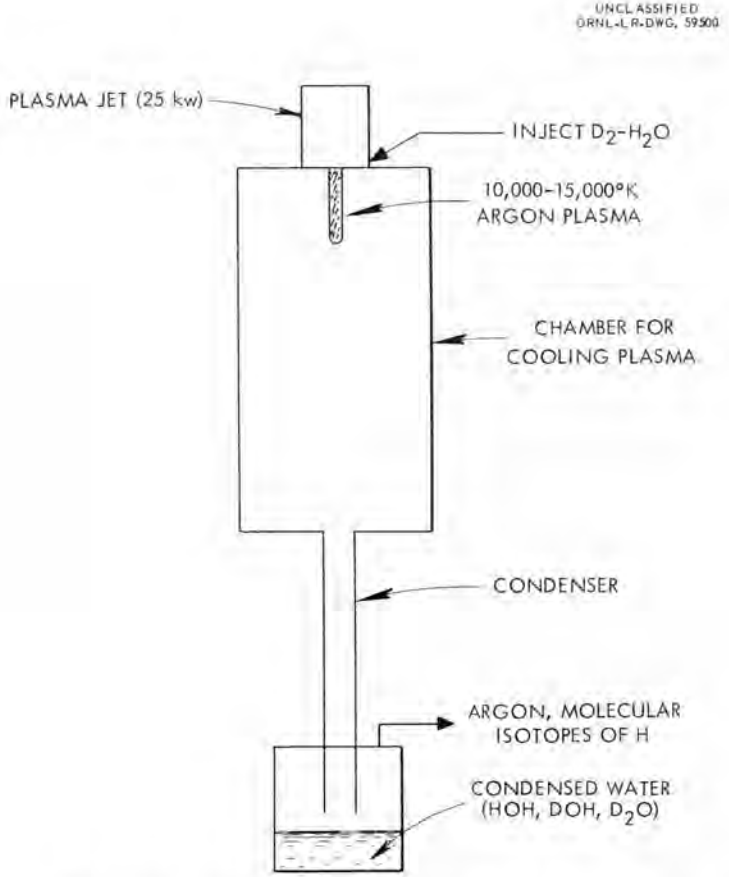

Fig. 22. Schematic of apparatus for plasma jet studies.

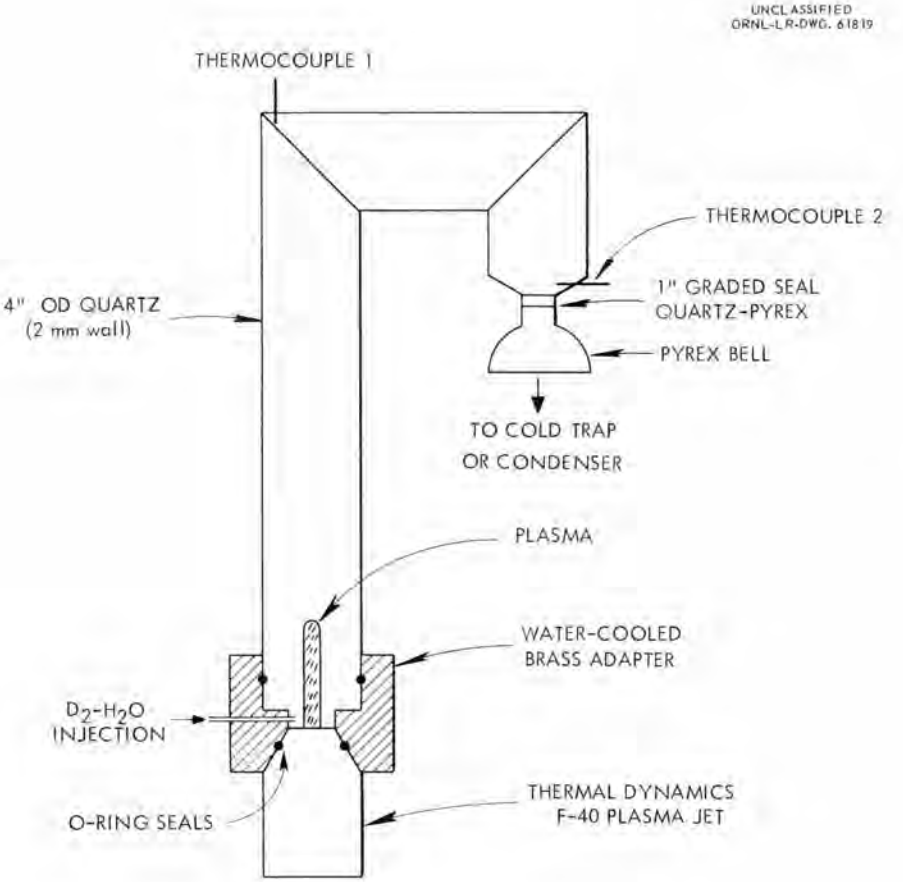

Fig. 23. Experimental apparatus.

9.0 REFERENCES

1. M. J. Bradley and L. M. Ferris, Ind. Eng. Chem., 53: 279 (1961).

2. M. J. Bradley and L. M. Ferris, Nuclear Sci. and Eng., 8: 432 (1960).

3. R. E. Blanco, "Monthly Progress Report for Chemical Development Section B, December 1960," ORNL-CF-60-12-100 (May 15, 1961).

4. "Quarterly Status Report on TURRET Reactor Experiment for Period Ending August 20, 1960," LAMS-2469 (Oct. 20, 1960).

5. M. J. Bradley and L. M. Ferris, "Processing of Uranium Carbide Reactor Fuels," ORNL-3101, (August 1961).

6. L. M. Litz, "Uranium Carbides - Their Preparation, Structure and Hydrolysis," PhD Thesis, Ohio State University, NP-1453 (1945).

7. "Proceedings of the Uranium Carbide Meeting," TID-7603, December 1960.

8. R. E. Blanco, "Proc. AEC Symposium for Chemical Processing of Irradiated Fuels from Power, Test, and Research Reactors," Richland, Washington, Oct. 20-21, 1959, TID-7583, p. 250.

9. T. A. Gens and R. L. Jolley, "New Laboratory Developments in the Zircex Process," ORNL-2992 (April 1961).

10. T. A. Gens, "An Oxyhydrochlorination Process for Preparing Uranium-Molybdenum Reactor Fuels for Solvent Extraction," ORNL-3019 (May 1961).

11. E. R. Johnson, L. M. Levy, R. L. Maddox, and J. Blum, "Oxidation of Chlorides in Raffinate Materials," FMPC-207 (April 1953).

12. R. H. Rainey and J. G. Moore, "Laboratory Development of the Acid Thorex Process for the Recovery of Consolidated Edison Thorium Reactor Fuel," ORNL-3155 (in press).

13. "Chemical Development Section C Progress Report, October-November, 1960," ORNL-CF-60-11-126.

14. L. M. Ferris and A. H. Kibbey, "Sulfex-Thorex and Darex-Thorex Processes for the Dissolution of Consolidated Edison Power Reactor Fuel: Laboratory Development, ORNL-2934.

15. R. E. Blanco, "Monthly Progress Report for Chemical Development Section B, October 1959," ORNL-CF-59-12-20 and "Unit Operation Monthly Progress Report, September 1959," ORNL-CF-59-9-69.

16. "Chemical Technology Division Annual Progress Report, August 31, 1961," ORNL-3153.

17. R. E. Blanco, "Monthly Progress Report for Chemical Development Section B, May 1959," ORNL-CF-59-6-64.

18. O. W. Parrott, "Modifications for the STR Fuel Recovery Process," IDO-14522, 1960.

19. R. E. Blanco, "Monthly Progress Report for Chemical Development Section B, March, 1961," ORNL-CF-61-4-108.

20. F. S. Martin and G. M. Gillies, "The Chemistry of Ruthenium, Part I. The Formation and Examination of an Extractable Ruthenium Nitrate in Macroscopic Amounts," AERE C/R 816 (1951).

21. R. E. Blanco, "Monthly Progress Report for Chemical Development Section B, February 1961," ORNL-CF-61-3-50.

22. R. E. Blanco, "Monthly Progress Report for Chemical Development Section B, March 1961," ORNL-CF-61-4-108.

23. R. E. Blanco, "Monthly Progress Report for Chemical Development Section B, January 1961," ORNL-CF-61-2-61.

24. "Chemical Technology Annual Progress Report, August 1961," ORNL-3153.

25. "Chemical Technology Annual Progress Report, August 1960," ORNL-2993.

26. P. D. Miller, C. L. Peterson, E. L. White, and F. W. Fink, "Evaluation of Container Materials for Zircex and Darex Nuclear Fuel Recovery Processes," BMI-1242, Dec. 11, 1957; (cf. Ind. Eng. Chem., 51 32-7 (1959)).

27. C. L. Peterson, P. D. Miller, J. D. Jackson, and F. W. Fink, "Construction Materials for Various Head-end Processes for the Aqueous Reprocessing of Spent Fuel Elements," BMI-1375, August 28, 1959.

28. R. E. Blanco, "Monthly Progress Report for Chemical Development Section B, February 1961," ORNL-CF-61-3-50.

29. R. E. Blanco, "Monthly Progress Report for Chemical Development Section B, March 1961, " ORNL-CF-61-4-108.

30. A. H. Samuel, R. S. Farrand, and W. E. Wilson, "Radiation Stability of Organic Liquids," Stanford Research Institute, Semi-Annual Report No. 1, Project Agreement No. 25, Contract AT(04-3)-115, January 31, 1961.

31. L. H. Towle and R. S. Farrand, "Radiation Stability of Organic Liquids," Semi-Annual Report No. 7, Subcontract 1081 with ORNL, June 15, 1960.

32. L. L. Burger, "The Decomposition Reactions of Tributyl Phosphate and Its Diluents and Their Effect on Uranium Recovery Processes," Chap. 7-5 in "Process Chemistry," Vol. 2, Series 3, Pergamon Press, N. Y., 1958.

33. W. Davis, Jr., "Radiation Densities and TBP Radiolysis During Thorex Short Decay Runs," ORNL-2764, Aug. 6, 1959.

34. R. E. Blanco, "Monthly Progress Report for Chemical Development Section B, January 1961," ORNL-CF-61-2-61.

35. R. E. Blanco, "Monthly Progress Report for Chemical Development Section B, February 1961," ORNL-CF-61-3-50.

36. G. B. Barton, T. L. Hepworth, E. D. McClanahan, Jr., R. L. Moore, and H. H. VanTuyl, Ind. Eng. Chem., 50, 212 (1958).

37. R. E. Blanco, "Monthly Progress Report for Chemical Development Section B, March 1961," ORNL-CF-61-4-108.

38. R. E. Blanco, "Monthly Progress Report for Chemical Development Section B, February 1961," ORNL-CF-61-3-50.

39. D. P. Evans, W. C. Davis, and W. J. Jones, J. Chem. Soc., 1930, p. 1310.

40. R. E. Blanco and E. G Struxness, "Waste Treatment and Disposal Progress Report for April and May 1961," ORNL-CF-61-7-3 (August 1961).

41. R. E. Blanco, "Monthly Progress Report for Chemical Development Section B, February 1961," ORNL-CF-61-3-50.

42. E. Glueckauf, British Patent 844,376 (August 10, 1960), "Improvements in or Relating to Method of Separating Strontium from Other Fission Products."

43. "Amberlite 200-Technical Notes," Technical Bulletin IE-48-60 issued by Rohm and Haas Company, The Resinous Products Division, Philadelphia 5, Pennsylvania (March 1960).

44. "Chemical Technology Division Annual Progress Report, August 31, 1960," ORNL-2993 (Sect. 18.1).

45. R. E. Blanco, "Monthly Progress Report for Chemical Development Section B, April 1960," ORNL-CF-60-5-106.

46. W. F. Libby, "Vibrational Frequencies of Isotopic Water Molecules: Equilibria with Isotopic Hydrogens," J. Chem. Phys. 11, 101 (1943).

47. W. M. Jones, "Thermodynamics Function for Tritium and Tritium Hydride. Equilibria of Tritium and Hydrogen with Tritium Hydride. The Dissociation of Tritium and Tritium Hydride," J. Chem. Phys. 16, 1077 (1948).

DISTRIBUTION

1. J. B. Adams
2-3. R. E. Blanco
4. J. O. Blomeke
5. J. C. Bresee
6. K. B. Brown
7. W. E. Clark
8. F. L. Culler
9. W. Davis
10. L. M. Ferris
11. D. E. Ferguson
12. J. R. Flanary
13. T. A. Gens
14. H. E Goeller
15. A. E. Goldman
16. J. M. Googin
17. A. T. Gresky
18. P. A. Haas
19. F. E. Harrington
20. R. F. Hibbs
21. J. M. Holmes
22. R. W. Horton
23. A. R. Irvine
24. W. H. Jordan
25. F. G. Kitts
26. Eugene Lamb
27. W. H. Lewis
28. R. B. Lindauer
29. A. P. Litman
30. J. T. Long
31. J. P. Nichols
32. E. L. Nicholson
33. R. H. Rainey
34. J. T. Roberts
35. A. D. Ryon
36-38. E. M. Shank
39. M. J. Skinner
40. S. H. Smiley
41. E. G. Struxness
42. J. C. Suddath
43. J. A. Swartout
44. J. W. Ullmann
45. C. D. Watson
46. M. E. Whatley
47. C. E. Winters
48. R. G. Wymer
49. E. L. Anderson, AEC, Washington
50. R. F. Benenati, General Atomic
51. S. Bernstein, Paducah
52. James A. Buckham, ICPP
53. J. T. Christy, AEC, Hanford
54. F. R. Dowling, AEC, Washington
55. R. A. Ewing, BMI
56. M. K. Harmon, Hanford
57. L. P. Hatch, Brookhaven
58. B. R. Hayward, Atomics International
59. O. F. Hill, Hanford
60. K. K. Kennedy, ICPP
61. E. M. Kinderman, SRI
62. S. Lawroski, ANL
63. J. A. Lieberman, AEC, Washington
64. J. A. McBride, ICPP
65. R. A. McGuire, ICPP
66. B. Manowitz, BNL
67. J. W. Morris, du Pont, Savannah River
68. D. M. Paige, ICPP
69. H. Pearlman, Atomics International
70. W. H. Reas, Hanford
71. Kenneth Rohde, ICPP
72. C. A. Rohrman, Hanford
73. H. Schoen, RAI
74. C. M. Slansky, ICPP
75. J. I. Stevens, ICPP
76. K. G. Steyer, General Atomics
77. V. R. Thayer, du Pont, Wilmington
78. R. E. Thomlinson, Hanford
79. J. Vanderryn, AEC ORO
80. F. M. Warzel, ICPP
81. Document Reference Section
82-83. Central Research Library
84-88. Laboratory Records
89. ORNL-RC
90-104. DTIE